

# CITATION REPORT

List of articles citing

## Surface science studies of the photoactivation of TiO<sub>2</sub>--new photochemical processes

DOI: 10.1021/cr050172k

Chemical Reviews, 2006, 106, 4428-53.

**Source:** <https://exaly.com/paper-pdf/39670261/citation-report.pdf>

**Version:** 2024-04-26

This report has been generated based on the citations recorded by exaly.com for the above article. For the latest version of this publication list, visit the link given above.

The third column is the impact factor (IF) of the journal, and the fourth column is the number of citations of the article.

#	Paper	IF	Citations
1872	Anisotropy in the electrical conductivity of rutile TiO <sub>2</sub> in the (110) plane. <b>2006</b> , 110, 22966-7		40
1871	Dynamics of efficient electron-hole separation in TiO <sub>2</sub> nanoparticles revealed by femtosecond transient absorption spectroscopy under the weak-excitation condition. <b>2007</b> , 9, 1453-60		234
1870	Mechanistic Insight into the TiO <sub>2</sub> Photocatalytic Reactions: Design of New Photocatalysts. <b>2007</b> , 111, 5259-5275		552
1869	Theoretical Study of Stable, Defect-Free (TiO <sub>2</sub> ) <sub>n</sub> Nanoparticles with $n = 10-16$ . <b>2007</b> , 111, 16808-16817		106
1868	Kinetics of Photogenerated Electrons Involved in Photocatalytic Reaction of Methanol on Pt/TiO <sub>2</sub> . <b>2007</b> , 20, 483-488		7
1867	Effect of protons on the optical properties of oxide nanostructures. <b>2007</b> , 129, 12491-6		43
1866	Characterization and optoelectronic properties of p-type N-doped CuAlO <sub>2</sub> films. <b>2007</b> , 90, 191117		43
1865	Photocatalytic Production of Hydrogen from Water with Visible Light Using Hybrid Catalysts of CdS Attached to Microporous and Mesoporous Silicas. <b>2007</b> , 111, 18195-18203		124
1864	Probing the electronic structure and band gap evolution of titanium oxide clusters (TiO <sub>2</sub> ) <sub>n</sub> (n = 1-10) using photoelectron spectroscopy. <b>2007</b> , 129, 3022-6		159
1863	Thin Coatings with Photo-Catalytic Activity Based on Inorganic-Organic Hybrid Polymers Modified with Anatase Nanoparticles. <b>2007</b> , 254, 196-202		7
1862	Titanium, zirconium and hafnium. <b>2007</b> , 103, 137		2
1861	Rate Enhancement and Rate Inhibition of Phenol Degradation over Irradiated Anatase and Rutile TiO <sub>2</sub> on the Addition of NaF: New Insight into the Mechanism. <b>2007</b> , 111, 19024-19032		119
1860	Partially hydroxylated polycrystalline ionic oxides: a new route toward electron-rich surfaces. <b>2007</b> , 129, 10575-81		26
1859	Visible-Light Photoactivity of Nitrogen-Doped TiO <sub>2</sub> : Photo-oxidation of HCO <sub>2</sub> H to CO <sub>2</sub> and H <sub>2</sub> O. <b>2007</b> , 111, 15357-15362		75
1858	Photocatalytic surface reactions on indoor wall paint. <b>2007</b> , 41, 6573-8		114
1857	Unexpected adsorption of oxygen on TiO <sub>2</sub> nanotube arrays: influence of crystal structure. <b>2007</b> , 7, 1091-4		72
1856	Photoexcitation of Local Surface Structures on Strontium Oxide Grains. <b>2007</b> , 111, 8069-8074		11

1855	Photochemistry of the indoor air pollutant acetone on Degussa P25 TiO <sub>2</sub> studied by chemical ionization mass spectrometry. <b>2007</b> , 111, 13023-31	38
1854	First Principles Study of Nitrogen Doping at the Anatase TiO <sub>2</sub> (101) Surface. <b>2007</b> , 111, 9275-9282	127
1853	Mechanistic Studies of Photocatalytic Reaction of Methanol for Hydrogen Production on Pt/TiO <sub>2</sub> by in situ Fourier Transform IR and Time-Resolved IR Spectroscopy. <b>2007</b> , 111, 8005-8014	167
1852	Surface Science Studies of the Photoactivation of TiO <sub>2</sub> [New Photochemical Processes. <b>2007</b> , 38, no	1
1851	Preparation and Characterization of Bi <sup>3+</sup> -TiO <sub>2</sub> and its Photocatalytic Activity. <b>2007</b> , 30, 577-582	39
1850	Nanostructured Titanium Oxynitride Porous Thin Films as Efficient Visible-Active Photocatalysts. <b>2007</b> , 17, 3348-3354	155
1849	Synthesis and characterization of visible-light absorbing ordered mesoporous titanosilicate incorporated with vanadium oxide. <b>2007</b> , 444, 161-166	8
1848	Time-resolved infrared absorption study of nine TiO <sub>2</sub> photocatalysts. <b>2007</b> , 339, 133-137	41
1847	Hydrogen activation at TiO <sub>2</sub> anatase nanocrystals. <b>2007</b> , 339, 138-145	46
1846	N-doped TiO <sub>2</sub> : Theory and experiment. <b>2007</b> , 339, 44-56	766
1845	A facile solution-phase synthesis of high quality water-soluble anatase TiO <sub>2</sub> nanocrystals. <b>2007</b> , 314, 337-40	37
1844	TiO <sub>2</sub> Nanobelts/CdSSe Quantum Dots Nanocomposite. <b>2007</b> , 111, 10389-10393	52
1843	Carbon and Nitrogen Co-doped TiO <sub>2</sub> with Enhanced Visible-Light Photocatalytic Activity. <b>2007</b> , 46, 2741-2746	468
1842	Femtosecond visible-to-IR spectroscopy of TiO <sub>2</sub> nanocrystalline films: dynamics of UV-generated charge carrier relaxation at different excitation wavelengths. <b>2007</b> ,	4
1841	Single-molecule detection of reactive oxygen species: application to photocatalytic reactions. <b>2007</b> , 17, 727-38	25
1840	Adsorption of iso-/n-butane on an anatase thin film: a molecular beam scattering and TDS study. <b>2007</b> , 116, 9-14	10
1839	CO Oxidation on Anatase TiO <sub>2</sub> Nanotubes Array and the Effect of Defects. <b>2007</b> , 118, 118-122	11
1838	Adsorption kinetics of alkanes on TiO <sub>2</sub> nanotubesarray [structure]activity relationship. <b>2007</b> , 601, 4620-4628	17

1837	The influence of cobalt doping on photocatalytic nano-titania: Crystal chemistry and amorphicity. <b>2007</b> , 180, 2905-2915	24
1836	Formation of impurity bands in iodine cation substitutionally doped TiO <sub>2</sub> and its effects on photoresponse and photogenerated carriers. <b>2008</b> , 372, 5901-5904	7
1835	Photooxidation of iodide ion on immobilized semiconductor powders. <b>2008</b> , 92, 490-494	21
1834	Synthesis and characterization of bamboo-like CdS/TiO <sub>2</sub> nanotubes composites with enhanced visible-light photocatalytic activity. <b>2008</b> , 10, 729-736	70
1833	In Situ FT-IR Study of Photocatalytic Decomposition of Formic Acid to Hydrogen on Pt/TiO <sub>2</sub> Catalyst. <b>2008</b> , 29, 105-107	62
1832	Advanced oxidation processes for water treatment: advances and trends for R&D. <b>2008</b> , 83, 769-776	624
1831	Probing defect sites on TiO <sub>2</sub> with [Re <sub>3</sub> (CO) <sub>12</sub> H <sub>3</sub> ]: spectroscopic characterization of the surface species. <b>2008</b> , 14, 1402-14	25
1830	Diffusion versus desorption: complex behavior of H atoms on an oxide surface. <b>2008</b> , 9, 253-6	118
1829	Charge separation in layered titanate nanostructures: effect of ion exchange induced morphology transformation. <b>2008</b> , 47, 1496-9	41
1828	Ladungstrennung in nanoskaligen Titanat-Schichten: Einfluss von Ionenaustausch und Morphologieumwandlung auf die photoelektronischen Eigenschaften. <b>2008</b> , 120, 1518-1522	4
1827	Synthesis and photoluminescence of well-dispersible anatase TiO <sub>2</sub> nanoparticles. <b>2008</b> , 318, 29-34	87
1826	Maintaining particle size in the transformation of anatase to rutile titania nanostructures. <b>2008</b> , 69, 2898-2906	13
1825	Visible-light driven TiO <sub>2</sub> photocatalysts from Ti-oxychloride precursors. <b>2008</b> , 199, 136-143	7
1824	Oxolinic acid photo-oxidation using immobilized TiO <sub>2</sub> . <b>2008</b> , 158, 460-4	37
1823	Technologies for the removal of phenol from fluid streams: a short review of recent developments. <b>2008</b> , 160, 265-88	897
1822	Metal ion induced room temperature phase transformation and stimulated infrared spectroscopy on TiO <sub>2</sub> -based surfaces. <b>2008</b> , 255, 718-721	3
1821	High efficient surface-complex-assisted photodegradation of phenolic compounds in single anatase titania under visible-light. <b>2008</b> , 318, 285-290	45
1820	Adsorption and photocatalytic decomposition of methylene blue on surface modified silica and silica-titania. <b>2008</b> , 325, 17-20	46

1819	Visible light photocatalytic properties of anion-doped TiO <sub>2</sub> materials prepared from a molecular titanium precursor. <b>2008</b> , 451, 75-79	30
1818	Photodegradation of methyl green using visible irradiation in ZnO suspensions: determination of the reaction pathway and identification of intermediates by a high-performance liquid chromatography-photodiode array-electrospray ionization-mass spectrometry method. <b>2008</b> , 1189, 355-65	85
1817	Photocatalytic performance of particulate semiconductors under natural sunshine. Oxidation of carboxylic acids. <b>2008</b> , 92, 588-593	44
1816	The effect of Pt on the photocatalytic degradation pathway of methylene blue over TiO <sub>2</sub> under ambient conditions. <b>2008</b> , 83, 277-285	73
1815	Improving visible-light photocatalytic activity of N-doped TiO <sub>2</sub> nanoparticles via sensitization by Zn porphyrin. <b>2008</b> , 255, 2879-2884	74
1814	Preparation, characterization and photocatalytic activity of transition metal-loaded BiVO <sub>4</sub> . <b>2008</b> , 147, 52-56	91
1813	Nitrogen-Doped Titanium Dioxide Active in Photocatalytic Reactions with Visible Light: A Multi-Technique Characterization of Differently Prepared Materials. <b>2008</b> , 112, 17244-17252	141
1812	Material Witness: Renewing old promises. <b>2008</b> , 7, 615	
1811	Crystal growth: Anatase shows its reactive side. <b>2008</b> , 7, 613-5	433
1810	A facile solvothermal route to photocatalytically active nanocrystalline anatase TiO <sub>2</sub> from peroxide precursors. <b>2008</b> , 10, 864-872	10
1809	Mechanism of Visible Light Photocatalytic Oxidation of Methanol in Aerated Aqueous Suspensions of Carbon-Doped TiO <sub>2</sub> . <b>2008</b> , 112, 15134-15139	44
1808	Reversible Wettability Changes in Colloidal TiO <sub>2</sub> Nanorod Thin-Film Coatings under Selective UV Laser Irradiation. <b>2008</b> , 112, 701-714	87
1807	Role of Surface/Interfacial Cu <sup>2+</sup> Sites in the Photocatalytic Activity of Coupled CuO/TiO <sub>2</sub> Nanocomposites. <b>2008</b> , 112, 19040-19044	285
1806	Synthesis of Pure and Mixed-Phase Titanium Dioxide for Photocatalytic Purposes: Relations between Phase Composition, Catalytic Activity, and Charge-Trapped Sites. <b>2008</b> , 20, 4051-4061	88
1805	Density Functional Theory and Electron Paramagnetic Resonance Study on the Effect of Nitrogen Codoping of TiO <sub>2</sub> . <b>2008</b> , 20, 3706-3714	178
1804	Excitation mechanism in the photoisomerization of a surface-bound azobenzene derivative: Role of the metallic substrate. <b>2008</b> , 129, 164102	71
1803	Diffusion-Controlled Self-Assembly and Dendrite Formation in Silver-Seeded Anatase Titania Nanospheres. <b>2008</b> , 112, 5439-5446	12
1802	The identification of hydroxyl groups on ZnO nanoparticles by infrared spectroscopy. <b>2008</b> , 10, 7092-7	272

1801	Chemical reactions on rutile TiO <sub>2</sub> (110). <b>2008</b> , 37, 2328-53	441
1800	Photocatalytic activity of MCM-organized TiO <sub>2</sub> materials in the oxygenation of cyclohexane with molecular oxygen. <b>2008</b> , 7, 819-25	19
1799	Ab initio study of the electronic states induced by oxygen vacancies in rutile and anatase TiO <sub>2</sub> . <b>2008</b> , 78,	221
1798	Photoformed electron transfer from TiO <sub>2</sub> to metal clusters. <b>2008</b> , 9, 1991-1995	54
1797	Low-Temperature UV-Processing of Nanocrystalline Nanoporous Thin TiO <sub>2</sub> Films: An Original Route toward Plastic Electrochromic Systems. <b>2008</b> , 20, 7260-7267	44
1796	A new role for Fe <sup>3+</sup> in TiO <sub>2</sub> hydrosol: accelerated photodegradation of dyes under visible light. <b>2008</b> , 42, 5759-64	50
1795	Synthesis of Coupled Semiconductor by Filling 1D TiO <sub>2</sub> Nanotubes with CdS. <b>2008</b> , 20, 6784-6791	307
1794	Modeling doped and defective oxides in catalysis with density functional theory methods: room for improvements. <b>2008</b> , 128, 182505	195
1793	Photoinduced degradation of orange II on different iron (hydr)oxides in aqueous suspension: rate enhancement on addition of hydrogen peroxide, silver nitrate, and sodium fluoride. <b>2008</b> , 24, 175-81	120
1792	The important role of tetrahedral Ti <sup>4+</sup> sites in the phase transformation and photocatalytic activity of TiO <sub>2</sub> nanocomposites. <b>2008</b> , 130, 5402-3	149
1791	Local structure and magnetic behaviour of Fe-doped TiO <sub>2</sub> anatase nanoparticles: experiments and calculations. <b>2008</b> , 20, 135210	41
1790	Enhanced Photocatalytic Activity in Anatase/TiO <sub>2</sub> (B) CoreShell Nanofiber. <b>2008</b> , 112, 20539-20545	171
1789	Origin of the Enhanced Photocatalytic Activities of Semiconductors: A Case Study of ZnO Doped with Mg <sup>2+</sup> . <b>2008</b> , 112, 12242-12248	211
1788	Real-Time Single-Molecule Imaging of the Spatial and Temporal Distribution of Reactive Oxygen Species with Fluorescent Probes: Applications to TiO <sub>2</sub> Photocatalysts. <b>2008</b> , 112, 1048-1059	77
1787	A Highly Efficient Visible-Light-Activated Photocatalyst Based on Bismuth- and Sulfur-Codoped TiO <sub>2</sub> . <b>2008</b> , 112, 6620-6626	153
1786	Nonhydrolytic synthesis of high-quality anisotropically shaped brookite TiO <sub>2</sub> nanocrystals. <b>2008</b> , 130, 11223-33	224
1785	Inorganic Materials as Catalysts for Photochemical Splitting of Water. <b>2008</b> , 20, 35-54	1846
1784	Molecular structures and energetics of the (TiO <sub>2</sub> ) <sub>n</sub> (n = 1-4) clusters and their anions. <b>2008</b> , 112, 6646-66	143

1783	The role of interstitial sites in the Ti3d defect state in the band gap of titania. <b>2008</b> , 320, 1755-9	744
1782	Biomimetic synthesis of titania nanoparticles induced by protamine. <b>2008</b> , 4165-71	63
1781	Photosensitization and Photocurrent Switching in Carminic Acid/Titanium Dioxide Hybrid Material. <b>2008</b> , 112, 19131-19141	33
1780	Photoinduced Dynamics of TiO <sub>2</sub> Doped with Cr and Sb. <b>2008</b> , 112, 1167-1173	102
1779	Synthesis, characterization, and photodegradation behavior of single-phase anatase TiO <sub>2</sub> materials synthesized from Ti-oxychloride precursors. <b>2008</b> , 24, 11111-8	6
1778	Facile synthesis of monoazidotitanium isopropoxides. <b>2008</b> , 47, 10804-6	6
1777	Formate adsorption onto thin films of rutile TiO <sub>2</sub> nanorods and nanowires. <b>2008</b> , 24, 14035-41	13
1776	Chemical state and environment of boron dopant in B,N-codoped anatase TiO <sub>2</sub> nanoparticles: an avenue for probing diamagnetic dopants in TiO <sub>2</sub> by electron paramagnetic resonance spectroscopy. <b>2008</b> , 130, 2760-1	104
1775	Preparation, Characterisation, and Photocatalytic Behaviour of Co-TiO <sub>2</sub> with Visible Light Response. <b>2008</b> , 2008, 1-9	34
1774	Gas-Phase Photodegradation of Decane and Methanol on TiO <sub>2</sub> : Dynamic Surface Chemistry Characterized by Diffuse Reflectance FTIR. <b>2008</b> , 2008, 1-9	11
1773	Excess electron states in reduced bulk anatase TiO <sub>2</sub> : comparison of standard GGA, GGA+U, and hybrid DFT calculations. <b>2008</b> , 129, 154113	429
1772	Interesting magnetic behavior from reduced titanium dioxide nanobelts. <b>2008</b> , 92, 232502	33
1771	Doping effects of Co(2+) ions on ZnO nanorods and their photocatalytic properties. <b>2008</b> , 19, 215703	93
1770	High Resolution Electron Energy Loss Spectroscopy on Perfect and Defective Oxide Surfaces. <b>2008</b> , 222, 927-964	29
1769	Electron-stimulated positive-ion desorption caused by charge transfer from adsorbate to substrate: Oxygen adsorbed on TiO <sub>2</sub> (110). <b>2009</b> , 79,	24
1768	First-principles study of thin TiO <sub>x</sub> and bulklike rutile nanowires. <b>2009</b> , 80,	21
1767	Theoretical study of the molecular and electronic structure of methanol on a TiO <sub>2</sub> (110) surface. <b>2009</b> , 80,	84
1766	Assignment of photoelectron spectra of (TiO <sub>2</sub> ) <sub>n</sub> with n = 1-3. <b>2009</b> , 130, 174308	12

1765	Magnetic properties of Fe-doped Zn-TiO <sub>2</sub> rutile nanoparticles. <b>2009</b> , 1201, 24	
1764	Photooxidation of Water Using Vertically Aligned Nanotube Arrays: A comparative study of TiO <sub>2</sub> , Fe <sub>2</sub> O <sub>3</sub> and TaON nanotubes. <b>2009</b> , 1171, 52	
1763	Band structure design and photocatalytic activity of In <sub>2</sub> O <sub>3</sub> /NiNbO <sub>4</sub> composite. <b>2009</b> , 95, 032107	47
1762	Nonlinear Modelling of Kinetic Data Obtained from Photocatalytic Mineralisation of 2,4-Dichlorophenol on a Titanium Dioxide Membrane. <b>2009</b> , 2009, 1-10	4
1761	TiO <sub>2</sub> and TiO <sub>2</sub> /WO <sub>3</sub> porous film electrodes for application in solar energy conversion. <b>2009</b> ,	
1760	Preparation of cuprous oxides with different sizes and their behaviors of adsorption, visible-light driven photocatalysis and photocorrosion. <b>2009</b> , 11, 129-138	248
1759	Preparation and characterization of S-doped TiO <sub>2</sub> nanoparticles, effect of calcination temperature and evaluation of photocatalytic activity. <b>2009</b> , 116, 376-382	107
1758	Nitrogen-doped TiO <sub>2</sub> nanotubes with enhanced photocatalytic activity synthesized by a facile wet chemistry method. <i>Materials Research Bulletin</i> , <b>2009</b> , 44, 146-150	5.1 91
1757	Reversibly Light-Switchable Wettability of Hybrid Organic/Inorganic Surfaces With Dual Micro-/Nanoscale Roughness. <b>2009</b> , 19, 1149-1157	106
1756	N-Doped Titania Thin Films Prepared by Atmospheric Pressure CVD using t-Butylamine as the Nitrogen Source: Enhanced Photocatalytic Activity under Visible Light. <b>2009</b> , 15, 171-174	30
1755	Substituent effect on nano TiO <sub>2</sub> - and ZnO-catalyzed phenol photodegradation rates. <b>2009</b> , 41, 275-283	18
1754	Semiconductor-photocatalyzed degradation of carboxylic acids: Enhancement by particulate semiconductor mixture. <b>2009</b> , 41, 716-726	10
1753	Photoreduction of chromium(VI) on ZrO <sub>2</sub> and ZnS surfaces. <b>2009</b> , 140, 1269-1274	17
1752	The 2 $\times$ 1 reconstruction of the rutile TiO <sub>2</sub> (011) surface: A combined density functional theory, X-ray diffraction, and scanning tunneling microscopy study. <b>2009</b> , 603, 138-144	96
1751	Scattering of F atoms and anions on a TiO <sub>2</sub> (1 1 0) surface. <b>2009</b> , 603, 1099-1105	1
1750	High performance nano-titania photocatalytic paper composite. Part II: Preparation and characterization of natural zeolite-based nano-titania composite sheets and study of their photocatalytic activity. <b>2009</b> , 164, 135-139	23
1749	A facile method to synthesize nitrogen and fluorine co-doped TiO <sub>2</sub> nanoparticles by pyrolysis of (NH <sub>4</sub> ) <sub>2</sub> TiF <sub>6</sub> . <b>2009</b> , 11, 303-313	44
1748	Photocatalytic properties of porous C-doped TiO <sub>2</sub> and Ag/C-doped TiO <sub>2</sub> nanomaterials by eggshell membrane templating. <b>2009</b> , 11, 375-384	34



1747	Synthesis and Characterization of Rare Earth Orthovanadate (RVO <sub>4</sub> ; R = La, Ce, Nd, Sm, Eu & Gd) Nanorods/Nanocrystals/Nanospindles by a Facile Sonochemical Method and Their Catalytic Properties. <b>2009</b> , 20, 291-305	95
1746	Optical properties of the HfO <sub>2</sub> / SiO <sub>2</sub> and TiO <sub>2</sub> / SiO <sub>2</sub> films prepared by ion beam sputtering. <b>2009</b> , 106, 72-77	15
1745	Reducing the Photocatalytic Activity of Zinc Oxide Quantum Dots by Surface Modification. <b>2009</b> , 92, 2083-2088	46
1744	Implantation of anatase thin film with 100 keV <sup>56</sup> Fe ions: Damage formation and magnetic behaviour. <b>2009</b> , 267, 2725-2730	6
1743	Chemical reactions on metal oxide surfaces investigated by vibrational spectroscopy. <b>2009</b> , 603, 1589-1599	45
1742	Reversible molecular switching at a metal surface: A case study of tetra-tert-butyl-azobenzene on Au(111). <b>2009</b> , 603, 1506-1517	84
1741	Photochemistry on TiO <sub>2</sub> : Mechanisms behind the surface chemistry. <b>2009</b> , 603, 1605-1612	173
1740	(Bi, C and N) codoped TiO <sub>2</sub> nanoparticles. <b>2009</b> , 161, 396-401	120
1739	Decolorization of C.I. Acid Blue 9 solution by UV/Nano-TiO <sub>2</sub> (2), Fenton, Fenton-like, electro-Fenton and electrocoagulation processes: a comparative study. <b>2009</b> , 161, 1225-33	248
1738	Photodegradation of phenol on Y <sub>2</sub> O <sub>3</sub> surface: synergism by semiconductors. <b>2009</b> , 167, 664-8	15
1737	Synthesis and characterization of TiO <sub>2</sub> -pillared Romanian clay and their application for azoic dyes photodegradation. <b>2009</b> , 167, 1050-6	50
1736	Photocatalytic degradation of three azo dyes using immobilized TiO <sub>2</sub> nanoparticles on glass plates activated by UV light irradiation: influence of dye molecular structure. <b>2009</b> , 168, 451-7	251
1735	The role of crystal phase in determining photocatalytic activity of nitrogen doped TiO <sub>2</sub> . <b>2009</b> , 329, 331-8	98
1734	Structural and adsorption characteristics and catalytic activity of titania and titania-containing nanomaterials. <b>2009</b> , 330, 125-37	21
1733	One-pot synthesis of peroxo-titania nanopowder and dual photochemical oxidation in aqueous methanol solution. <b>2009</b> , 331, 132-7	27
1732	Degradation of phenol by mechanical activation of a rutile catalyst. <b>2009</b> , 339, 133-9	7
1731	A simple route towards low-temperature processing of nanoporous thin films using UV-irradiation: Application for dye solar cells. <b>2009</b> , 205, 70-76	34
1730	Nitrogen-doped and nitrogen/fluorine-codoped titanium dioxide. Nature and concentration of the photoactive species and their role in determining the photocatalytic activity under visible light. <b>2009</b> , 205, 93-97	59

1729	N, S co-doped and N-doped Degussa P-25 powders with visible light response prepared by mechanical mixing of thiourea and urea. Reactivity towards E. coli inactivation and phenol oxidation. <b>2009</b> , 205, 109-115	82
1728	Enhanced photocatalytic activity under visible light in N-doped TiO <sub>2</sub> thin films produced by APCVD preparations using t-butylamine as a nitrogen source and their potential for antibacterial films. <b>2009</b> , 207, 244-253	100
1727	Preparation and spectroscopic characterization of visible light sensitized N doped TiO <sub>2</sub> (rutile). <b>2009</b> , 182, 160-164	65
1726	Photoinduced electron dynamics at the chromophore-semiconductor interface: A time-domain ab initio perspective. <b>2009</b> , 84, 30-68	155
1725	The interaction between adsorbed OH and O <sub>2</sub> on TiO <sub>2</sub> surfaces. <b>2009</b> , 84, 155-176	111
1724	Operando FTIR study of the photocatalytic oxidation of acetone in air over TiO <sub>2</sub> /ZrO <sub>2</sub> thin films. <b>2009</b> , 143, 364-373	47
1723	Photodegradation of carboxylic acids on Pr <sub>6</sub> O <sub>11</sub> surface. Enhancement by semiconductors. <b>2009</b> , 151, 46-50	5
1722	Photocatalytic mineralization of phenol catalyzed by pure and mixed phase hydrothermal titanium dioxide. <b>2009</b> , 88, 497-504	37
1721	Abatement of organics and Escherichia coli by N, S co-doped TiO <sub>2</sub> under UV and visible light. Implications of the formation of singlet oxygen ( <sup>1</sup> O <sub>2</sub> ) under visible light. <b>2009</b> , 88, 398-406	188
1720	Highly active TiO <sub>2</sub> /N <sub>x</sub> F <sub>y</sub> visible photocatalyst prepared under supercritical conditions in NH <sub>4</sub> F/EtOH fluid. <b>2009</b> , 89, 543-550	89
1719	Is sulfur-doped TiO <sub>2</sub> an effective visible light photocatalyst for remediation?. <b>2009</b> , 91, 554-562	118
1718	Synthesis, characterization and photocatalytic activities of rare earth-loaded BiVO <sub>4</sub> catalysts. <b>2009</b> , 256, 597-602	78
1717	Cr/Sb co-doped TiO <sub>2</sub> from first principles calculations. <b>2009</b> , 469, 166-171	79
1716	The nitrogen photoactive centre in N-doped titanium dioxide formed via interaction of N atoms with the solid. Nature and energy level of the species. <b>2009</b> , 477, 135-138	80
1715	Quick screening method for the photocatalytic activity of nanoparticles and powdery materials. <b>2009</b> , 352, 271-276	4
1714	Photocatalytic behavior of TOPO-capped TiO <sub>2</sub> nanocrystals for degradation of endocrine disrupting chemicals. <b>2009</b> , 91, 619-627	33
1713	Comparison of the substrate dependent performance of Pt-, Au- and Ag-doped TiO <sub>2</sub> photocatalysts in H <sub>2</sub> -production and in decomposition of various organics. <b>2009</b> , 98, 215-225	53
1712	Reduced and n-Type Doped TiO <sub>2</sub> : Nature of Ti <sup>3+</sup> Species. <b>2009</b> , 113, 20543-20552	572

1711	On the Origin of the Spectral Bands in the Visible Absorption Spectra of Visible-Light-Active TiO <sub>2</sub> Specimens Analysis and Assignments. <b>2009</b> , 113, 15110-15123	192
1710	Enhanced Photoactivity of Oxygen-Deficient Anatase TiO <sub>2</sub> Sheets with Dominant {001} Facets. <b>2009</b> , 113, 21784-21788	341
1709	Equilibrium adsorption of stilbenoids at metal oxides. <b>2009</b> , 45, 19-24	2
1708	Interaction of stilbenes with TiO <sub>2</sub> studied by Fourier IR spectroscopy. <b>2009</b> , 45, 685-692	2
1707	Selectivity in photocatalysis by particulate semiconductors. <b>2009</b> , 7, 134-137	13
1706	Solar-driven electrochemically assisted semiconductor-catalyzed iodide ion oxidation. Enhanced efficiency by oxide mixtures. <b>2009</b> , 7, 519-523	2
1705	Chemical State of Nitrogen and Visible Surface and Schottky Barrier Driven Photoactivities of N-Doped TiO <sub>2</sub> Thin Films. <b>2009</b> , 113, 13341-13351	58
1704	Highly stable molecular layers on nanocrystalline anatase TiO <sub>2</sub> through photochemical grafting. <b>2009</b> , 25, 10676-84	37
1703	Solid-State <sup>13</sup> C NMR Characterization of Carbon-Modified TiO <sub>2</sub> . <b>2009</b> , 21, 1187-1197	39
1702	Photochemical grafting and patterning of biomolecular layers onto TiO <sub>2</sub> thin films. <b>2009</b> , 1, 1013-22	34
1701	Single-molecule observation of photocatalytic reaction in TiO <sub>2</sub> nanotube: importance of molecular transport through porous structures. <b>2009</b> , 131, 934-6	78
1700	Decorating Titanate Nanotubes with CeO <sub>2</sub> Nanoparticles. <b>2009</b> , 113, 20234-20239	50
1699	Boron-Doped Anatase TiO <sub>2</sub> : Pure and Hybrid DFT Calculations. <b>2009</b> , 113, 220-228	146
1698	Final State Distributions of O <sub>2</sub> Photodesorbed from TiO <sub>2</sub> (110). <b>2009</b> , 113, 13180-13191	60
1697	Nature of the Oxidizing Species Formed upon UV Photolysis of C-TiO <sub>2</sub> Aqueous Suspensions. <b>2009</b> , 113, 12489-12494	20
1696	Effect of Rapid Infrared Annealing on the Photoelectrochemical Properties of Anodically Fabricated TiO <sub>2</sub> Nanotube Arrays. <b>2009</b> , 113, 7996-7999	48
1695	Formation and diffusion of water dimers on rutile TiO <sub>2</sub> (110). <b>2009</b> , 102, 226101	80
1694	Synergistic effect between anatase and rutile TiO <sub>2</sub> nanoparticles in dye-sensitized solar cells. <b>2009</b> , 10078-85	178

1693	First-Principle Calculations of Solvated Electrons at Protic Solvent-TiO <sub>2</sub> Interfaces with Oxygen Vacancies. <b>2009</b> , 113, 7236-7245		17
1692	Thermal Decomposition of a Chemical Warfare Agent Simulant (DMMP) on TiO <sub>2</sub> : Adsorbate Reactions with Lattice Oxygen as Studied by Infrared Spectroscopy. <b>2009</b> , 113, 15684-15691		87
1691	A Density Functional Theory + U Study of Oxygen Vacancy Formation at the (110), (100), (101), and (001) Surfaces of Rutile TiO <sub>2</sub> . <b>2009</b> , 113, 7322-7328		192
1690	ESR Study on the Reversible Electron Transfer from O <sub>2</sub> to Ti <sup>4+</sup> on TiO <sub>2</sub> Nanoparticles Induced by Visible-Light Illumination. <b>2009</b> , 113, 1160-1163		29
1689	Anomalous Photocathodic Behavior of CdS within the Urbach Tail Region. <b>2009</b> , 113, 6774-6784		41
1688	Nature of Ti Interstitials in Reduced Bulk Anatase and Rutile TiO <sub>2</sub> . <b>2009</b> , 113, 3382-3385		132
1687	Surface-mediated visible-light photo-oxidation on pure TiO <sub>2</sub> (001). <b>2009</b> , 131, 14670-2		86
1686	Mixed-phase TiO <sub>2</sub> nanoparticles preparation using sol-gel method. <i>Journal of Alloys and Compounds</i> , <b>2009</b> , 478, 586-589	5-7	72
1685	Crystallization behaviors of TiO <sub>2</sub> films derived from thermal oxidation of evaporated and sputtered titanium films. <i>Journal of Alloys and Compounds</i> , <b>2009</b> , 480, 938-941	5-7	18
1684	Photocatalytic removal of C.I. Basic Red 46 on immobilized TiO <sub>2</sub> nanoparticles: artificial neural network modelling. <b>2009</b> , 30, 1155-68		79
1683	Development of alternative photocatalysts to TiO <sub>2</sub> : Challenges and opportunities. <b>2009</b> , 2, 1231		1024
1682	An efficient photocatalyst structure: TiO <sub>2</sub> (B) nanofibers with a shell of anatase nanocrystals. <b>2009</b> , 131, 17885-93		448
1681	On the Origin of the Decay of the Photocatalytic Activity of TiO <sub>2</sub> Powders Ground at High Energy. <b>2009</b> , 113, 16589-16602		35
1680	UV Raman Spectroscopic Study on TiO <sub>2</sub> . II. Effect of Nanoparticle Size on the Outer/Inner Phase Transformations. <b>2009</b> , 113, 1698-1704		98
1679	A metal matrix composite prepared from electrospun TiO <sub>2</sub> nanofibers and an Al 1100 alloy via friction stir processing. <b>2009</b> , 1, 987-91		14
1678	SnO <sub>2</sub> nanostructures-TiO <sub>2</sub> nanofibers heterostructures: controlled fabrication and high photocatalytic properties. <b>2009</b> , 48, 7261-8		278
1677	Polyol-Mediated Synthesis of Ultrafine TiO <sub>2</sub> Nanocrystals and Tailored Physiochemical Properties by Ni Doping. <b>2009</b> , 113, 9210-9217		43
1676	A new visible-light photocatalyst: CdS quantum dots embedded mesoporous TiO <sub>2</sub> . <b>2009</b> , 43, 7079-85		391

1675	Band-to-Band Visible-Light Photon Excitation and Photoactivity Induced by Homogeneous Nitrogen Doping in Layered Titanates. <b>2009</b> , 21, 1266-1274	259
1674	Analysis of Surface OH Groups on TiO <sub>2</sub> Single Crystal with Polarization Modulation Infrared External Reflection Spectroscopy. <b>2009</b> , 113, 20322-20327	28
1673	Photo-induced effects on self-organized TiO <sub>2</sub> nanotube arrays: the influence of surface morphology. <b>2009</b> , 20, 045603	71
1672	Single-molecule fluorescence imaging of TiO(2) photocatalytic reactions. <b>2009</b> , 25, 7791-802	81
1671	Characterization of Fe-TiO <sub>2</sub> films synthesized by sol-gel method for application in energy conversion devices. <b>2009</b> ,	2
1670	Stability and photoelectronic properties of layered titanate nanostructures. <b>2009</b> , 131, 6198-206	98
1669	Structure and Phase Transition Behavior of Sn <sup>4+</sup> -Doped TiO <sub>2</sub> Nanoparticles. <b>2009</b> , 113, 18121-18124	99
1668	New approach toward nanosized ferrous ferric oxide and Fe(3)O(4)-doped titanium dioxide photocatalysts. <b>2009</b> , 1, 2453-61	54
1667	Highly thermal stable and highly crystalline anatase TiO <sub>2</sub> for photocatalysis. <b>2009</b> , 43, 5423-8	94
1666	Efficient Promotion of Anatase TiO <sub>2</sub> Photocatalysis via Bifunctional Surface-Terminating TiO <sub>2</sub> Structures. <b>2009</b> , 113, 12317-12324	109
1665	TiO <sub>2</sub> -catalyzed photodegradation of porphyrins: mechanistic studies and application in monolayer photolithography. <b>2009</b> , 25, 5398-403	10
1664	Density functional theory based first-principle calculation of Nb-doped anatase TiO <sub>2</sub> and its interactions with oxygen vacancies and interstitial oxygen. <b>2009</b> , 131, 034702	75
1663	Femtosecond Visible-to-IR Spectroscopy of TiO <sub>2</sub> Nanocrystalline Films: Elucidation of the Electron Mobility before Deep Trapping. <b>2009</b> , 113, 11741-11746	158
1662	Band gap narrowing of titanium oxide semiconductors by noncompensated anion-cation codoping for enhanced visible-light photoactivity. <b>2009</b> , 103, 226401	325
1661	Stability of Pt nanoparticles and enhanced photocatalytic performance in mesoporous Pt-(anatase/TiO <sub>2</sub> (B)) nanoarchitecture. <b>2009</b> , 19, 7055	65
1660	When Fewer Photons Do More: A Comparative O <sub>2</sub> Photoadsorption Study on Vapor-Deposited TiO <sub>2</sub> and ZrO <sub>2</sub> Nanocrystal Ensembles. <b>2009</b> , 113, 9175-9181	13
1659	Wettability conversion of colloidal TiO <sub>2</sub> nanocrystal thin films with UV-switchable hydrophilicity. <b>2009</b> , 11, 3692-700	44
1658	Enhancement of electroluminescence from TiO <sub>2</sub> /p+-Si heterostructure-based devices through engineering of oxygen vacancies in TiO <sub>2</sub> . <b>2009</b> , 95, 252102	20

1657	Role of Coverage and Surface Oxidation Degree in the Adsorption of Acetone on TiO <sub>2</sub> (110). A Density Functional Study. <b>2009</b> , 113, 19973-19980	22
1656	Synthesis of rutileanatase coreshell structured TiO <sub>2</sub> for photocatalysis. <b>2009</b> , 19, 6590	108
1655	Hierarchically nanostructured rutile arrays: acid vapor oxidation growth and tunable morphologies. <b>2009</b> , 3, 1212-8	98
1654	Ordered Co <sub>3</sub> O <sub>4</sub> hierarchical nanorod arrays: tunable superhydrophilicity without UV irradiation and transition to superhydrophobicity. <b>2009</b> , 19, 8366	116
1653	Observation of all the intermediate steps of a chemical reaction on an oxide surface by scanning tunneling microscopy. <b>2009</b> , 3, 517-26	92
1652	The electronic structure of oxygen atom vacancy and hydroxyl impurity defects on titanium dioxide (110) surface. <b>2009</b> , 130, 124502	183
1651	Nitrogen diffusion in doped TiO <sub>2</sub> (110) single crystals: a combined XPS and SIMS study. <b>2009</b> , 19, 8418	59
1650	Controlled growth of monocrystalline rutile nanoshuttles in anatase TiO <sub>2</sub> particles under mild conditions. <b>2009</b> , 11, 564	20
1649	Synthesis of Poly(methyl methacrylate) Encapsulated TiO <sub>2</sub> Nanocomposite Particles in Supercritical CO <sub>2</sub> . <b>2009</b> , 514, 25/[355]-35/[365]	8
1648	Energetics and diffusion of intrinsic surface and subsurface defects on anatase TiO <sub>2</sub> (101). <b>2009</b> , 131, 054703	126
1647	Changing the physical and chemical properties of titanium oxynitrides TiN <sub>1-x</sub> O <sub>x</sub> by changing the composition. <b>2009</b> , 80,	36
1646	Iodine doped anatase TiO <sub>2</sub> photocatalyst with ultra-long visible light response: correlation between geometric/electronic structures and mechanisms. <b>2009</b> , 19, 2822	119
1645	Properties of hydrogen and hydrogenvacancy complexes in the rutile phase of titanium dioxide. <b>2009</b> , 80,	54
1644	Surface Area, Pore Size, and Particle Size Engineering of Titania with Seeding Technique and Phosphate Modification. <b>2009</b> , 113, 13750-13757	27
1643	Efficiency of clay-TiO <sub>2</sub> nanocomposites on the photocatalytic elimination of a model hydrophobic air pollutant. <b>2009</b> , 43, 1500-6	97
1642	A new dual-purpose ultrahigh vacuum infrared spectroscopy apparatus optimized for grazing-incidence reflection as well as for transmission geometries. <b>2009</b> , 80, 113108	65
1641	Crystallite phase-controlled preparation, characterisation and photocatalytic properties of titanium dioxide nanoparticles. <b>2009</b> , 4, 121-137	36
1640	Enhanced Photocatalytic Activity of Ag <sub>3</sub> VO <sub>4</sub> Loaded with Rare-Earth Elements under Visible-Light Irradiation. <b>2009</b> , 48, 10771-10778	77

1639	Photocatalytic Purification of Water and Air over Nanoparticulate TiO <sub>2</sub> . <b>2009</b> , 579-603	1
1638	Polyolefin Clay Nanocomposites. <b>2009</b> , 129-164	
1637	Structure of Adsorbents, Ion Exchangers, Ion Conductors, Catalysts, and Permeable Materials. <b>2009</b> , 63-102	
1636	Heterogeneous Catalysis and Surface Reactions. <b>2009</b> , 421-466	
1635	Influence of Crystalline Forms of Titania on Desorption/Ionization Efficiency in Titania-Based Surface-Assisted Laser Desorption/Ionization Mass Spectrometry. <b>2010</b> , 58, 221-228	9
1634	Properties of titanium glykolates as precursors for the synthesis of titanium dioxide. <b>2010</b> , 44, 755-761	1
1633	Specific features of the photocatalytic destruction of Safranin T on mechanochemically produced barium titanate. <b>2010</b> , 83, 1799-1803	4
1632	Defining the Role of Excess Electrons in the Surface Chemistry of TiO <sub>2</sub> . <b>2010</b> , 114, 5891-5897	179
1631	Dye-sensitized solar cells. <i>Chemical Reviews</i> , <b>2010</b> , 110, 6595-663	68.1 7291
1630	Fabrication of Rutile TiO <sub>2</sub> /Anatase TiO <sub>2</sub> Heterostructure and Its Application in Visible-Light Photocatalysis. <b>2010</b> , 114, 3627-3633	132
1629	Titania-water interactions: a review of theoretical studies. <b>2010</b> , 20, 10319	228
1628	Self-organized TiO <sub>2</sub> Nanotube Arrays: Critical Effects on Morphology and Growth. <b>2010</b> , 50, 453-467	79
1627	Photocatalytic treatment of a dye solution using immobilized TiO <sub>2</sub> nanoparticles combined with photoelectro-Fenton process: Optimization of operational parameters. <b>2010</b> , 648, 143-150	85
1626	Photocatalytic degradation of 1-naphthol by oxide ceramics with added bacterial disinfection. <b>2010</b> , 181, 708-15	26
1625	Pillaring and photocatalytic properties of mesoporous Fe <sub>2</sub> O <sub>3</sub> /titanate nanocomposites via an exfoliation and restacking route. <b>2010</b> , 71, 841-847	20
1624	Photocatalytic O <sub>2</sub> evolution performances of Cd <sub>1-x</sub> In <sub>2x</sub> S <sub>x</sub> O <sub>4</sub> (x=0.1, 0.3, 0.5, 0.7, 1.0) conducting oxides. <b>2010</b> , 71, 880-883	3
1623	Kinetics of Ag/TiO <sub>2</sub> -photocatalyzed iodide ion oxidation. <b>2010</b> , 141, 529-537	11
1622	Large scale photochemical synthesis of M@TiO <sub>2</sub> nanocomposites (M = Ag, Pd, Au, Pt) and their optical properties, CO oxidation performance, and antibacterial effect. <b>2010</b> , 3, 244-255	223

1621	Solar photocatalytic decomposition of two azo dyes on multi-walled carbon nanotubes (MWCNTs)/TiO <sub>2</sub> composites. <b>2010</b> , 4, 311-320	7
1620	The Synergistic Effects of Two Co-catalysts on Zn <sub>2</sub> GeO <sub>4</sub> on Photocatalytic Water Splitting. <b>2010</b> , 134, 78-86	100
1619	Ion exchanged potassium titanoniobate as photocatalyst under visible light. <b>2010</b> , 24, 110-114	11
1618	Comparison of magnetic-nanometer titanium dioxide/ferriferous oxide (TiO <sub>2</sub> /Fe <sub>3</sub> O <sub>4</sub> ) composite photocatalyst prepared by acid-sol and homogeneous precipitation methods. <b>2010</b> , 45, 6018-6024	34
1617	Water Adsorption on TiO <sub>2</sub> . <b>2010</b> , 53, 423-430	91
1616	Photomineralization of phenol on Al <sub>2</sub> O <sub>3</sub> : synergistic photocatalysis by semiconductors. <b>2010</b> , 36, 361-371	12
1615	Preparation and characterization of antimicrobial Ce-doped ZnO nanoparticles for photocatalytic detoxification of cyanide. <b>2010</b> , 123, 585-594	145
1614	Hydrogen loading of oxide powder particles: a transmission IR study for the case of zinc oxide. <b>2010</b> , 11, 3604-7	34
1613	Dilute doping, defects, and ferromagnetism in metal oxide systems. <b>2010</b> , 22, 3125-55	325
1612	Fundamental Reactions on Rutile TiO <sub>2</sub> (110) Model Photocatalysts Studied by High-Resolution Scanning Tunneling Microscopy. 91-122	1
1611	Fourier-Transform Infrared and Raman Spectroscopy of Pure and Doped TiO <sub>2</sub> Photocatalysts. 189-238	0
1610	Correlation of the catalytic activity for oxidation taking place on various TiO <sub>2</sub> surfaces with surface OH groups and surface oxygen vacancies. <b>2010</b> , 16, 1202-11	92
1609	Voltage-Induced Payload Release and Wettability Control on TiO <sub>2</sub> and TiO <sub>2</sub> Nanotubes. <b>2010</b> , 122, 361-364	15
1608	Voltage-induced payload release and wettability control on TiO <sub>2</sub> and TiO <sub>2</sub> nanotubes. <b>2010</b> , 49, 351-4	102
1607	Role of Cl <sup>-</sup> ions in photooxidation of propylene on TiO <sub>2</sub> surface. <b>2010</b> , 256, 2132-2137	14
1606	Facile synthesis of TiO <sub>2</sub> (B) crystallites/nanopores structure: a highly efficient photocatalyst. <b>2010</b> , 350, 417-20	7
1605	Enhanced phenol-photodegradation by particulate semiconductor mixtures: interparticle electron-jump. <b>2010</b> , 176, 799-806	48
1604	Nonaqueous seeded growth of flower-like mixed-phase titania nanostructures for photocatalytic applications. <b>2010</b> , 183, 1917-1924	28



1603	Lanthanide absorption spectral probe in titania nanoparticles synthesized by ultrasonic assistant sol-gel method. <b>2010</b> , 71, 971-975	1
1602	Enhancement of photocatalytic oxidation of oxalic acid by gold modified WO <sub>3</sub> /TiO <sub>2</sub> photocatalysts under UV and visible light irradiation. <b>2010</b> , 327, 51-57	124
1601	Artificial neural networks modeling of contaminated water treatment processes by homogeneous and heterogeneous nanocatalysis. <b>2010</b> , 331, 86-100	129
1600	High performance nano-titania photocatalytic paper composite. Part I: Experimental design study for TiO <sub>2</sub> composite sheet using a natural zeolite microparticle system and its photocatalytic property. <b>2010</b> , 166, 127-131	26
1599	ERD analysis and modification of TiO <sub>2</sub> thin films with heavy ions. <b>2010</b> , 268, 1893-1898	47
1598	Immobilization of TiO <sub>2</sub> nanoparticles on activated carbon fiber and its photodegradation performance for organic pollutants. <b>2010</b> , 8, 272-278	89
1597	Photo-electro catalytic oxidation of aromatic alcohols on visible light-absorbing nitrogen-doped TiO <sub>2</sub> . <b>2010</b> , 55, 7788-7795	38
1596	The influence of pressure on the structure and the self-cleaning properties of sputter deposited TiO <sub>2</sub> layers. <b>2010</b> , 518, 4242-4246	23
1595	Photocatalytic activity of N, S co-doped and N-doped commercial anatase TiO <sub>2</sub> powders towards phenol oxidation and E. coli inactivation under simulated solar light irradiation. <b>2010</b> , 84, 37-43	142
1594	Solar-powered potentially induced TiO <sub>2</sub> , ZnO and SnO <sub>2</sub> -catalyzed iodine generation. <b>2010</b> , 94, 900-906	13
1593	Photocatalytic activity of poly(3-hexylthiophene)/titanium dioxide composites for degrading methyl orange. <b>2010</b> , 94, 1658-1664	73
1592	Facile synthesis and photocatalytic activity of ZnO@CuO nanocomposite. <b>2010</b> , 47, 615-623	201
1591	Dissociative and molecular oxygen chemisorption channels on reduced rutile TiO <sub>2</sub> (110): An STM and TPD study. <b>2010</b> , 604, 1945-1960	116
1590	Effect of applied potential on photocatalytic phenol degradation using nanocrystalline TiO <sub>2</sub> electrodes. <b>2010</b> , 93, 205-211	49
1589	Design of mesostructured H <sub>3</sub> PW <sub>12</sub> O <sub>40</sub> /titania materials with controllable structural orderings and pore geometries and their simulated sunlight photocatalytic activity towards diethyl phthalate degradation. <b>2010</b> , 99, 364-375	54
1588	Photocatalytic activity of La <sub>2</sub> O <sub>3</sub> -modified silver vanadates catalyst for Rhodamine B dye degradation under visible light irradiation. <b>2010</b> , 160, 33-41	81
1587	Photocatalytic degradation of phenol by base metal-substituted orthovanadates. <b>2010</b> , 161, 136-145	22
1586	Decontamination of textile wastewater via TiO <sub>2</sub> /activated carbon composite materials. <b>2010</b> , 159, 130-43	89

1585	Probing the electronic structure of early transition metal oxide clusters: Molecular models towards mechanistic insights into oxide surfaces and catalysis. <b>2010</b> , 500, 185-195	90
1584	Nanosized N-doped TiO <sub>2</sub> and gold modified semiconductors [photocatalysts for combined UV-visible light destruction of oxalic acid in aqueous solution. <i>Desalination</i> , <b>2010</b> , 260, 101-106	103 44
1583	Study of erbium (III) doped titanium dioxide nanoparticles by photoacoustic spectroscopy. <b>2010</b> , 28, 211-214	7
1582	Preparation and photocatalytic activity of B, Y co-doped nanosized TiO <sub>2</sub> catalyst. <b>2010</b> , 28, 737-741	14
1581	Self-organized TiO <sub>2</sub> nanotubes: Factors affecting their morphology and properties. <b>2010</b> , 247, 2424-2435	72
1580	Structure and properties of nitrogen-doped titanium dioxide thin films produced by reactive magnetron sputtering. <b>2010</b> , 42, 970-973	16
1579	Combining degradation and contact angle data in assessing the photocatalytic TiO <sub>2</sub> :N surface. <b>2010</b> , 42, 947-954	13
1578	Electron diffractive imaging of oxygen atoms in nanocrystals at sub-ångström resolution. <b>2010</b> , 5, 360-5	53
1577	In Situ Preparation of TiO <sub>2</sub> Composite Layer upon Ti Alloy Substrate Using Micro-Arc Oxidation and its Photocatalytic Property. <b>2010</b> , 663-665, 3-11	1
1576	Electrochemical and photocatalytic properties of TiO <sub>2</sub> /WO <sub>3</sub> photoelectrodes. <b>2010</b> ,	1
1575	An Overview of Semi-Conductor Photocatalysis: Modification of TiO <sub>2</sub> Nanomaterials. <b>2010</b> , 162, 239-260	57
1574	UV-A and Solar Photodegradation of Ibuprofen and Carbamazepine Catalyzed by TiO <sub>2</sub> . <b>2010</b> , 45, 1564-1570	71
1573	Electrochemical Fabrication of TiO <sub>2</sub> /Au Nanocomposites. <b>2010</b> , 157, D5	4
1572	New Photocatalyst Electrodes and Their Photocatalytic Degradation Properties of Organics. <b>2010</b> , 14, 709-727	4
1571	Intrinsic defects and their influence on the chemical and optical properties of TiO <sub>2</sub> films. <b>2010</b> , 43, 485402	42
1570	Nature of Defect States in Nitrogen-Doped MgO. <b>2010</b> , 114, 1350-1356	33
1569	Self-doped Ti <sup>3+</sup> enhanced photocatalyst for hydrogen production under visible light. <b>2010</b> , 132, 11856-7	1038
1568	Development of modified N doped TiO <sub>2</sub> photocatalyst with metals, nonmetals and metal oxides. <b>2010</b> , 3, 715	543

1567	Modelling nano-clusters and nucleation. <b>2010</b> , 12, 786-811	160
1566	Ab Initio Study of the Interaction of Dimethyl Methylphosphonate with Rutile (110) and Anatase (101) TiO <sub>2</sub> Surfaces. <b>2010</b> , 114, 3063-3074	33
1565	Electron-Transfer Reaction of Oxygen Species on TiO <sub>2</sub> Nanoparticles Induced by Sub-band-gap Illumination. <b>2010</b> , 114, 1240-1245	106
1564	Surface properties and electronic structure of low-index stoichiometric anatase TiO(2) surfaces. <b>2010</b> , 22, 175008	42
1563	Deep versus Shallow Behavior of Intrinsic Defects in Rutile and Anatase TiO <sub>2</sub> Polymorphs. <b>2010</b> , 114, 21694-21704	126
1562	Biocompatible Anatase Single-Crystal Photocatalysts with Tunable Percentage of Reactive Facets. <b>2010</b> , 10, 1130-1137	113
1561	The Effect of Addition of Pt on the Gas Phase Photocatalysis over TiO <sub>2</sub> . <b>2010</b> , 479-501	1
1560	Electronic and Optical Properties of Doped and Undoped (TiO <sub>2</sub> ) <sub>n</sub> Nanoparticles. <b>2010</b> , 114, 17333-17343	92
1559	Bacterial Synthesis of Photocatalytically Active and Biocompatible TiO <sub>2</sub> and ZnO Nanoparticles. <b>2010</b> , 2, P80-P99	9
1558	Thermal chemistry and photochemistry of hexafluoroacetone on rutile TiO <sub>2</sub> (110). <b>2010</b> , 12, 8084-91	16
1557	Acetone Adsorption on Oxidized and Reduced TiO <sub>2</sub> (110): A Scanning Tunneling Microscope Study. <b>2010</b> , 114, 14579-14582	13
1556	Stability and dynamics of carbon and nitrogen dopants in anatase TiO <sub>2</sub> : A density functional theory study. <b>2010</b> , 81,	36
1555	Direct Observation of Surface-Mediated Electron-Hole Pair Recombination in TiO <sub>2</sub> (110). <b>2010</b> , 114, 3098-3101	95
1554	Synthesis of activated carbon-surrounded and carbon-doped anatase TiO <sub>2</sub> nanocomposites. <b>2010</b> , 20, 5682	47
1553	Unraveling the Diffusion of Bulk Ti Interstitials in Rutile TiO <sub>2</sub> (110) by Monitoring Their Reaction with O Adatoms. <b>2010</b> , 114, 3059-3062	79
1552	Enhanced Bonding of Silver Nanoparticles on Oxidized TiO <sub>2</sub> (110) <b>2010</b> , 114, 16964-16972	20
1551	Photosensitized Solid-state Polymerization of Diacetylenes in Nanoporous TiO <sub>2</sub> Structures. <b>2010</b> , 47, 1161-1166	5
1550	Band Gap Narrowing versus Formation of Electronic States in the Gap in N-doped TiO <sub>2</sub> Thin Films. <b>2010</b> , 114, 22546-22557	29

1549	Synthesis and Photocatalytic Activities of NaNbO <sub>3</sub> Rods Modified by In <sub>2</sub> O <sub>3</sub> Nanoparticles. <b>2010</b> , 114, 6157-6162		147
1548	Hydrolysis of TiCl <sub>4</sub> : initial steps in the production of TiO <sub>2</sub> . <b>2010</b> , 114, 7561-70		90
1547	Visible-light-driven Cu(II)-(Sr(1-y)Na(y))(Ti(1-x)Mo(x))O <sub>3</sub> photocatalysts based on conduction band control and surface ion modification. <b>2010</b> , 132, 15259-67		178
1546	Electron-mediated CO oxidation on the TiO <sub>2</sub> (110) surface during electronic excitation. <b>2010</b> , 132, 12804-7		46
1545	A potential site for trapping photogenerated holes on rutile TiO <sub>2</sub> surface as revealed by EPR spectroscopy: an avenue for enhancing photocatalytic activity. <b>2010</b> , 132, 10982-3		31
1544	Off-Normal CO <sub>2</sub> Desorption from the Photooxidation of CO on Reduced TiO <sub>2</sub> (110). <i>Journal of Physical Chemistry Letters</i> , <b>2010</b> , 1, 2508-2513	6.4	47
1543	IR Spectroscopic Measurement of Diffusion Kinetics of Chemisorbed Pyridine through TiO <sub>2</sub> Particles. <b>2010</b> , 114, 16649-16659		17
1542	Nanosheet-Based Bi <sub>2</sub> MoxW <sub>1-x</sub> O <sub>6</sub> Solid Solutions with Adjustable Band Gaps and Enhanced Visible-Light-Driven Photocatalytic Activities. <b>2010</b> , 114, 18812-18818		77
1541	Solar Light and Dopant-Induced Recombination Effects: Photoactive Nitrogen in TiO <sub>2</sub> as a Case Study. <b>2010</b> , 114, 18067-18072		51
1540	Photochemistry of 1,1,1-Trifluoroacetone on Rutile TiO <sub>2</sub> (110) □ <b>2010</b> , 114, 16900-16908		14
1539	Adsorption of CO on Rutile TiO <sub>2</sub> (110)-1 □ Surface with Preadsorbed O Adatoms. <b>2010</b> , 114, 18222-18227		35
1538	Titania-based photocatalysts □ crystal growth, doping and heterostructuring. <b>2010</b> , 20, 831-843		953
1537	Single-molecule, single-particle fluorescence imaging of TiO <sub>2</sub> -based photocatalytic reactions. <b>2010</b> , 39, 4802-19		142
1536	Supported silver nanoparticles as photocatalysts under ultraviolet and visible light irradiation. <b>2010</b> , 12, 414		242
1535	Charge Separation and Trapping in N-Doped TiO <sub>2</sub> Photocatalysts: A Time-Resolved Microwave Conductivity Study. <i>Journal of Physical Chemistry Letters</i> , <b>2010</b> , 1, 3261-3265	6.4	86
1534	Reactive and Organosoluble Anatase Nanoparticles by a Surfactant-Free Nonhydrolytic Synthesis. <b>2010</b> , 22, 4519-4521		26
1533	Visible-light absorption and photocatalytic activity in molybdenum- and nitrogen-codoped TiO <sub>2</sub> . <b>2010</b> , 11, 331-335		62
1532	Photocatalytic hydrogenation of acetophenone derivatives and diaryl ketones on polycrystalline titanium dioxide. <b>2010</b> , 11, 1049-1053		46

1531	Adjusting the Crystal Phase and Morphology of Titania via a Soft Chemical Process. <b>2010</b> , 10, 2185-2191	22
1530	Effect of fluorination on the surface properties of titania P25 powder: an FTIR study. <b>2010</b> , 26, 2521-7	103
1529	Advances in computational studies of energy materials. <b>2010</b> , 368, 3379-456	110
1528	Systematic Control of Monoclinic CdWO <sub>4</sub> Nanophase for Optimum Photocatalytic Activity. <b>2010</b> , 114, 1512-1519	80
1527	Nanoassemblies for photovoltaic applications. <b>2010</b> ,	
1526	Wetting properties of polycrystalline TiO <sub>2</sub> surfaces: a scaling approach to the roughness factors. <b>2010</b> , 26, 15875-82	35
1525	Photoinduced charge transfer in ZnO/Cu(2)O heterostructure films studied by surface photovoltage technique. <b>2010</b> , 12, 15476-81	116
1524	Photoinduced Dissociation of O <sub>2</sub> on Rutile TiO <sub>2</sub> (110). <i>Journal of Physical Chemistry Letters</i> , <b>2010</b> , 1, 17586, 1762-73	
1523	Synthesis, Characterization, and Photocatalytic Activities of Nanoparticulate N, S-Codoped TiO <sub>2</sub> Having Different Surface-to-Volume Ratios. <b>2010</b> , 114, 2717-2723	93
1522	EPR characterization and reactivity of surface-localized inorganic radicals and radical ions. <i>Chemical Reviews</i> , <b>2010</b> , 110, 1320-47	68.1 145
1521	Vibrational Spectroscopic Observation of Weakly Bound Adsorbed Molecular Oxygen on Powdered Titanium Dioxide. <b>2010</b> , 114, 11924-11930	27
1520	Design of self-cleaning TiO <sub>2</sub> coating on clay roofing tiles. <b>2010</b> , 90, 2989-3002	23
1519	Decreasing the oxidative potential of TiO <sub>2</sub> nanoparticles through modification of the surface with carbon: a new strategy for the production of safe UV filters. <b>2010</b> , 46, 8478-80	38
1518	Diffusion of oxygen vacancies on a strained rutile TiO <sub>2</sub> (110) surface. <b>2010</b> , 82,	23
1517	Peroxide and superoxide states of adsorbed O(2) on anatase TiO(2) (101) with subsurface defects. <b>2010</b> , 12, 12956-60	115
1516	Monitoring electronic structure changes of TiO <sub>2</sub> (110) via sign reversal of adsorbate vibrational bands. <b>2010</b> , 12, 3649-52	28
1515	Nitrogen/gold codoping of the TiO <sub>2</sub> (101) anatase surface. A theoretical study based on DFT calculations. <b>2011</b> , 13, 11340-50	34
1514	Hierarchical Bi <sub>2</sub> O <sub>2</sub> CO <sub>3</sub> microspheres with improved visible-light-driven photocatalytic activity. <b>2011</b> , 13, 4010	155

1513	Enhancement of visible light photocatalysis by grafting ZnO nanoplatelets with exposed (0001) facets onto a hierarchical substrate. <b>2011</b> , 47, 10797-9	81
1512	EDTA-mediated shape-selective synthesis of Bi <sub>2</sub> WO <sub>6</sub> hierarchical self-assemblies with high visible-light-driven photocatalytic activities. <b>2011</b> , 13, 7267	76
1511	The nitrogen-boron paramagnetic center in visible light sensitized N-B co-doped TiO <sub>2</sub> . Experimental and theoretical characterization. <b>2011</b> , 13, 136-43	47
1510	Urea derivatives enhance the photocatalytic activity of dye-modified titanium dioxide. <b>2011</b> , 10, 623-5	29
1509	Single-crystalline and reactive facets exposed anatase TiO <sub>2</sub> nanofibers with enhanced photocatalytic properties. <b>2011</b> , 21, 6718	30
1508	Biogenic N-I-codoped TiO <sub>2</sub> photocatalyst derived from kelp for efficient dye degradation. <b>2011</b> , 4, 172-180	103
1507	Bandgap narrowing of titanium oxide nanosheets: homogeneous doping of molecular iodine for improved photoreactivity. <b>2011</b> , 21, 14672	27
1506	Synthesis and photocatalytic activity of undoped and doped TiO <sub>2</sub> nanopowders. <b>2011</b> ,	
1505	Understanding Acetaldehyde Thermal Chemistry on the TiO <sub>2</sub> (110) Rutile Surface: From Adsorption to Reactivity. <b>2011</b> , 115, 2819-2825	20
1504	N <sub>3</sub> -dye-induced visible laser anatase-to-rutile phase transition on mesoporous TiO <sub>2</sub> films. <b>2011</b> , 27, 9094-9	15
1503	CO <sub>2</sub> Adsorption, Diffusion, and Electron-Induced Chemistry on Rutile TiO <sub>2</sub> (110): A Low-Temperature Scanning Tunneling Microscopy Study. <b>2011</b> , 115, 12095-12105	48
1502	Shallow Electron Trap, Interfacial Water, and Outer-Sphere Adsorbed Oxalate IR Absorptions Correlate during UV Irradiation of Photocatalytic TiO <sub>2</sub> Films in Aqueous Solution <b>2011</b> , 115, 902-907	27
1501	Molecular oxygen adsorption behaviors on the rutile TiO <sub>2</sub> (110)-1 $\bar{1}$ surface: an in situ study with low-temperature scanning tunneling microscopy. <b>2011</b> , 133, 2002-9	135
1500	Potential-dependent recombination kinetics of photogenerated electrons in n- and p-type GaN photoelectrodes studied by time-resolved IR absorption spectroscopy. <b>2011</b> , 133, 11351-7	42
1499	Interaction of CO with Oxygen Adatoms on TiO <sub>2</sub> (110). <b>2011</b> , 115, 4163-4167	21
1498	A Finite Cluster Approach to an Extended Transition Metal Oxide: A Wave Function Based Study. <b>2011</b> , 115, 17540-17557	10
1497	Hydrolysis and Complexation of N,N-Dimethylformamide in New Nanostructured Titanium Oxide Hybrid Organic-Inorganic Sols and Gel. <b>2011</b> , 115, 12269-12274	55
1496	CdS and CdTeS quantum dot decorated TiO <sub>2</sub> nanowires. Synthesis and photoefficiency. <b>2011</b> , 22, 065603	24

1495	Direct evidence for ethanol dissociation on rutile TiO <sub>2</sub> (110). <b>2011</b> , 107, 136102	53
1494	Photogenerated defects in shape-controlled TiO <sub>2</sub> anatase nanocrystals: a probe to evaluate the role of crystal facets in photocatalytic processes. <b>2011</b> , 133, 17652-61	288
1493	Tuning the relative concentration ratio of bulk defects to surface defects in TiO <sub>2</sub> nanocrystals leads to high photocatalytic efficiency. <b>2011</b> , 133, 16414-7	830
1492	Increasing solar absorption for photocatalysis with black hydrogenated titanium dioxide nanocrystals. <b>2011</b> , 331, 746-50	4625
1491	Photocatalytic Degradation of Methyl Orange Using Nanosized TiO <sub>2</sub> Photocatalyst Doped with Cerium. <b>2011</b> ,	
1490	Preparation and photocatalytic activity of eccentric Au-titania core-shell nanoparticles by block copolymer templates. <b>2011</b> , 13, 2809-14	26
1489	Controllable Morphology of Engelhard Titanium Silicates ETS-4: Synthetic, Photocatalytic, and Calorimetric Studies. <b>2011</b> , 23, 1166-1173	8
1488	Structural Defects in W-Doped TiO <sub>2</sub> (101) Anatase Surface: Density Functional Study. <b>2011</b> , 115, 16970-16976	31
1487	An experimental study of OH solubility in rutile at 500-800 °C, 0.5-2 GPa, and a range of oxygen fugacities. <b>2011</b> , 96, 1291-1299	13
1486	Synthesis and photocatalytic activity of iodine-doped ZnO nanoflowers. <b>2011</b> , 21, 10982	61
1485	STM studies of single molecules: molecular orbital aspects. <b>2011</b> , 47, 2747-62	8
1484	Visible light photoactivity from a bonding assembly of titanium oxide nanocrystals. <b>2011</b> , 47, 4219-21	39
1483	Oxygen Photochemistry on TiO <sub>2</sub> (110): Recyclable, Photoactive Oxygen Produced by Annealing Adsorbed O <sub>2</sub> . <i>Journal of Physical Chemistry Letters</i> , <b>2011</b> , 2, 2790-2796	6.4 36
1482	Advanced Oxidation Processes. <b>2011</b> , 377-408	31
1481	Mapping the photocatalytic activity or potential free radical toxicity of nanoscale titania. <b>2011</b> , 4, 439-443	10
1480	Electric Charge of Single Au Atoms Adsorbed on TiO <sub>2</sub> (110) and Associated Band Bending. <b>2011</b> , 115, 23848-23853	33
1479	Mechanism of O <sub>2</sub> Production from Water Splitting: Nature of Charge Carriers in Nitrogen Doped Nanocrystalline TiO <sub>2</sub> Films and Factors Limiting O <sub>2</sub> Production. <b>2011</b> , 115, 3143-3150	111
1478	Modification of Metal Nanoparticles with TiO <sub>2</sub> and Metal-Support Interaction in Photodeposition. <i>ACS Catalysis</i> , <b>2011</b> , 1, 187-192	13.1 64

1477	Constructing WO <sub>3</sub> /TiO <sub>2</sub> composite structure towards sufficient use of solar energy. <b>2011</b> , 47, 4231-3	76
1476	Catalysis by Supported Gold Nanoparticles. <b>2011</b> , 1-11	2
1475	On the Nature of Reduced States in Titanium Dioxide As Monitored by Electron Paramagnetic Resonance. I: The Anatase Case. <b>2011</b> , 115, 25413-25421	122
1474	The Annealing Effect on the Microstructures and Phase Transformation of the TiO <sub>2</sub> Layer in ZnO/TiO <sub>2</sub> Core/Shell Nanostructures. <b>2011</b> , 11, 367-371	14
1473	Synthesis of high-reactive facets dominated anatase TiO <sub>2</sub> . <b>2011</b> , 21, 7052	223
1472	BACK MATTER. <b>2011</b> , 132-196	
1471	BiO <sub>2</sub> COOH hierarchical nanostructures: Shape-controlled solvothermal synthesis and photocatalytic degradation performances. <b>2011</b> , 13, 2381	82
1470	Pillared Nanocomposite TiO <sub>2</sub> /Bi-Doped Hexaniobate with Visible-Light Photocatalytic Activity. <b>2011</b> , 115, 6531-6539	65
1469	Role of Fe doping in tuning the band gap of TiO <sub>2</sub> for the photo-oxidation-induced cytotoxicity paradigm. <b>2011</b> , 133, 11270-8	290
1468	Surface-modification of TiO <sub>2</sub> with new metalloporphyrins and their photocatalytic activity in the degradation of 4-nitrophenol. <b>2011</b> , 258, 940-945	45
1467	Chemical etching preparation of BiOI/Bi <sub>2</sub> O <sub>3</sub> heterostructures with enhanced photocatalytic activities. <b>2011</b> , 12, 660-664	156
1466	Effect of Si doping on the photocatalytic activity and photoelectrochemical property of TiO <sub>2</sub> nanoparticles. <b>2011</b> , 13, 14-17	40
1465	Stable TiO <sub>2</sub> /ractorite: Preparation, characterization and photocatalytic activity. <b>2011</b> , 51, 335-340	49
1464	Density functional theory study of dopants in polycrystalline TiO <sub>2</sub> . <b>2011</b> , 83,	30
1463	Configurations, electronic properties, and diffusion of carbon and nitrogen dopants in rutile TiO <sub>2</sub> : A density functional theory study. <b>2011</b> , 84,	14
1462	Electron transfer between colloidal ZnO nanocrystals. <b>2011</b> , 133, 4228-31	43
1461	Micro-arc oxidation of TC4 substrates to fabricate TiO <sub>2</sub> /YAG:Ce <sup>3+</sup> compound films with enhanced photocatalytic activity. <i>Journal of Alloys and Compounds</i> , <b>2011</b> , 509, L137-L141	5-7 32
1460	Size and shape dependence of the photocatalytic activity of TiO <sub>2</sub> nanocrystals: a total scattering Debye function study. <b>2011</b> , 133, 3114-9	95



1459	The importance of bulk Ti <sup>3+</sup> defects in the oxygen chemistry on titania surfaces. <b>2011</b> , 133, 6529-32	179
1458	TiO <sub>2</sub> -B/anatase core-shell heterojunction nanowires for photocatalysis. <b>2011</b> , 3, 4444-50	149
1457	Cu(II) Oxide Amorphous Nanoclusters Grafted Ti <sup>3+</sup> Self-Doped TiO <sub>2</sub> : An Efficient Visible Light Photocatalyst. <b>2011</b> , 23, 5282-5286	232
1456	Photocatalytic Activities of Different Well-defined Single Crystal TiO <sub>2</sub> Surfaces: Anatase versus Rutile. <i>Journal of Physical Chemistry Letters</i> , <b>2011</b> , 2, 2461-2465	6.4 140
1455	Evidence for crystal-face-dependent TiO <sub>2</sub> photocatalysis from single-molecule imaging and kinetic analysis. <b>2011</b> , 133, 7197-204	511
1454	TiO <sub>2</sub> Photocatalysis for the Redox Conversion of Aquatic Pollutants. <i>ACS Symposium Series</i> , <b>2011</b> , 199-2224	14
1453	Rutile nanowire arrays: tunable surface densities, wettability and photochemistry. <b>2011</b> , 21, 15806	15
1452	Theoretical Study of Adsorption of Ag Clusters on the Anatase TiO <sub>2</sub> (100) Surface. <b>2011</b> , 115, 17368-17377	49
1451	Distribution of Ti <sup>3+</sup> Surface Sites in Reduced TiO <sub>2</sub> . <b>2011</b> , 115, 7562-7572	204
1450	Fast Synthesis of Highly Dispersed Anatase TiO <sub>2</sub> Nanocrystals in a Microfluidic Reactor. <b>2011</b> , 40, 1371-1373	8
1449	Photocatalytic removal of nitrogen oxides from air on TiO <sub>2</sub> modified with bases and platinum. <b>2011</b> , 52, 518-524	3
1448	Photocatalytic activity of Ho-doped anatase titanium dioxide coated magnetite. <b>2011</b> , 87, 626-31	10
1447	Formation of single-crystalline rutile TiO <sub>2</sub> splitting microspheres for dye-sensitized solar cells. <b>2011</b> , 85, 2697-2703	18
1446	Structure differences between TiO <sub>2</sub> and phosphorus implanted TiO <sub>2</sub> films caused by thermal treatment. <b>2011</b> , 206, 1024-1028	5
1445	Determination of photo-catalytic activity of un-doped and Mn-doped TiO <sub>2</sub> anatase powders on acetaldehyde under UV and visible light. <b>2011</b> , 520, 1195-1201	66
1444	Ag <sub>0</sub> -loaded brookite/anatase composite with enhanced photocatalytic performance towards the degradation of methyl orange. <b>2011</b> , 348, 114-119	27
1443	Thermally stable and photocatalytically active titania for ceramic surfaces. <b>2011</b> , 31, 2887-2896	16
1442	Preparation and characterization of visible-light-driven europium doped mesoporous titania photocatalyst. <b>2011</b> , 29, 929-933	16

1441	Efficient photo-degradation of 4-nitrophenol by using new CuPp-TiO <sub>2</sub> photocatalyst under visible light irradiation. <b>2011</b> , 16, 90-93		44
1440	Electron- and Hole-Mediated Reactions in UV-Irradiated O <sub>2</sub> Adsorbed on Reduced Rutile TiO <sub>2</sub> (110). <b>2011</b> , 115, 152-164		60
1439	Bulk and Surface Polarons in Photoexcited Anatase TiO <sub>2</sub> . <i>Journal of Physical Chemistry Letters</i> , <b>2011</b> , 2, 2223-2228	6.4	191
1438	Plasmonic photosensitization of a wide band gap semiconductor: converting plasmons to charge carriers. <b>2011</b> , 11, 5548-52		345
1437	Review on modified TiO <sub>2</sub> photocatalysis under UV/visible light: selected results and related mechanisms on interfacial charge carrier transfer dynamics. <b>2011</b> , 115, 13211-41		1497
1436	Photocatalytic oxidation of organic dyes with nanostructured zinc dioxide modified with silver metals. <b>2011</b> , 85, 1416-1422		11
1435	Characterization, activity and mechanisms of a visible light driven photocatalyst: Manganese and iron co-modified TiO <sub>2</sub> nanoparticles. <b>2011</b> , 85, 1825-1831		14
1434	Synthesis and properties of TiO <sub>2</sub> -based nanomaterials. <b>2011</b> , 45, 731-738		5
1433	Photocatalytic Titanium Dioxide Nanostructures for Self-Regenerating Relative Humidity Sensors. <b>2011</b> , 11, 1713-1719		6
1432	Multiple aspects of the interaction of biomacromolecules with inorganic surfaces. <b>2011</b> , 63, 1186-209		129
1431	Synthesis and characterization of nanocrystalline TiO <sub>2</sub> thin films. <b>2011</b> , 22, 260-264		22
1430	Preparation and characterization of mesoporous TiO <sub>2</sub> -pillared titanate photocatalyst. <b>2011</b> , 18, 185-193		13
1429	Synthesis, Characterization and Photocatalytic Performance of TiO <sub>2</sub> Codoped with Bismuth and Nitrogen. <b>2011</b> , 141, 1371-1377		20
1428	Photocatalytic mechanisms of modified titania under visible light. <b>2011</b> , 37, 91-102		58
1427	Complete oxidation of egg albumin on photoirradiated TiO <sub>2</sub> : factors determining catalytic performance in solid-solid heterogeneous systems. <b>2011</b> , 37, 587-598		1
1426	Synthesis, characterization and photocatalytic properties of tungsten-doped hydrothermal TiO <sub>2</sub> . <b>2011</b> , 57, 43-50		18
1425	Effect of silver incorporation on crystallization and microstructural properties of sol-gel derived titania thin films on glass. <b>2011</b> , 58, 277-289		22
1424	Sol-gel and impregnated prepared silver TiO <sub>2</sub> semiconductors as photocatalysts for the UV decomposition of 2,4-d: a comparative study of the preparation method. <b>2011</b> , 59, 57-62		7

1423	Photocatalytic Decomposition of Synthetic Alizarin Red S by Nickel Doped TiO <sub>2</sub> . <b>2011</b> , 54, 490-495	11
1422	Photoelectrochemical Hydrogen Production from Aqueous Solution Containing Cyanide Using Bi <sub>2</sub> MnNbO <sub>7</sub> (M = Al, Fe, Ga, In) Films on Stainless Steel as Photoanodes. <b>2011</b> , 54, 244-249	9
1421	Mechanistic pathways differences between P25-TiO(2) and Pt-TiO(2) mediated CV photodegradation. <b>2011</b> , 185, 227-35	89
1420	Microemulsion-mediated solvothermal synthesis and photocatalytic properties of crystalline titania with controllable phases of anatase and rutile. <b>2011</b> , 192, 651-7	51
1419	Integrating efficient filtration and visible-light photocatalysis by loading Ag-doped zeolite Y particles on filtration membrane of alumina nanofibers. <b>2011</b> , 375, 69-74	25
1418	TiO <sub>2</sub> nanocrystals grafted on macroporous silica: A novel hybrid organic/inorganic sol-gel approach for the synthesis of highly photoactive composite material. <b>2011</b> , 104, 282-290	27
1417	A surface science perspective on TiO <sub>2</sub> photocatalysis. <b>2011</b> , 66, 185-297	1592
1416	Anti-fingerprints fluorinated coating for anodized titanium avoiding color alteration. <b>2011</b> , 8, 153-160	16
1415	Visible light photocatalytic properties of novel molybdenum treated carbon nanotube/titania composites. <b>2011</b> , 34, 543-549	3
1414	Synthesis and photocatalytic properties of lanthanum doped anatase TiO <sub>2</sub> coated Fe <sub>3</sub> O <sub>4</sub> composites. <b>2011</b> , 30, 252-257	19
1413	A review of TiO <sub>2</sub> nanoparticles. <b>2011</b> , 56, 1639-1657	798
1412	Solar photocatalytic detoxification of cyanide by different forms of TiO <sub>2</sub> . <b>2011</b> , 28, 1214-1220	12
1411	Temperature-dependent grain growth and phase transformation in mixed anatase-rutile nanocrystalline TiO <sub>2</sub> films. <b>2011</b> , 208, 1635-1640	6
1410	Control Over the Crystallinity and Defect Chemistry of YVO <sub>4</sub> Nanocrystals for Optimum Photocatalytic Property. <b>2011</b> , 2011, 2211-2220	48
1409	Probing the Local Environment of Ti <sup>3+</sup> Ions in TiO <sub>2</sub> (Rutile) by 17O HYSCORE. <b>2011</b> , 123, 8188-8190	4
1408	TiO <sub>2</sub> nanotubes: synthesis and applications. <b>2011</b> , 50, 2904-39	2393
1407	Probing the local environment of Ti <sup>3+</sup> ions in TiO <sub>2</sub> (rutile) by 17O HYSCORE. <b>2011</b> , 50, 8038-40	51
1406	The role of surface and subsurface point defects for chemical model studies on TiO <sub>2</sub> : a first-principles theoretical study of formaldehyde bonding on rutile TiO <sub>2</sub> (110). <b>2011</b> , 17, 4496-506	66

1405	Visible-light-induced dye degradation over copper-modified reduced graphene oxide. <b>2011</b> , 17, 2428-34	74
1404	On the reactions of methyl radicals with TiO <sub>2</sub> nanoparticles and granular powders immersed in aqueous solutions. <b>2011</b> , 17, 9226-31	13
1403	A family of visible-light responsive photocatalysts obtained by dispersing CrO <sub>6</sub> octahedra into a hydroxalcite matrix. <b>2011</b> , 17, 13175-81	79
1402	The application of titanium dioxide for deactivation of bioparticulates: An overview. <b>2011</b> , 169, 249-257	215
1401	Photochemical synthesis and photocatalytic activity in simulated solar light of nanosized Ag doped TiO <sub>2</sub> nanoparticle composite. <b>2011</b> , 42, 579-583	70
1400	Surface doping is more beneficial than bulk doping to the photocatalytic activity of vanadium-doped TiO <sub>2</sub> . <b>2011</b> , 101, 333-342	114
1399	BiOI-sensitized TiO <sub>2</sub> in phenol degradation: A novel efficient semiconductor sensitizer. <b>2011</b> , 508, 102-106	65
1398	Preparation of B, N-codoped nanotube arrays and their enhanced visible light photoelectrochemical performances. <b>2011</b> , 13, 121-124	46
1397	Preparation and characterization of TiO <sub>2</sub> /carbon composite thin films with enhanced photocatalytic activity. <b>2011</b> , 335, 136-144	23
1396	Influence of neodymium ions on photocatalytic activity of TiO <sub>2</sub> synthesized by sol-gel and precipitation methods. <b>2011</b> , 336, 58-63	33
1395	Heterogeneous photocatalysis of a dye solution using supported TiO <sub>2</sub> nanoparticles combined with homogeneous photoelectrochemical process: Molecular degradation products. <b>2011</b> ,	5
1394	Improvement in the methylene blue adsorption capacity and photocatalytic activity of H <sub>2</sub> -reduced rutile-TiO <sub>2</sub> caused by Ni(II)porphyrin preadsorption. <b>2011</b> ,	1
1393	Superhydrophilicity and photocatalytic enhancement of titania nano thin films. <b>2011</b> , 257, 3780-3785	23
1392	Photocatalytic and superhydrophilicity properties of N-doped TiO <sub>2</sub> nanothin films. <b>2011</b> , 257, 7179-7183	33
1391	Nanoparticulate silver coated-titania thin filmsPhoto-oxidative destruction of stearic acid under different light sources and antimicrobial effects under hospital lighting conditions. <b>2011</b> , 220, 113-123	64
1390	CdWO <sub>4</sub> polymorphs: Selective preparation, electronic structures, and photocatalytic activities. <b>2011</b> , 184, 357-364	61
1389	Preparation and photocatalytic activity of cerium doped anatase titanium dioxide coated magnetite composite. <b>2011</b> , 42, 652-657	56
1388	Preparation and photocatalytic activity of TiO <sub>2</sub> nanoparticles co-doped with Fe and La. <b>2011</b> , 9, 260-264	21

1387	New photocatalysts based on MIL-53 metal-organic frameworks for the decolorization of methylene blue dye. <b>2011</b> , 190, 945-51	336
1386	Development of visible light sensitive titania photocatalysts by combined nitrogen and silver doping. <b>2011</b> , 17, 358-363	26
1385	Fe-doped and ZnO-pillared titanates as visible-light-driven photocatalysts. <b>2011</b> , 358, 360-8	42
1384	Reliable and fast sensor for in vitro evaluation of solar protection factor based on the photobleaching kinetics of a nanocrystalline TiO <sub>2</sub> /dye UV-dosimeter. <b>2011</b> , 156, 325-331	3
1383	A study of stabilization of P3HT/PCBM organic solar cells by photochemical active TiO <sub>x</sub> layer. <b>2011</b> , 95, 1123-1130	47
1382	Single-step preparation, characterization and photocatalytic mechanism of mesoporous Fe-doped sulfated titania. <b>2011</b> , 605, 1281-1286	16
1381	Isotropic photo-decomposition of spherical organic polymers on rutile TiO <sub>2</sub> (110) surfaces. <b>2011</b> , 22, 155705	1
1380	Effects of Calcination Temperature on Photoreduction Activity of Cu/TiO <sub>2</sub> Nanoparticles. <b>2011</b> , 55-57, 1648-1652	
1379	Preparation of Silver-Doped TiO <sub>2</sub> Photoatylst via a Simple Sol-Hydrothermal and their Visible Light Photocatalytic Activity. <b>2011</b> , 694, 824-830	3
1378	Calcination Temperature Influence on the Microstructure and the Photocatalytic Properties of TiO <sub>2</sub> Pillared Rectorite. <b>2011</b> , 197-198, 790-795	
1377	Metal surface oxidation and surface interactions. <b>2011</b> , 102-142	5
1376	Photocatalytic Mechanism of Action of Apatite-Coated Ag/Agbr/Tio <sub>2</sub> on Phenol and Escherichia Coli and Bacillus Subtilis Bacteria Under Various Conditions. <b>2011</b> , 36, 38-52	15
1375	Study on photocatalytic activity of titania loaded on zeolite. <b>2011</b> ,	
1374	Photocatalytic Degradation of Organic Contaminants on Mineral Surfaces. <b>2011</b> , 91-111	1
1373	First principles theoretical study of the hole-assisted conversion of CO to CO <sub>2</sub> on the anatase TiO <sub>2</sub> (101) surface. <b>2011</b> , 134, 104701	34
1372	One-Step Nonaqueous Synthesis of Pure Phase TiO <sub>2</sub> Nanocrystals from TiCl <sub>4</sub> in Butanol and Their Photocatalytic Properties. <b>2011</b> , 2011, 1-6	4
1371	Photocatalytic Properties of Nanotubular-ShapedTiO <sub>2</sub> Powders with Anatase Phase Obtained from Titanate Nanotube Powder through Various Thermal Treatments. <b>2011</b> , 2011, 1-7	26
1370	Oxidative stress studies of six TiO <sub>2</sub> and two CeO <sub>2</sub> nanomaterials: immuno-spin trapping results with DNA. <b>2011</b> , 5, 546-56	19

- 1369 Synthesis of Anatase-Based Titania Nanostructures Using Extreme Hydrothermal Conditions. **2012**, 463-464, 1493-1496
- 1368 Synthesis of Ag, Pd-Loaded Bi<sub>2</sub>WO<sub>6</sub> and its Photocatalytic Activities. **2012**, 518-523, 833-836 5
- 1367 Study on the Dispersion of Nanometer TiO<sub>2</sub> Powder by Sol-Gel Method. **2012**, 599, 104-107
- 1366 Electron stimulated desorption, DIET, and photochemistry at surfaces: a personal recollection. **2012**, 137, 091701 3
- 1365 Helium mediated deposition: modeling the He-TiO<sub>2</sub>(110)-(1 $\bar{1}$ ) interaction potential and application to the collision of a helium droplet from density functional calculations. **2012**, 136, 124703 27
- 1364 Toward photochemistry of integrated heterogeneous systems. **2012**, 137, 091705
- 1363 Study on Strategy to Incorporate Carbon and Nitrogen in Nanostructured TiO<sub>2</sub>: Modification of Low Bandgap Initiated by Broad Spectrum Response and Its Photoelectrochemical Properties. **2012**, 137, 091705
- 1362 Superhydrophilic TiO<sub>2</sub> surfaces generated by reactive oxygen treatment. **2012**, 30, 051402 11
- 1361 Influence of hydrogen addition to an Ar plasma on the structural properties of TiO<sub>2</sub> thin films deposited by RF sputtering. **2012**, 45, 345302 50
- 1360 Preparation, Characterization and Photocatalytic Activity of Lanthanum Doped Mesoporous Titanium Dioxide. **2012**, 25, 96-102 20
- 1359 SILVER PHOSPHATE BASED PLASMONIC PHOTOCATALYST: HIGHLY ACTIVE VISIBLE-LIGHT-ENHANCED PHOTOCATALYTIC PROPERTY AND PHOTOSENSITIZED DEGRADATION OF POLLUTANTS. **2012**, 05, 1250047 5
- 1358 Investigation on the Photoelectrocatalytic Activity of Well-Aligned TiO<sub>2</sub>Nanotube Arrays. **2012**, 2012, 1-7 6
- 1357 Titanium Oxide Modeling and Design for Innovative Biomedical Surfaces: A Concise Review. **2012**, 35, 629-641 19
- 1356 Analysis of Functional Groups at Buried Liquid/Solid Interfaces Utilizing Polarization Modulation Infrared External Reflection Spectroscopy. **2012**, 361-372
- 1355 Adsorbate-Induced Modification of Surface Electronic Structure: Pyrocatechol Adsorption on the Anatase TiO<sub>2</sub> (101) and Rutile TiO<sub>2</sub> (110) Surfaces. **2012**, 116, 23515-23525 44
- 1354 High intensity UV radiation ozone treatment of nanocrystalline TiO<sub>2</sub> layers for high efficiency of dye-sensitized solar cells. **2012**, 358, 2496-2500 17
- 1353 Importance of Diffusion in Methanol Photochemistry on TiO<sub>2</sub>(110). **2012**, 116, 25465-25469 62
- 1352 Preparation and Strongly Enhanced Visible Light Photocatalytic Activity of TiO<sub>2</sub> Nanoparticles Modified by Conjugated Derivatives of Polyisoprene. **2012**, 116, 25806-25815 68

1351	Experimental and computational studies of nitrogen doped Degussa P25 TiO <sub>2</sub> : application to visible-light driven photo-oxidation of As(III). <b>2012</b> , 2, 784	32
1350	Inhibitive influence of oxygen vacancies for photoactivity on TiO <sub>2</sub> (110). <b>2012</b> , 109, 266103	35
1349	Titanium dioxide photocatalysis in atmospheric chemistry. <i>Chemical Reviews</i> , <b>2012</b> , 112, 5919-48	68.1 604
1348	Preparation and photocatalytic performance of porous ZnO microrods loaded with Ag. <b>2012</b> , 22, 873-878	32
1347	Titanium oxide modeling and design for innovative biomedical surfaces: a concise review. <b>2012</b> , 35, 629-41	7
1346	Comparative study of photocatalytic performance of titanium oxide spheres assembled by nanorods, nanoplates and nanosheets. <b>2012</b> , 3, 72-80	4
1345	Oxygen vacancies contained TiO <sub>2</sub> spheres: facile fabrication and enhanced ferromagnetism. <b>2012</b> , 14, 1	7
1344	Photocatalytic Overall Water Splitting Promoted by an p-n Phase Junction on Ga <sub>2</sub> O <sub>3</sub> . <b>2012</b> , 124, 13266-13269	75
1343	Photocatalytic overall water splitting promoted by an p-n phase junction on Ga <sub>2</sub> O <sub>3</sub> . <b>2012</b> , 51, 13089-92	511
1342	Hydrophilicity control of visible-light hydrogen evolution and dynamics of the charge-separated state in dye/TiO <sub>2</sub> /Pt hybrid systems. <b>2012</b> , 18, 15368-81	47
1341	Electron transfer in dye-sensitised semiconductors modified with molecular cobalt catalysts: photoreduction of aqueous protons. <b>2012</b> , 18, 15464-75	104
1340	Effect of particle morphology on the photocatalytic activity of BiFeO <sub>3</sub> microcrystallites. <b>2012</b> , 23, 1869-1874	24
1339	Reduced step edges on rutile TiO <sub>2</sub> (110) as competing defects to oxygen vacancies on the terraces and reactive sites for ethanol dissociation. <b>2012</b> , 109, 155501	41
1338	Intrinsic nature of the excess electron distribution at the TiO <sub>2</sub> (110) surface. <b>2012</b> , 108, 126803	62
1337	Enhanced photocatalytic activity of nc-TiO <sub>2</sub> by promoting photogenerated electrons captured by the adsorbed oxygen. <b>2012</b> , 14, 8530-6	68
1336	Versatile grafting chemistry for creation of stable molecular layers on oxides. <b>2012</b> , 22, 1046-1053	19
1335	Sunlight active antibacterial nanostructured N-doped TiO <sub>2</sub> thin films synthesized by an ultrasonic spray pyrolysis technique. <b>2012</b> , 2, 10639	14
1334	Final state distributions of methyl radical desorption from ketone photooxidation on TiO <sub>2</sub> (110). <b>2012</b> , 14, 13630-7	11


1333	Oxidation kinetics of nitrogen doped TiO <sub>2</sub> thin films. <b>2012</b> , 14, 12930-7		10
1332	Porous vanadium-doped titania with active hydrogen: a renewable reductant for chemoselective hydrogenation of nitroarenes under ambient conditions. <b>2012</b> , 48, 9032-4		28
1331	Rapid synthesis of Zn <sup>2+</sup> doped SnWO <sub>4</sub> nanowires with the aim of exploring doping effects on highly enhanced visible photocatalytic activities. <b>2012</b> , 2, 6266		38
1330	Photocatalytic oxidation surfaces on anatase TiO <sub>2</sub> crystals revealed by single-particle chemiluminescence imaging. <b>2012</b> , 48, 3300-2		34
1329	Visible-Light Photocatalytic Degradation of Methylene Blue with Porphyrin-Sensitized TiO <sub>2</sub> . <b>2012</b> , 441, 544-548		1
1328	Charge-Carrier Dynamics in Nitrogen-Doped TiO <sub>2</sub> Powder Studied by Femtosecond Time-Resolved Diffuse Reflectance Spectroscopy. <b>2012</b> , 116, 1286-1292		49
1327	Making Photo-selective TiO <sub>2</sub> Materials by Cation/Anion Codoping: From Structure and Electronic Properties to Photoactivity. <b>2012</b> , 116, 18759-18767		25
1326	Probing the influence from residual Ti interstitials on water adsorption on TiO <sub>2</sub> (110). <b>2012</b> , 86,		26
1325	Ethanol Diffusion on Rutile TiO <sub>2</sub> (110) Mediated by H Adatoms. <i>Journal of Physical Chemistry Letters</i> , <b>2012</b> , 3, 283-8	6.4	33
1324	Probing redox photocatalysis of trapped electrons and holes on single Sb-doped titania nanorod surfaces. <b>2012</b> , 134, 3946-9		55
1323	Biomaterialized N-doped CNT/TiO <sub>2</sub> core/shell nanowires for visible light photocatalysis. <b>2012</b> , 6, 935-43		167
1322	Binding of a Benzoate Dye-Molecule Analogue to Rutile Titanium Dioxide Surfaces. <b>2012</b> , 116, 1020-1026		14
1321	Photochemical grafting of organic alkenes to single-crystal TiO <sub>2</sub> surfaces: a mechanistic study. <b>2012</b> , 28, 12085-93		12
1320	On a novel catalytic system based on electrospun nanofibers and M-POSS. <b>2012</b> , 4, 604-7		28
1319	Adsorptive and Kinetic Properties on Photocatalytic Hydrogenation of Aromatic Ketones upon UV Irradiated Polycrystalline Titanium Dioxide: Differences between Acetophenone and Its Trifluoromethylated Derivative. <b>2012</b> , 116, 17705-17713		27
1318	Adsorption of Co-Phthalocyanine on the Rutile TiO <sub>2</sub> (110) Surface: A Scanning Tunneling Microscopy/Spectroscopy Study. <b>2012</b> , 116, 20300-20305		36
1317	Direct Imaging of Site-Specific Photocatalytical Reactions of O on TiO(110). <i>Journal of Physical Chemistry Letters</i> , <b>2012</b> , 3, 102-106	6.4	52
1316	UV-resistant amorphous fluorinated coating for anodized titanium surfaces. <b>2012</b> , 74, 794-800		21



1315	Visible light induced photodesorption of NO from the $\text{Cr}_2\text{O}_3(0001)$ surface. <b>2012</b> , 606, 505-509	11
1314	Calculation of point defects in rutile $\text{TiO}_2$ by the screened-exchange hybrid functional. <b>2012</b> , 86,	81
1313	Electroless deposition of multi-functional zinc oxide surfaces displaying photoconductive, superhydrophobic, photowetting, and antibacterial properties. <b>2012</b> , 22, 3859	31
1312	Some critical factors for photocatalysis on self-organized $\text{TiO}_2$ nanotubes. <b>2012</b> , 16, 3499-3504	33
1311	Solvothermal Preparation of Carbon-Enhanced $\text{TiO}_2$ /Graphene Composite and Its Visible Light Photocatalytic Properties. <b>2012</b> , 138, 152-158	6
1310	Synthesis of $\text{TiO}_2$ nanoparticles using novel titanium oxalate complex towards visible light-driven photocatalytic reduction of $\text{CO}_2$ to $\text{CH}_3\text{OH}$ . <b>2012</b> , 437-438, 28-35	72
1309	Visible light assisted photodecolorization of eosin-Y in aqueous solution using hesperidin modified $\text{TiO}_2$ nanoparticles. <b>2012</b> , 258, 4592-4600	44
1308	Tuning electronic structure and photocatalytic properties by Ag incorporated on (001) surface of anatase $\text{TiO}_2$ . <b>2012</b> , 258, 4806-4812	19
1307	Structural characteristics of mixed oxides $\text{MO}_x/\text{SiO}_2$ affecting photocatalytic decomposition of methylene blue. <b>2012</b> , 258, 6288-6296	11
1306	Effect of nitrogen doping on anatase-rutile phase transformation of $\text{TiO}_2$ . <b>2012</b> , 258, 7997-8001	37
1305	Enhanced adsorption and photocatalytic activity of $\text{BiOI-MWCNT}$ composites towards organic pollutants in aqueous solution. <b>2012</b> , 229-230, 72-82	82
1304	Study on defect properties of nanocrystalline $\text{TiO}_2$ during phase transition by positron annihilation lifetime. <b>2012</b> , 353, 55-58	12
1303	DFT study of the adsorption of Ni on Anatase (0 0 1) surface. <b>2012</b> , 981, 59-67	20
1302	The past, present and future of heterogeneous catalysis. <b>2012</b> , 189, 2-27	256
1301	First-principles investigation of adsorption of $\text{N}_2\text{O}$ on the anatase $\text{TiO}_2$ (101) and the CO pre-adsorbed $\text{TiO}_2$ surfaces. <b>2012</b> , 58, 24-30	21
1300	First-row transition metal atoms adsorption on rutile $\text{TiO}_2(110)$ surface. <b>2012</b> , 23, 1309-1321	15
1299	Boron oxynitride nanoclusters on tungsten trioxide as a metal-free cocatalyst for photocatalytic oxygen evolution from water splitting. <b>2012</b> , 4, 1267-70	44
1298	A review of photocatalysis using self-organized $\text{TiO}_2$ nanotubes and other ordered oxide nanostructures. <b>2012</b> , 8, 3073-103	533

1297	Volumes and issues. <b>2012</b> , 3, 27	10
1296	Photoluminescence of TiO <sub>2</sub> : effect of UV light and adsorbed molecules on surface band structure. <b>2012</b> , 134, 324-32	118
1295	CHAPTER 8: Toxicology of Designer/Engineered Metallic Nanoparticles. <b>2012</b> , 190-212	6
1294	Template-free fabrication of TiO <sub>2</sub> hollow spheres and their photocatalytic properties. <b>2012</b> , 4, 860-5	140
1293	Structure selection based on high vertical electron affinity for TiO <sub>2</sub> clusters. <b>2012</b> , 108, 106801	48
1292	Controllable Synthesis and Photocatalytic Activity of Anatase TiO <sub>2</sub> Single Crystals with Exposed {110} Facets. <b>2012</b> , 33, 1743-1753	17
1291	A red anatase TiO <sub>2</sub> photocatalyst for solar energy conversion. <b>2012</b> , 5, 9603	332
1290	Influence of pH on Surface States Behavior in TiO <sub>2</sub> Nanotubes. <b>2012</b> , 116, 22139-22148	23
1289	Optically and thermally induced molecular switching processes at metal surfaces. <b>2012</b> , 24, 394001	52
1288	Surface photochemistry probed by two-photon photoemission spectroscopy. <b>2012</b> , 5, 6833	26
1287	Inactivation of TiO <sub>2</sub> nano-powders for the preparation of photo-stable sunscreens via carbon-based surface modification. <b>2012</b> , 22, 19105	26
1286	Growth mechanism of palladium clusters on rutile TiO <sub>2</sub> (110) surface. <b>2012</b> , 21, 544-555	8
1285	Heterostructured Tin oxide-pillared tetratitanate with enhanced photocatalytic activity. <b>2012</b> , 386, 1-8	13
1284	Facile in situ synthesis of the bismuth oxychloride/bismuth niobate/TiO <sub>2</sub> composite as a high efficient and stable visible light driven photocatalyst. <b>2012</b> , 386, 373-80	28
1283	A new sight on hydrogenation of F and N-F doped {001} facets dominated anatase TiO <sub>2</sub> for efficient visible light photocatalyst. <b>2012</b> , 127, 28-35	75
1282	Fabrication of metallic platinum doped ordered mesoporous titania/silica materials with excellent simulated sunlight and visible light photocatalytic activity. <b>2012</b> , 415, 399-405	15
1281	Adsorption performance of titanium dioxide (TiO <sub>2</sub> ) coated air filters for volatile organic compounds. <b>2012</b> , 243, 340-9	64
1280	Monodispersed Ag nanoparticles loaded on the surface of spherical Bi <sub>2</sub> WO <sub>6</sub> nanoarchitectures with enhanced photocatalytic activities. <b>2012</b> , 22, 4751	182

1279	Assessing the importance of Van der Waals interactions on the adsorption of azobenzene on the rutile TiO <sub>2</sub> (110) surface. <b>2012</b> , 545, 60-65	10
1278	Fabrication of composite photocatalyst g-C <sub>3</sub> N <sub>4</sub> -ZnO and enhancement of photocatalytic activity under visible light. <b>2012</b> , 41, 6756-63	475
1277	Efficient Contaminant Removal by Bi <sub>2</sub> WO <sub>6</sub> Films with Nanoleaflike Structures through a Photoelectrocatalytic Process. <b>2012</b> , 116, 19413-19418	41
1276	Mo + N Codoped TiO <sub>2</sub> sheets with dominant {001} facets for enhancing visible-light photocatalytic activity. <b>2012</b> , 22, 17700	142
1275	Ag <sub>2</sub> O/Bi <sub>2</sub> O <sub>3</sub> composites: synthesis, characterization and high efficient photocatalytic activities. <b>2012</b> , 14, 5705	42
1274	Sulfur dioxide adsorption and photooxidation on isotopically-labeled titanium dioxide nanoparticle surfaces: roles of surface hydroxyl groups and adsorbed water in the formation and stability of adsorbed sulfite and sulfate. <b>2012</b> , 14, 6957-66	80
1273	Nanostructure Transition on Anodic Titanium: Structure Control via a Competition Strategy between Electrochemical Oxidation and Chemical Etching. <b>2012</b> , 116, 22359-22364	20
1272	Photo-induced hydrophilicity and self-cleaning: models and reality. <b>2012</b> , 5, 7491	187
1271	Ab initio study of neutral (TiO <sub>2</sub> ) <sub>n</sub> clusters and their interactions with water and transition metal atoms. <b>2012</b> , 24, 305301	22
1270	Synthesis of Efficient Nanosized Rutile TiO <sub>2</sub> and Its Main Factors Determining Its Photodegradation Activity: Roles of Residual Chloride and Adsorbed Oxygen. <b>2012</b> , 116, 17094-17100	41
1269	Observation of photocatalytic dissociation of water on terminal Ti sites of TiO <sub>2</sub> (110)-1 × 1 surface. <b>2012</b> , 134, 9978-85	137
1268	Probe of NH <sub>3</sub> and CO adsorption on the very outermost surface of a porous TiO <sub>2</sub> adsorbent using photoluminescence spectroscopy. <b>2012</b> , 28, 5652-9	12
1267	First-Principles Studies on Photocatalytic TiO <sub>2</sub> /H <sub>2</sub> O Interfaces on the Atomic Scale. <b>2012</b> , 33, 345-350	
1266	Hydrogen Production by Photoreforming of Renewable Substrates. <b>2012</b> , 2012, 1-21	47
1265	Acetic Acid Adsorption on Anatase TiO <sub>2</sub> (101). <b>2012</b> , 116, 11643-11651	56
1264	Anatase TiO <sub>2</sub> -pillared hexaniobate mesoporous nanocomposite with enhanced photocatalytic activity. <b>2012</b> , 147, 79-85	20
1263	Photocatalytic H <sub>2</sub> production on Pt/TiO <sub>2</sub> /Bi <sub>2</sub> O <sub>3</sub> with tuned surface-phase structures: enhancing activity and reducing CO formation. <b>2012</b> , 5, 6345-6351	86
1262	Advanced nanoarchitectures for solar photocatalytic applications. <i>Chemical Reviews</i> , <b>2012</b> , 112, 1555-6148.1	1888

1261	A carbon nitride/TiO <sub>2</sub> nanotube array heterojunction visible-light photocatalyst: synthesis, characterization, and photoelectrochemical properties. <b>2012</b> , 22, 17900	184
1260	Photocatalytic Activity of Fe and Ce Co-doped Mesoporous TiO <sub>2</sub> Catalyst under UV and Visible Light. <b>2012</b> , 59, 614-620	18
1259	Direct Synthesis of Anatase Films with ~100% (001) Facets and [001] Preferred Orientation. <b>2012</b> , 24, 2324-2329	40
1258	TiO <sub>2</sub> -assisted photodegradation of pharmaceuticals  review. <b>2012</b> , 10, 989-1027	31
1257	Selective photoreduction of nitric oxide to nitrogen by nanostructured TiO <sub>2</sub> photocatalysts: role of oxygen vacancies and iron dopant. <b>2012</b> , 134, 9369-75	194
1256	Surface chemistry of ruthenium dioxide in heterogeneous catalysis and electrocatalysis: from fundamental to applied research. <i>Chemical Reviews</i> , <b>2012</b> , 112, 3356-426	68.1 484
1255	Nonaqueous synthesis of TiO <sub>2</sub> nanocrystals using TiF <sub>4</sub> to engineer morphology, oxygen vacancy concentration, and photocatalytic activity. <b>2012</b> , 134, 6751-61	745
1254	Titanium-oxo-clusters with dicarboxylates: single-crystal structure and photochromic effect. <b>2012</b> , 51, 8982-8	62
1253	Heteroatom-Modulated Switching of Photocatalytic Hydrogen and Oxygen Evolution Preferences of Anatase TiO <sub>2</sub> Microspheres. <b>2012</b> , 22, 3233-3238	114
1252	Hierarchically Structured Porous Materials for Energy Conversion and Storage. <b>2012</b> , 22, 4634-4667	697
1251	Two-dimensional nanoarchitectures for lithium storage. <b>2012</b> , 24, 4097-111	444
1250	Metal-organic framework templated synthesis of Fe <sub>2</sub> O <sub>3</sub> /TiO <sub>2</sub> nanocomposite for hydrogen production. <b>2012</b> , 24, 2014-8	369
1249	Fabrication and deodorizing efficiency of nanostructured core-sheath TiO <sub>2</sub> nanofibers. <b>2012</b> , 125, 2929-2935	5
1248	Inorganic photocatalysts for overall water splitting. <b>2012</b> , 7, 642-57	139
1247	Visible Light Active Phosphorus-Doped TiO <sub>2</sub> Nanoparticles: An EPR Evidence for the Enhanced Charge Separation. <b>2012</b> , 116, 16191-16197	107
1246	Improved visible-light photocatalytic activity of titania activated by nitrogen and indium modification. <b>2012</b> , 22, 14443	41
1245	Infrared Spectroscopic Studies of Conduction Band and Trapped Electrons in UV-Photoexcited, H-Atom n-Doped, and Thermally Reduced TiO <sub>2</sub> . <b>2012</b> , 116, 4535-4544	104
1244	Photooxidation Mechanism of Methanol on Rutile TiO <sub>2</sub> Nanoparticles. <b>2012</b> , 116, 6623-6635	86

1243	Band bending in semiconductors: chemical and physical consequences at surfaces and interfaces. <i>Chemical Reviews</i> , <b>2012</b> , 112, 5520-51	68.1	1464
1242	Tartaric acid-assisted preparation and photocatalytic performance of titania nanoparticles with controllable phases of anatase and brookite. <b>2012</b> , 47, 5743-5751		35
1241	Synthesis, characterization and visible-light photocatalytic activity of TiO <sub>2</sub> /BiO <sub>2</sub> composite modified with zinc porphyrins. <b>2012</b> , 62, 432-440		9
1240	One-Pot Construction of Titania-AlOOH Nanocomposites Employed for Photocatalytic Degradation. <b>2012</b> , 223, 2073-2081		5
1239	Transition metal oxide loaded MCM catalysts for photocatalytic degradation of dyes. <b>2012</b> , 124, 385-393		16
1238	Correlating the visible light photoactivity of N-doped TiO <sub>2</sub> with brookite particle size and bridged-nitro surface species. <b>2012</b> , 17, 1-7		21
1237	Dissociation of formic acid on anatase TiO <sub>2</sub> (101) probed by vibrational spectroscopy. <b>2012</b> , 182, 12-15		52
1236	Effects of the crystal reduction state on the interaction of oxygen with rutile TiO <sub>2</sub> (1 1 0). <b>2012</b> , 182, 25-38		37
1235	Sol-gel derived mesoporous titania nanoparticles: Effects of calcination temperature and alcoholic solvent on the photocatalytic behavior. <b>2012</b> , 38, 2233-2237		26
1234	Physisorption of helium on a TiO <sub>2</sub> (110) surface: Periodic and finite cluster approaches. <b>2012</b> , 399, 272-280		10
1233	Photocatalytic activity of single and mixed nanosheet-like Bi <sub>2</sub> WO <sub>6</sub> and TiO <sub>2</sub> for Rhodamine B degradation under sunlike and visible illumination. <b>2012</b> , 423-424, 34-41		39
1232	Preparation of boron and phosphor co-doped TiO <sub>2</sub> nanotube arrays and their photoelectrochemical property. <b>2012</b> , 19, 127-130		27
1231	Photocatalytic activity of cerium-doped mesoporous TiO <sub>2</sub> coated Fe <sub>3</sub> O <sub>4</sub> magnetic composite under UV and visible light. <b>2012</b> , 30, 355-360		21
1230	Effects of calcining temperature on photocatalytic activity of Fe-doped sulfated titania. <b>2012</b> , 88, 816-23		12
1229	Nanostructured Photocatalysts with Enhanced Visible-Light Activity by a Low-Temperature Sol-Gel Process. <b>2012</b> , 95, 2330-2338		7
1228	Excited nanoscale-TiO <sub>2</sub> induced interfacial electron transfer reaction of redox active cobalt(III)alkyl amine complex and the solid surface. <b>2012</b> , 134, 747-754		4
1227	Phase and morphology changes induced by acid treatment following alkaline reaction of mesoporous anatase: Effect of anions. <b>2012</b> , 134, 1020-1029		4
1226	Photocatalytic degradation of p-cresol on Pt/Al <sub>2</sub> O <sub>3</sub> /TiO <sub>2</sub> mixed oxides: Effect of oxidizing and reducing pre-treatments. <b>2012</b> , 236, 21-25		12

1225	Defects in TiO <sub>2</sub> films on p+-Si studied by positron annihilation spectroscopy. <b>2012</b> , 177, 625-628	1
1224	Facile synthesis of monodispersed nanocrystalline anatase TiO <sub>2</sub> particles with large surface area and enhanced photocatalytic activity for degradation of organic contaminant in wastewaters. <b>2012</b> , 15, 108-111	21
1223	A first-principles study of the effect of oxygen vacancy on rutile Ti <sub>1-x</sub> Cd <sub>x</sub> O <sub>2</sub> . <b>2012</b> , 152, 142-146	1
1222	Synthesis and catalytic activity of Au-supported porous TiO <sub>2</sub> nanospheres for CO oxidation. <b>2012</b> , 217, 585-590	10
1221	Visible-light-driven Nb-codoped TiO <sub>2</sub> powders derived from different ammonium oxofluorotitanate precursors. <b>2012</b> , 218, 140-148	28
1220	Influence of Pt promoter on the photo-oxidative degradation by visible-light plasmonic Pt-titania catalyst. <b>2012</b> , 46, 133-138	3
1219	Preparation and photocatalytic activity of magnetic samarium-doped mesoporous titanium dioxide at the decomposition of methylene blue under visible light. <b>2012</b> , 86, 1326-1331	11
1218	Evaluation of sun protection factor of cosmetic formulations by a simple visual in vitro method mimicking the in vivo method. <b>2012</b> , 101, 726-32	5
1217	Nano-photocatalytic materials: possibilities and challenges. <b>2012</b> , 24, 229-51	2967
1216	Enhancement of thermal stability of TiO <sub>2</sub> nanowires embedded in anodic aluminum oxide template. <b>2012</b> , 47, 739-745	4
1215	Simulated Sunlight-Driven Degradation of Rhodamine B by Porous Peanut-Like TiO <sub>2</sub> /BiVO <sub>4</sub> Composite. <b>2013</b> , 24, 771-785	12
1214	Hydrothermal Synthesis and Characterization of Visible-Light-Driven Dumbbell-Like BiVO <sub>4</sub> and Ag/BiVO <sub>4</sub> Photocatalysts. <b>2013</b> , 24, 531-547	18
1213	Analysis of the origin of lateral interactions in the adsorption of small organic molecules on oxide surfaces. <b>2013</b> , 132, 1	5
1212	Role of steps in the dissociative adsorption of water on rutile TiO <sub>2</sub> (110). <b>2013</b> , 110, 146101	54
1211	Au@TiO <sub>2</sub> -CdS ternary nanostructures for efficient visible-light-driven hydrogen generation. <b>2013</b> , 5, 8088-92	157
1210	STM tip-assisted single molecule chemistry. <b>2013</b> , 15, 12428-41	21
1209	Synthesis of hybrid Zn-Al mixed metal oxides/carbon nanotubes composite and enhanced visible-light-induced photocatalytic performance. <b>2013</b> , 282, 937-946	29
1208	Enhancement of photocatalytic H <sub>2</sub> evolution over nitrogen-deficient graphitic carbon nitride. <b>2013</b> , 1, 11754	257

1207	Preparation and photo-catalytic activity of TiO <sub>2</sub> -coated medical stone-based porous ceramics. <b>2013</b> , 20, 593-597		7
1206	Effect of rare earth dopants on the morphologies and photocatalytic activities of BiFeO <sub>3</sub> microcrystallites. <b>2013</b> , 24, 1530-1535		20
1205	Characterization and photocatalytic activity of nitrogen-doped titanium(IV) oxide prepared by doping titania with TiN powder. <b>2013</b> , 455, 86-91		11
1204	Solar Photocatalytic Disinfection of Bacteria. <b>2013</b> , 243-262		
1203	Current Development of Photocatalysts for Solar Energy Conversion. <b>2013</b> , 279-304		1
1202	Photocatalytic Nanooxides: The Case of TiO <sub>2</sub> and ZnO. <b>2013</b> , 245-266		2
1201	Graphitized carbon dots emitting strong green photoluminescence. <b>2013</b> , 1, 4902		61
1200	In Situ Loading Transition Metal Oxide Clusters on TiO <sub>2</sub> Nanosheets As Co-catalysts for Exceptional High Photoactivity. <i>ACS Catalysis</i> , <b>2013</b> , 3, 2052-2061	13.1	135
1199	Effects of copper and vanadium deposition in multi-walled hydrogen trititanate and mixed-phase anatase/trititanate nanotubes. <b>2013</b> , 42, 12148-56		2
1198	Photoinactivation of Escherichia coli by sulfur-doped and nitrogen-fluorine-codoped TiO <sub>2</sub> nanoparticles under solar simulated light and visible light irradiation. <b>2013</b> , 47, 9988-96		113
1197	Optimizing Nanoscale TiO <sub>2</sub> for Adsorption-Enhanced Photocatalytic Degradation of Low-Concentration Air Pollutants. <b>2013</b> , 5, 3114-3123		25
1196	A simple strategy to incorporate Pt into TiO <sub>2</sub> nanosponges via wet oxidation of multilayered films. <b>2013</b> , 3, 19971		3
1195	Photoinduced Decomposition of Formaldehyde on a TiO <sub>2</sub> (110) Surface, Assisted by Bridge-Bonded Oxygen Atoms. <i>Journal of Physical Chemistry Letters</i> , <b>2013</b> , 4, 2668-2673	6.4	44
1194	Physical properties of nano-titania hollow fibers and their photocatalytic activity in the decomposition of phenol. <b>2013</b> , 87, 69-73		8
1193	Growth of Ag and Au Nanoparticles on Reduced and Oxidized Rutile TiO <sub>2</sub> (110) Surfaces. <b>2013</b> , 56, 1460-1476		25
1192	A series of MOFs based on a tricarboxylic acid and various N-donor ligands: syntheses, structures, and properties. <b>2013</b> , 15, 6986		46
1191	TiO <sub>2</sub> /T-PVA Composites Immobilized on Cordierite: Structure and Photocatalytic Activity for Degrading RhB Under Visible Light. <b>2013</b> , 224, 1		10
1190	A Comparative Study of Immobilization Techniques for Photocatalytic Degradation of Rhodamine B using Nanoparticles of Titanium Dioxide. <b>2013</b> , 224, 1		10

1189	Nanotubes and Peapods. <b>2013</b> , 925-940	
1188	Titania Embedded with Nanostructured Sodium Titanate: Reduced Thermal Conductivity for Thermoelectric Application. <b>2013</b> , 42, 1680-1687	3
1187	Low-temperature catalytic reduction of NO by NH <sub>3</sub> over vanadia-based nanoparticles prepared by flame-assisted spray pyrolysis: Influence of various supports. <b>2013</b> , 140-141, 289-298	89
1186	Time-resolved infrared spectroscopic investigation of roles of valence states of Cr in (La,Cr)-doped SrTiO <sub>3</sub> photocatalysts. <b>2013</b> , 34, 2036-2040	12
1185	Microwave-assisted solvothermal synthesis of flower-like Ag/AgBr/BiOBr microspheres and their high efficient photocatalytic degradation for p-nitrophenol. <b>2013</b> , 206, 308-316	51
1184	Disordered Co <sub>1.28</sub> Mn <sub>1.71</sub> O <sub>4</sub> as a visible-light-responsive photocatalyst for hydrogen evolution. <b>2013</b> , 19, 4123-7	19
1183	Zinc oxysulfide ternary alloy nanocrystals: A bandgap modulated photocatalyst. <b>2013</b> , 102, 2331-10	19
1182	Mesoporous cobalt-intercalated layered tantalotungstate with high visible-light photocatalytic activity. <b>2013</b> , 172, 105-111	10
1181	Room temperature aqueous solution synthesis of pinacol (C <sub>6</sub> ) by photocatalytic CC coupling of isopropanol. <b>2013</b> , 272, 1-5	17
1180	Effect of ion doping in different sites on the morphology and photocatalytic activity of BiFeO <sub>3</sub> microcrystals. <i>Journal of Alloys and Compounds</i> , <b>2013</b> , 570, 57-60	5-7 39
1179	Facile synthesis of defect-mediated TiO <sub>2</sub> with enhanced visible light photocatalytic activity. <b>2013</b> , 1, 10099	82
1178	Modulation and effects of surface groups on photoluminescence and photocatalytic activity of carbon dots. <b>2013</b> , 5, 11665-71	141
1177	Photocatalytic activity and mechanism of nano-cubic barium titanate prepared by a hydrothermal method. <b>2013</b> , 44, 660-669	73
1176	Electron Hopping through TiO <sub>2</sub> Powder: A Study by Photoluminescence Spectroscopy. <b>2013</b> , 117, 24189-24195	29
1175	Nanomaterials: A Danger or a Promise?. <b>2013</b> ,	33
1174	Electrochemical reduction induced self-doping of Ti <sup>3+</sup> for efficient water splitting performance on TiO <sub>2</sub> based photoelectrodes. <b>2013</b> , 15, 15637-44	150
1173	A study on the active sites for visible-light photocatalytic activity of phosphorus-doped titanium(IV) oxide particles prepared using a phosphide compound. <b>2013</b> , 140-141, 327-332	19
1172	CNTs/TiO <sub>2</sub> composites and its electrochemical properties after UV light irradiation. <b>2013</b> , 23, 164-169	26



1171	Fabrication and photocatalysis of TiO <sub>2</sub> -graphene sandwich nanosheets with smooth surface and controlled thickness. <b>2013</b> , 229, 569-576	33
1170	Photocatalytic Oxidation Processes for Toluene Oxidation over TiO <sub>2</sub> Catalysts. <b>2013</b> , 3, 219-231	28
1169	Incorporation of nonmetal impurities at the anatase TiO <sub>2</sub> (001)-(1 1 1) surface. <b>2013</b> , 110, 016101	21
1168	A novel magnetic recyclable photocatalyst based on a core-shell metal-organic framework Fe <sub>3</sub> O <sub>4</sub> @MIL-100(Fe) for the decolorization of methylene blue dye. <b>2013</b> , 1, 14329	307
1167	Preparation and characterization of N-TiO <sub>2</sub> photocatalyst with high crystallinity and enhanced photocatalytic inactivation of bacteria. <b>2013</b> , 24, 335705	31
1166	Synthesis of TiO <sub>2</sub> nanoparticles on mesoporous aluminosilicate Al-SBA-15 in supercritical CO <sub>2</sub> for photocatalytic decolorization of methylene blue. <b>2013</b> , 39, 3823-3829	17
1165	Sol-gel synthesis of titanium dioxide by hydrolysis of titanium glycerolates and peroxides. <b>2013</b> , 39, 398-402	1
1164	One-pot synthesis of homogeneous core-shell Cu <sub>2</sub> O films with nanoparticle-composed multishells and their photocatalytic properties. <b>2013</b> , 3, 25010	21
1163	A combined experimental and computational study on the adsorption and reactions of NO on rutile TiO <sub>2</sub> . <b>2013</b> , 15, 466-72	21
1162	Inorganic Nanoparticles and Nanomaterials Based on Titanium (Ti): Applications in Medicine. <b>2013</b> , 754, 21-87	4
1161	Interaction of TiO <sub>2</sub> with water: infrared photodissociation spectroscopy and density functional calculations. <b>2013</b> , 15, 17126-33	16
1160	Synergetic promotion of the photocatalytic activity of TiO <sub>2</sub> by gold deposition under UV-visible light irradiation. <b>2013</b> , 49, 11767-9	58
1159	Si quantum dot-assisted synthesis of mesoporous black TiO <sub>2</sub> nanocrystals with high photocatalytic activity. <b>2013</b> , 1, 4162	7
1158	Metallic zinc- assisted synthesis of Ti <sup>3+</sup> self-doped TiO <sub>2</sub> with tunable phase composition and visible-light photocatalytic activity. <b>2013</b> , 49, 868-70	143
1157	Synthesis and photocatalytic activity of N-doped TiO <sub>2</sub> produced in a solid phase reaction. <b>2013</b> , 74, 286-290	16
1156	Self-assembly and enhanced visible-light-driven photocatalytic activities of Bi <sub>2</sub> MoO <sub>6</sub> by tungsten substitution. <b>2013</b> , 265, 424-430	36
1155	Tailored preparation of titania with controllable phases of anatase and brookite by an alkaline hydrothermal route. <b>2013</b> , 201, 151-158	50
1154	Antibacterial studies on Eu-Ag codoped TiO <sub>2</sub> surfaces. <b>2013</b> , 39, 1695-1705	29

1153	Visible-light photocatalysis with phosphorus-doped titanium(IV) oxide particles prepared using a phosphide compound. <b>2013</b> , 132-133, 39-44	49
1152	Ionic-liquid-assisted synthesis of uniform fluorinated B/C-codoped TiO <sub>2</sub> nanocrystals and their enhanced visible-light photocatalytic activity. <b>2013</b> , 19, 2433-41	134
1151	Theoretical approaches to excited-state-related phenomena in oxide surfaces. <i>Chemical Reviews</i> , <b>2013</b> , 113, 4456-95	68.1 69
1150	Syntheses, structures, photoluminescence, photocatalysis, and photoelectronic effects of 3D mixed high-connected metal-organic frameworks based on octanuclear and dodecanuclear secondary building units. <b>2013</b> , 42, 1567-80	79
1149	Enhancing the photocatalytic activity of anatase TiO <sub>2</sub> by improving the specific facet-induced spontaneous separation of photogenerated electrons and holes. <b>2013</b> , 8, 282-9	113
1148	The role of interfacial lattice Ag <sup>+</sup> on titania based photocatalysis. <b>2013</b> , 130-131, 218-223	7
1147	Modeling materials and processes in dye-sensitized solar cells: understanding the mechanism, improving the efficiency. <b>2014</b> , 352, 151-236	18
1146	Electrical property measurements of Cr-N codoped TiO <sub>2</sub> epitaxial thin films grown by pulsed laser deposition. <b>2013</b> , 102, 172108	11
1145	Synthesis of hierarchical Bi <sub>2</sub> WO <sub>6</sub> microspheres with high visible-light-driven photocatalytic activities by sol-gel-hydrothermal route. <b>2013</b> , 108, 84-87	21
1144	Synthesis of La-doped Ag <sub>1.4</sub> K <sub>0.6</sub> Ta <sub>4</sub> O <sub>11</sub> nanocomposites as efficient photocatalysts for hydrogen production and organic pollutants degradation. <b>2013</b> , 467, 335-341	4
1143	Enhancement of visible light-induced surface photo-activity of nanostructured N-TiO <sub>2</sub> thin films modified by ion implantation. <b>2013</b> , 582, 95-99	11
1142	Anatase TiO <sub>2</sub> single crystals with dominant {001} facets: Facile fabrication from Ti powders and enhanced photocatalytic activity. <b>2013</b> , 274, 117-123	33
1141	Enhanced visible light activity and mechanism of TiO <sub>2</sub> codoped with molybdenum and nitrogen. <b>2013</b> , 178, 425-430	16
1140	Direct solvothermal growth of hierarchical porous TiO <sub>2</sub> nanosheets with high photocatalytic activity. <b>2013</b> , 111, 161-164	6
1139	Super-resolution mapping of reactive sites on titania-based nanoparticles with water-soluble fluorogenic probes. <b>2013</b> , 7, 263-75	70
1138	Mesoporous cobalt-intercalated layered tetratitanate for efficient visible-light photocatalysis. <b>2013</b> , 215-216, 396-403	29
1137	Ultrafast plasmon induced electron injection mechanism in gold-TiO <sub>2</sub> nanoparticle system. <b>2013</b> , 15, 21-30	96
1136	Recent progress in biomedical applications of titanium dioxide. <b>2013</b> , 15, 4844-58	334

1135	Photocatalytic activity of a nitrogen-doped TiO <sub>2</sub> modified zeolite in the degradation of Reactive Yellow 125 azo dye. <b>2013</b> , 44, 270-278		51
1134	Molecular-level insights into photocatalysis from scanning probe microscopy studies on TiO <sub>2</sub> (110). <i>Chemical Reviews</i> , <b>2013</b> , 113, 4428-55	68.1	202
1133	Photocatalytic cross-coupling of methanol and formaldehyde on a rutile TiO <sub>2</sub> (110) surface. <b>2013</b> , 135, 5212-9		110
1132	Low temperature synthesis of ordered mesoporous stable anatase nanocrystals: the phosphorus dendrimer approach. <b>2013</b> , 5, 2850-6		29
1131	Modified Photocatalysts. <b>2013</b> , 103-143		4
1130	Green synthetic approach for Ti <sup>3+</sup> self-doped TiO(2-x) nanoparticles with efficient visible light photocatalytic activity. <b>2013</b> , 5, 1870-5		194
1129	Characterization of the Active Surface Species Responsible for UV-Induced Desorption of O <sub>2</sub> from the Rutile TiO <sub>2</sub> (110) Surface. <b>2013</b> , 117, 5774-5784		36
1128	Defect-Electron Spreading on the TiO <sub>2</sub> (110) Semiconductor Surface by Water Adsorption. <i>Journal of Physical Chemistry Letters</i> , <b>2013</b> , 4, 674-9	6.4	26
1127	Reduced TiO <sub>2</sub> nanotube arrays for photoelectrochemical water splitting. <b>2013</b> , 1, 5766		429
1126	N-TiO <sub>2</sub> Photocatalysts highly active under visible irradiation for NO <sub>x</sub> abatement and 2-propanol oxidation. <b>2013</b> , 206, 19-25		37
1125	Copper(I) Oxide Nanocrystals [One Step Synthesis, Characterization, Formation Mechanism, and Photocatalytic Properties. <b>2013</b> , 2013, 2640-2651		85
1124	Inherent electronic trap states in TiO <sub>2</sub> nanocrystals: effect of saturation and sintering. <b>2013</b> , 6, 1221		68
1123	Single-molecule catalysis mapping quantifies site-specific activity and uncovers radial activity gradient on single 2D nanocrystals. <b>2013</b> , 135, 1845-52		160
1122	Defective TiO <sub>2</sub> with oxygen vacancies: synthesis, properties and photocatalytic applications. <b>2013</b> , 5, 3601-14		1426
1121	Charge trapping in TiO <sub>2</sub> polymorphs as seen by Electron Paramagnetic Resonance spectroscopy. <b>2013</b> , 15, 9435-47		162
1120	Trends in non-metal doping of anatase TiO <sub>2</sub> : B, C, N and F. <b>2013</b> , 206, 12-18		238
1119	Quantum chemical elucidation of the mechanism for hydrogenation of TiO <sub>2</sub> anatase crystals. <b>2013</b> , 138, 154705		30
1118	Optical properties of Nb-doped TiO <sub>2</sub> thin films prepared by sol-gel method. <b>2013</b> , 39, 4771-4776		55

1117	Theoretical insights into photoinduced charge transfer and catalysis at oxide interfaces. <i>Chemical Reviews</i> , <b>2013</b> , 113, 4496-565	68.1	392
1116	N-doped rutile TiO <sub>2</sub> nano-rods show tunable photocatalytic selectivity. <i>Journal of Alloys and Compounds</i> , <b>2013</b> , 575, 40-47	5.7	51
1115	Self-Organized Arrays of Single-Metal Catalyst Particles in TiO <sub>2</sub> Cavities: A Highly Efficient Photocatalytic System. <b>2013</b> , 125, 7662-7665		10
1114	Self-organized arrays of single-metal catalyst particles in TiO <sub>2</sub> cavities: a highly efficient photocatalytic system. <b>2013</b> , 52, 7514-7		82
1113	Waterborne Escherichia coli Inactivation by TiO <sub>2</sub> Photoassisted Processes: A Brief Overview. <b>2013</b> , 295-309		2
1112	Low-temperature crystallization of anodized TiO <sub>2</sub> nanotubes at the solid-gas interface and their photoelectrochemical properties. <b>2013</b> , 5, 6139-44		24
1111	Single-Molecule Fluorescence Detection of Effective Adsorption Sites at the Metal Oxide/Solution Interface. <b>2013</b> , 117, 11219-11228		12
1110	Electronic structure and quantum dynamics of photoinitiated dissociation of O <sub>2</sub> on rutile TiO <sub>2</sub> nanocluster. <b>2013</b> , 138, 194705		4
1109	Low-temperature synthesis of water-dispersible anatase titanium dioxide nanoparticles for photocatalysis. <b>2013</b> , 396, 90-4		29
1108	Exceptional Photocatalytic Activity of 001-Facet-Exposed TiO <sub>2</sub> Mainly Depending on Enhanced Adsorbed Oxygen by Residual Hydrogen Fluoride. <i>ACS Catalysis</i> , <b>2013</b> , 3, 1378-1385	13.1	122
1107	Ultraviolet and Visible Photochemistry of Methanol at 3D Mesoporous Networks: TiO <sub>2</sub> and Au/TiO <sub>2</sub> . <b>2013</b> , 117, 15035-15049		42
1106	Photocatalytic Degradation of Polyethylene Glycol by Nano-Titanium Dioxide Modified With Ferric Acetylacetonate. <b>2013</b> , 43, 321-324		5
1105	Surface Structure and Reactivity of Anatase TiO <sub>2</sub> Crystals with Dominant {001} Facets. <b>2013</b> , 117, 6358-6362		78
1104	High-performance UV photodetection of unique ZnO nanowires from zinc carbonate hydroxide nanobelts. <b>2013</b> , 5, 5861-7		35
1103	Searching for the Formation of Ti-B Bonds in B-Doped TiO <sub>2</sub> /Rutile. <b>2013</b> , 117, 13163-13172		21
1102	Energy-level matching of Fe(III) ions grafted at surface and doped in bulk for efficient visible-light photocatalysts. <b>2013</b> , 135, 10064-72		235
1101	Hydrothermal synthesis and visible-light photocatalytic activity of porous peanut-like BiVO <sub>4</sub> and BiVO <sub>4</sub> /Fe <sub>3</sub> O <sub>4</sub> submicron structures. <b>2013</b> , 39, 9163-9172		21
1100	Adsorption of 2-propanol on anatase TiO <sub>2</sub> (101) and (001) surfaces: A density functional theory study. <b>2013</b> , 616, 76-84		17

1099	Enhanced photocatalytic activity of titania with unique surface indium and boron species. <b>2013</b> , 273, 638-644	19
1098	Photocatalytic Degradation of Toluene Over Spindle-like Porphyrinoid Nanostructures. <b>2013</b> , 18, 353-358	1
1097	A facile modification of g-C <sub>3</sub> N <sub>4</sub> with enhanced photocatalytic activity for degradation of methylene blue. <b>2013</b> , 280, 967-974	139
1096	Molecular hydrogen formation from photocatalysis of methanol on TiO <sub>2</sub> (110). <b>2013</b> , 135, 10206-9	90
1095	Single-Molecule Reactive Oxygen Species Detection in Photocatalytic Reactions. <b>2013</b> ,	
1094	Bi <sub>2</sub> WO <sub>6</sub> Quantum Dots Decorated Reduced Graphene Oxide: Improved Charge Separation and Enhanced Photoconversion Efficiency. <b>2013</b> , 117, 9113-9120	118
1093	Understanding electronic and optical properties of anatase TiO <sub>2</sub> photocatalysts co-doped with nitrogen and transition metals. <b>2013</b> , 15, 9549-61	76
1092	A review on non metal ion doped titania for the photocatalytic degradation of organic pollutants under UV/solar light: Role of photogenerated charge carrier dynamics in enhancing the activity. <b>2013</b> , 140-141, 559-587	426
1091	Photocatalysis on supported gold and silver nanoparticles under ultraviolet and visible light irradiation. <b>2013</b> , 15, 1814	469
1090	Graphene oxide-epoxy hybrid material as innovative photocatalyst. <b>2013</b> , 48, 5204-5208	11
1089	Structure of clean and adsorbate-covered single-crystal rutile TiO <sub>2</sub> surfaces. <i>Chemical Reviews</i> , <b>2013</b> , 113, 3887-948	68.1 257
1088	Nonadiabatic dynamics of positive charge during photocatalytic water splitting on GaN(10-10) surface: charge localization governs splitting efficiency. <b>2013</b> , 135, 8682-91	90
1087	Photoinduced charge transfer and acetone sensitivity of single-walled carbon nanotube-titanium dioxide hybrids. <b>2013</b> , 135, 9015-22	68
1086	Photocatalytic degradation of methylene blue by visible-light-driven yttrium-doped mesoporous titania coated magnetite photocatalyst. <b>2013</b> , 51, 7101-7108	4
1085	Metal buffer layer mediated wettability of nanostructured TiO <sub>2</sub> films. <b>2013</b> , 92, 151-153	10
1084	Synergism between Fe <sub>2</sub> O <sub>3</sub> and WO <sub>3</sub> particles: Photocatalytic activity enhancement and reaction mechanism. <b>2013</b> , 367, 103-107	46
1083	Four-faceted nanowires generated from densely-packed TiO <sub>2</sub> rutile surfaces: Ab initio calculations. <b>2013</b> , 608, 226-240	18
1082	Synproportionation Reaction for the Fabrication of Sn <sup>2+</sup> Self-Doped SnO <sub>2-x</sub> Nanocrystals with Tunable Band Structure and Highly Efficient Visible Light Photocatalytic Activity. <b>2013</b> , 117, 24157-24166	85

1081	Lanthanoid Oxide Layers on Rhodium-Loaded (Ga <sub>1-x</sub> Zn <sub>x</sub> )(N <sub>1-x</sub> O <sub>x</sub> ) Photocatalyst as a Modifier for Overall Water Splitting under Visible-Light Irradiation. <b>2013</b> , 117, 14000-14006		45
1080	Thermal properties of the stationary current in mesoporous Pt/TiO <sub>2</sub> structures in an oxyhydrogen atmosphere. <b>2013</b> , 5, 12375-9		20
1079	Catalytic Role of Surface Oxygens in TiO <sub>2</sub> Photooxidation Reactions: Aqueous Benzene Photooxidation with Ti(18)O <sub>2</sub> under Anaerobic Conditions. <i>Journal of Physical Chemistry Letters</i> , <b>2013</b> , 4, 1415-22	6.4	53
1078	Tuning the surface structure of nitrogen-doped TiO <sub>2</sub> nanofibres--an effective method to enhance photocatalytic activities of visible-light-driven green synthesis and degradation. <b>2013</b> , 19, 5731-41		30
1077	Sulfurization-Assisted Cobalt Deposition on Sm <sub>2</sub> Ti <sub>2</sub> S <sub>2</sub> O <sub>5</sub> Photocatalyst for Water Oxidation under Visible Light Irradiation. <b>2013</b> , 117, 376-382		35
1076	Electron-Phonon Coupling Dynamics at Oxygen Evolution Sites of Visible-Light-Driven Photocatalyst: Bismuth Vanadate. <b>2013</b> , 117, 9881-9886		59
1075	Facile oxidative conversion of TiH <sub>2</sub> to high-concentration Ti(3+)-self-doped rutile TiO <sub>2</sub> with visible-light photoactivity. <b>2013</b> , 52, 3884-90		150
1074	Strong photon energy dependence of the photocatalytic dissociation rate of methanol on TiO <sub>2</sub> (110). <b>2013</b> , 135, 19039-45		49
1073	Toward the Nanoscale. <b>2013</b> , 261-294		
1072	Optical Transition and Photocatalytic Performance of d <sup>1</sup> Metallic Perovskites. <b>2013</b> , 117, 5593-5598		30
1071	Monohafnium oxide clusters HfO(n)- and HfO(n) (n = 1-6): oxygen radicals, superoxides, peroxides, diradicals, and triradicals. <b>2013</b> , 117, 1042-52		20
1070	Fabrication of reduced graphene oxide/BiOCl hybrid material via a novel benzyl alcohol route and its enhanced photocatalytic activity. <b>2013</b> , 15, 1		30
1069	Nonmetal Doping in TiO <sub>2</sub> Toward Visible-Light-Induced Photocatalysis. <b>2013</b> , 87-113		1
1068	Degradation of Toluene Using Modified TiO <sub>2</sub> as Photocatalysts. <b>2013</b> , 669, 7-18		3
1067	Photons, Electrons and Holes: Fundamentals of Photocatalysis with Semiconductors. <b>2013</b> , 5-33		2
1066	Kinetics Study of Photocatalytic Activity of Flame-Made Unloaded and Fe-Loaded CeO <sub>2</sub> Nanoparticles. <b>2013</b> , 2013, 1-9		21
1065	Facile Postsynthesis of N-Doped TiO <sub>2</sub> -SBA-15 and Its Photocatalytic Activity. <b>2013</b> , 2013, 1-8		3
1064	Titanium Dioxide in Photocatalysis. <b>2013</b> , 153-188		8

1063	Synergistic modification of electronic and photocatalytic properties of TiO <sub>2</sub> nanotubes by implantation of Au and N atoms. <b>2013</b> , 14, 2800-7	5
1062	Kinetics and Dynamics of Photocatalyzed Dissociation of Ethanol on TiO <sub>2</sub> (110). <b>2013</b> , 26, 1-7	8
1061	STRUCTURES AND ELECTRONIC PROPERTIES OF A Co <sub>2</sub> P CLUSTER DEPOSITED ON THE RUTILE TiO <sub>2</sub> (110) SURFACE BY FIRST PRINCIPLES CALCULATIONS. <b>2013</b> , 12, 1250102	4
1060	Photoresponse on the Desorption of an Atomic Hydrogen on Titanium Dioxide Surface Induced by a Tip of Scanning Tunneling Microscope. <b>2013</b> , 42, 942-943	4
1059	Vibrational spectroscopic studies on pure and metal-covered metal oxide surfaces. <b>2013</b> , 250, 1204-1221	18
1058	Fabrication of anatase titanium dioxide microspheres via homogeneous precipitation method. <b>2013</b> , 17, 117-121	0
1057	Zeolites: Promised Materials for the Sustainable Production of Hydrogen. <b>2013</b> , 2013, 1-19	23
1056	Low-temperature growth of well-aligned zinc oxide nanorod arrays on silicon substrate and their photocatalytic application. <b>2014</b> , 9, 2109-15	15
1055	Regulating Photocatalytic Selectivity of Anatase TiO <sub>2</sub> with {101}, {001}, and {111} Facets. <b>2014</b> , 97, 4005-4010	26
1054	Second Generation Nitrogen Doped Titania Nanoparticles: A Comprehensive Electronic and Microstructural Picture. <b>2014</b> , 32, 1195-1213	14
1053	Photocatalytic and Photovoltaic Properties of TiO <sub>2</sub> Nanoparticles Investigated by Ab Initio Simulations. <b>2014</b> , 118, 29928-29942	27
1052	Probing Photocatalytic Characteristics of Sb-Doped TiO <sub>2</sub> under Visible Light Irradiation. <b>2014</b> , 2014, 1-6	4
1051	Preparation of Cerium Modified Titanium Dioxide Nanoparticles and Investigation of Their Visible Light Photocatalytic Performance. <b>2014</b> , 2014, 1-9	6
1050	Fabrication of CdS/H-TiO <sub>2</sub> Nanotube Arrays and Their Application for the Degradation of Methyl Orange in Aqueous Solutions. <b>2014</b> , 2014, 1-7	1
1049	Optically modulated charge transfer in TiO <sub>2</sub> -Au nano-complexes. <b>2014</b> , 1, 045033	5
1048	Enhanced Photo-Oxidation of Formaldehyde on Highly Reduced o-TiO <sub>2</sub> (110). <b>2014</b> , 118, 29242-29251	27
1047	Optimization of photocatalytic degradation of naphthol using nano TiO <sub>2</sub> -activated carbon composite. <b>2014</b> , 1-12	1
1046	Structural, spectroscopic aspects, and electronic properties of (TiO <sub>2</sub> ) <sub>n</sub> clusters: a study based on the use of natural algorithms in association with quantum chemical methods. <b>2014</b> , 35, 51-61	27

1045	Infrared spectroscopy study of adsorption and photodecomposition of formic acid on reduced and defective rutile TiO <sub>2</sub> (110) surfaces. <b>2014</b> , 32, 061402	12
1044	Fe(III) doped and grafted PbTiO <sub>3</sub> film photocathode with enhanced photoactivity for hydrogen production. <b>2014</b> , 105, 082903	13
1043	Water on titanium dioxide surface: a revisiting by reactive molecular dynamics simulations. <b>2014</b> , 30, 14832-40	51
1042	Controlled Vacancy-Assisted C–C Couplings of Acetaldehyde on Rutile TiO <sub>2</sub> (110). <b>2014</b> , 118, 27920-27924	13
1041	Evidence of Facilitated Electron Transfer on Hydrogenated Self-Doped TiO <sub>2</sub> Nanocrystals. <b>2014</b> , 1, 1415-1421	10
1040	Solar Hydrogen Generation: Photocatalytic and Photoelectrochemical Methods. <b>2014</b> , 27-49	1
1039	Atomic defects in titanium dioxide. <b>2014</b> , 14, 923-34	17
1038	Band structure engineering of anatase TiO <sub>2</sub> by metal-assisted P-O coupling. <b>2014</b> , 140, 174705	23
1037	Dynamics of the Photogenerated Hole at the Rutile TiO <sub>2</sub> (110)/Water Interface: A Nonadiabatic Simulation Study. <b>2014</b> , 118, 27393-27401	30
1036	Catalytic role of TiO <sub>2</sub> terminal oxygen atoms in liquid-phase photocatalytic reactions: oxidation of aromatic compounds in anhydrous acetonitrile. <b>2014</b> , 15, 2311-20	17
1035	Probing the role of surface energetics of electrons and their accumulation in photoreduction processes on TiO <sub>2</sub> . <b>2014</b> , 20, 7759-65	14
1034	New reconstructions of the (110) surface of rutile TiO <sub>2</sub> predicted by an evolutionary method. <b>2014</b> , 113, 266101	50
1033	Preparation of TiO <sub>2</sub> /SiO <sub>2</sub> nanocomposite with non-ionic surfactants via sol-gel process and their photocatalytic study. <b>2014</b> , 30, 1577-1584	15
1032	Tailoring the interplay between electromagnetic fields and nanomaterials toward applications in life sciences: a review. <b>2014</b> , 19, 101507	13
1031	Ag-Loaded Wool Spherical-Like Bi <sub>2</sub> WO <sub>6</sub> Nanoarchitectures Photocatalyst Degrade Pigments. <b>2014</b> , 496-500, 30-37	1
1030	8th Congress on Electronic Structure: Principles and Applications (ESPA 2012). <b>2014</b> ,	
1029	The facile preparation of 5,10,15,20-tetrakis(4-carboxyl phenyl) porphyrin-CdS nanocomposites and their photocatalytic activity. <b>2014</b> , 188, 106-113	10
1028	Influence of Nd-Doping on Photocatalytic Properties of TiO <sub>2</sub> Nanoparticles and Thin Film Coatings. <b>2014</b> , 2014, 1-10	21



1027	Titania Nanotubes by Electrochemical Anodization for Solar Energy Conversion. <b>2014</b> , 161, D3066-D3077	26
1026	Coverage dependence of the level alignment for methanol on TiO <sub>2</sub> (1 1 0). <b>2014</b> , 1040-1041, 259-265	13
1025	Realizing high visible-light-induced carriers mobility in TiO <sub>2</sub> -based photoanodes. <b>2014</b> , 251, 195-201	3
1024	The role of oxygen pressure in nitrogen and carbon co-doped TiO <sub>2</sub> thin films prepared by pulsed laser deposition method. <b>2014</b> , 241, 148-153	15
1023	Considerations to improve adsorption and photocatalysis of low concentration air pollutants on TiO <sub>2</sub> . <b>2014</b> , 225, 24-33	62
1022	Nb <sub>2</sub> O <sub>5</sub> /TiO <sub>2</sub> heterojunctions: Synthesis strategy and photocatalytic activity. <b>2014</b> , 152-153, 280-288	164
1021	Synthesis and characterization of N-doped TiO <sub>2</sub> photocatalysts with tunable response to solar radiation. <b>2014</b> , 305, 281-291	44
1020	Self-assembly synthesis of ZnO with adjustable morphologies and their photocatalytic performance. <b>2014</b> , 40, 2973-2978	7
1019	Surface modification of nano-TiO <sub>2</sub> with trimellitylimido-amino acid-based diacids for preventing aggregation of nanoparticles. <b>2014</b> , 25, 348-353	45
1018	Visible light driven photocatalysis mediated via ligand-to-metal charge transfer (LMCT): an alternative approach to solar activation of titania. <b>2014</b> , 7, 954	293
1017	Stable blue TiO <sub>2</sub> nanoparticles for efficient visible light photocatalysts. <b>2014</b> , 2, 4429	262
1016	Visible-light photocatalysis of ZnO deposited on nanoporous Au. <b>2014</b> , 114, 1061-1066	4
1015	Hydrothermal synthesis of SrTiO <sub>3</sub> nanocubes: Characterization, photocatalytic activities, and degradation pathway. <b>2014</b> , 45, 1927-1936	90
1014	BiFeO <sub>3</sub> /TiO <sub>2</sub> nanotube arrays composite electrode: construction, characterization, and enhanced photoelectrochemical properties. <b>2014</b> , 6, 671-9	135
1013	Superwetting of TiO <sub>2</sub> by light-induced water-layer growth via delocalized surface electrons. <b>2014</b> , 111, 5784-9	24
1012	A novel 3D structured reduced graphene oxide/TiO <sub>2</sub> composite: synthesis and photocatalytic performance. <b>2014</b> , 2, 3605-3612	57
1011	Engineering the TiO <sub>2</sub> -graphene interface to enhance photocatalytic H <sub>2</sub> production. <b>2014</b> , 7, 618-26	72
1010	Photocatalytic treatment of 2,4,6-trinitotoluene in red water by multi-doped TiO <sub>2</sub> with enhanced visible light photocatalytic activity. <b>2014</b> , 452, 103-108	19

1009	Hierarchical porous TiO <sub>2</sub> templated from natural Artemia cyst shells for photocatalysis applications. <b>2014</b> , 4, 20393-20397	7
1008	TiO <sub>2</sub> nanoparticles as functional building blocks. <i>Chemical Reviews</i> , <b>2014</b> , 114, 9283-318	68.1 340
1007	Surface chemistry of CO <sub>2</sub> Adsorption of carbon dioxide on clean surfaces at ultrahigh vacuum. <b>2014</b> , 89, 161-217	109
1006	Ag/Bi <sub>2</sub> WO <sub>6</sub> plasmonic composites with enhanced visible photocatalytic activity. <b>2014</b> , 40, 6495-6501	42
1005	Effects of Cocatalyst on Carrier Dynamics of a Titanate Photocatalyst with Layered Perovskite Structure. <b>2014</b> , 118, 10972-10979	14
1004	Molecular hydrogen formation from photocatalysis of methanol on anatase-TiO <sub>2</sub> (101). <b>2014</b> , 136, 602-5	78
1003	Self-doped Ti <sup>3+</sup> @TiO <sub>2</sub> visible light photocatalyst: Influence of synthetic parameters on the H <sub>2</sub> production activity. <b>2014</b> , 39, 711-717	53
1002	High-Efficiency Solar Cells. <b>2014</b> ,	16
1001	Significantly enhancement of photocatalytic performances via core-shell structure of ZnO@mpg-C <sub>3</sub> N <sub>4</sub> . <b>2014</b> , 147, 554-561	188
1000	Solid-state NMR investigation of the <sup>16</sup> O/ <sup>17</sup> O isotope exchange of oxygen species in pure-anatase and mixed-phase TiO <sub>2</sub> . <b>2014</b> , 594, 34-40	6
999	Heterojunctions in g-C <sub>3</sub> N <sub>4</sub> /TiO <sub>2</sub> (B) nanofibres with exposed (001) plane and enhanced visible-light photoactivity. <b>2014</b> , 2, 2071-2078	218
998	Adsorption and Photocatalytic Degradation of 3-Fluoroaniline on Anatase TiO <sub>2</sub> (101): A Photoemission and Near-Edge X-ray Absorption Fine Structure Study. <b>2014</b> , 118, 2028-2036	7
997	Solar photocatalytic activity of anatase TiO <sub>2</sub> nanocrystals synthesized by non-hydrolytic sol-gel method. <b>2014</b> , 101, 321-332	95
996	Temperature-programed surface reaction study of CO oxidation over Au/TiO <sub>2</sub> at low temperature: An insight into nature of the reaction process. <b>2014</b> , 311, 71-79	26
995	Influence of La-doping on phase transformation and photocatalytic properties of ZnTiO <sub>3</sub> nanoparticles synthesized via modified sol-gel method. <b>2014</b> , 16, 728-35	73
994	Enhanced photocatalytic activity and stability of interstitial Ga-doped CdS: Combination of experiment and calculation. <b>2014</b> , 224, 104-113	32
993	Effect of different base structures on the performance of the hierarchical TiO <sub>2</sub> photocatalysts. <b>2014</b> , 225, 74-79	16
992	Photo-catalytic degradation of 2,4-DCP wastewater using MWCNT/TiO <sub>2</sub> nano-composite activated by UV and solar light. <b>2014</b> , 1-2, 24-29	15

991	Fabrication and Characterization of CuO-ZnO-Cu <sub>2</sub> O Nano-Composites by Sol-Gel Route: Effect of Calcinations Temperature. <b>2014</b> , 44, 1358-1362	4
990	TiO <sub>2</sub> -coated nanostructures for dye photo-degradation in water. <b>2014</b> , 9, 458	43
989	Viable Photocatalysts under Solar-Spectrum Irradiation: Nonplasmonic Metal Nanoparticles. <b>2014</b> , 126, 2979-2984	28
988	Synthesis and hydrophilic properties of Mo doped TiO <sub>2</sub> thin films. <b>2014</b> , 115, 213501	10
987	One-Pot Polyvinyl Alcohol-Assisted Hydrothermal Synthesis of Hierarchical Flower-Like BiOCl Nanoplates with Enhancement of Photocatalytic Activity for Degradation of Rhodamine B. <b>2014</b> , 42, 521-527	15
986	Active hydrogen species on TiO <sub>2</sub> for photocatalytic H <sub>2</sub> production. <b>2014</b> , 16, 7051-7	49
985	In situ surface hydrogenation synthesis of Ti <sup>3+</sup> self-doped TiO <sub>2</sub> with enhanced visible light photoactivity. <b>2014</b> , 6, 9078-84	137
984	Experimental and theoretical studies of H <sub>2</sub> O oxidation by neutral Ti <sub>2</sub> O <sub>4,5</sub> clusters under visible light irradiation. <b>2014</b> , 16, 13900-8	18
983	Defect self-doped TiO <sub>2</sub> for visible light activity and direct noble metal anchoring. <b>2014</b> , 16, 21876-81	25
982	Photocatalytic and photoelectrochemical oxidation mechanisms of methanol on TiO <sub>2</sub> in aqueous solution. <b>2014</b> , 319, 44-49	38
981	An N-doped anatase/rutile TiO <sub>2</sub> hybrid from low-temperature direct nitridization: enhanced photoactivity under UV-/visible-light. <b>2014</b> , 4, 420-427	38
980	Intermediate band in the gap of photosensitive hybrid gel based on titanium oxide: role of coordinated ligands during photoreduction. <b>2014</b> , 2, 11499-11508	18
979	Recent advances in TiO <sub>2</sub> -based photocatalysis. <b>2014</b> , 2, 12642	371
978	Efficient charge separation and photooxidation on cobalt phosphate-loaded TiO <sub>2</sub> mesocrystal superstructures. <b>2014</b> , 2, 3381-3388	46
977	Effect of phase composition, morphology, and specific surface area on the photocatalytic activity of TiO <sub>2</sub> nanomaterials. <b>2014</b> , 4, 47031-47038	88
976	Metabolomic effects in HepG2 cells exposed to four TiO <sub>2</sub> and two CeO <sub>2</sub> nanomaterials. <b>2014</b> , 1, 466-477	29
975	localized order-disorder transitions induced by Li segregation in amorphous TiO <sub>2</sub> nanoparticles. <b>2014</b> , 6, 18962-70	6
974	Coexistence of an anatase/TiO <sub>2</sub> (B) heterojunction and an exposed (001) facet in TiO <sub>2</sub> nanoribbon photocatalysts synthesized via a fluorine-free route and topotactic transformation. <b>2014</b> , 6, 5329-37	39

973	Towards highly efficient photoanodes: boosting sunlight-driven semiconductor nanomaterials for water oxidation. <b>2014</b> , 6, 7142-64	150
972	Formation and sintering of Pt nanoparticles on vicinal rutile TiO <sub>2</sub> surfaces. <b>2014</b> , 16, 21289-99	13
971	Probing the photochemistry of chemisorbed oxygen on TiO <sub>2</sub> (110) with Kr and other co-adsorbates. <b>2014</b> , 16, 2338-46	22
970	Cu(II) nanocluster-grafted, Nb-doped TiO <sub>2</sub> as an efficient visible-light-sensitive photocatalyst based on energy-level matching between surface and bulk states. <b>2014</b> , 2, 13571-13579	46
969	Plasmon-mediated, highly enhanced photocatalytic degradation of industrial textile dyes using hybrid ZnO@Ag core-shell nanorods. <b>2014</b> , 4, 58930-58940	100
968	UHV-FTIRS studies on molecular competitive adsorption: 12CO, 13CO and CO <sub>2</sub> on reduced TiO <sub>2</sub> (110) surfaces. <b>2014</b> , 16, 23711-5	5
967	Kinetic study on photocatalytic hydrogenation of acetophenone derivatives on titanium dioxide. <b>2014</b> , 4, 1084	34
966	Spectral Features of Photostimulated Oxygen Isotope Exchange and NO Adsorption on Self-Sensitized TiO <sub>2</sub> /TiO <sub>2</sub> in UV-Vis Region. <b>2014</b> , 118, 21986-21994	7
965	Cobalt sulfide quantum dots modified TiO <sub>2</sub> nanoparticles for efficient photocatalytic hydrogen evolution. <b>2014</b> , 39, 15387-15393	49
964	Enhanced Visible-Light Photoactivity of CuWO <sub>4</sub> through a Surface-Deposited CuO. <b>2014</b> , 118, 9982-9989	72
963	Adsorption Properties of Two-Dimensional NaCl: A Density Functional Theory Study of the Interaction of Co, Ag, and Au Atoms with NaCl/Au(111) Ultrathin Films. <b>2014</b> , 118, 12353-12363	5
962	Synergistic effect of interfacial lattice Ag(+) and Ag(0) clusters in enhancing the photocatalytic performance of TiO <sub>2</sub> . <b>2014</b> , 16, 19358-64	32
961	Super-resolution mapping of photogenerated electron and hole separation in single metal-semiconductor nanocatalysts. <b>2014</b> , 136, 1398-408	121
960	High surface area stainless steel wire mesh-supported TiO <sub>2</sub> prepared by sacrificial template accelerated hydrolysis. A monolithic photocatalyst superior to P25 TiO <sub>2</sub> . <b>2014</b> , 2, 2229-2235	9
959	Vicinal Rutile TiO <sub>2</sub> Surfaces and Their Interactions with O <sub>2</sub> . <b>2014</b> , 118, 3620-3628	12
958	Assessing the performance of dispersionless and dispersion-accounting methods: helium interaction with cluster models of the TiO <sub>2</sub> (110) surface. <b>2014</b> , 118, 6367-84	29
957	Titanium Dioxide Nanoparticle Surface Reactivity with Atmospheric Gases, CO <sub>2</sub> , SO <sub>2</sub> , and NO <sub>2</sub> : Roles of Surface Hydroxyl Groups and Adsorbed Water in the Formation and Stability of Adsorbed Products. <b>2014</b> , 118, 23011-23021	60
956	Fluorine- and Niobium-Doped TiO <sub>2</sub> : Chemical and Spectroscopic Properties of Polycrystalline n-Type-Doped Anatase. <b>2014</b> , 118, 8462-8473	56

955	Nitrogen doped anatase TiO <sub>2</sub> sheets with dominant {001} facets for enhancing visible-light photocatalytic activity. <b>2014</b> , 27, 47-50		10
954	Highly Crystalline Mesoporous TiO <sub>2</sub> (B) Nanofibers. <b>2014</b> , 118, 3049-3055		18
953	Comprehensive Kinetic and Mechanistic Analysis of TiO <sub>2</sub> Photocatalytic Reactions According to the Direct/Indirect Model: (II) Experimental Validation. <b>2014</b> , 118, 14276-14290		46
952	Ionic liquid assisted chemical strategy to TiO <sub>2</sub> hollow nanocube assemblies with surface-fluorination and nitridation and high energy crystal facet exposure for enhanced photocatalysis. <b>2014</b> , 6, 10283-95		35
951	Sandwich SrTiO <sub>3</sub> /TiO <sub>2</sub> /H-Titanate nanofiber composite photocatalysts for efficient photocatalytic hydrogen evolution. <b>2014</b> , 315, 314-322		26
950	Defect Sites in H <sub>2</sub> -Reduced TiO <sub>2</sub> Convert Ethylene to High Density Polyethylene without Activator. <i>ACS Catalysis</i> , <b>2014</b> , 4, 986-989	13.1	33
949	An enhanced photocatalytic response of nanometric TiO <sub>2</sub> wrapping of Au nanoparticles for eco-friendly water applications. <b>2014</b> , 6, 11189-95		50
948	Significantly Enhanced Visible-Light-Induced Photocatalytic Performance of Hybrid ZnO/r Layered Double Hydroxide/Graphene Nanocomposite and the Mechanism Study. <b>2014</b> , 53, 12943-12952		67
947	Titanium dioxide-based nanomaterials for photocatalytic fuel generations. <i>Chemical Reviews</i> , <b>2014</b> , 114, 9987-10043	68.1	1794
946	Multiscale Modelling of Organic and Hybrid Photovoltaics. <b>2014</b> ,		12
945	Controlling surface defects and photophysics in TiO <sub>2</sub> nanoparticles. <b>2014</b> , 118, 10631-8		33
944	Synthesis of Titanium Dioxide Nanoparticles for Photocatalytic Degradation of Cyanide in Wastewater. <b>2014</b> , 47, 1772-1782		43
943	Band Structure Tuning of TiO <sub>2</sub> for Enhanced Photoelectrochemical Water Splitting. <b>2014</b> , 118, 7451-7457		77
942	Probing the optical property and electronic structure of TiO <sub>2</sub> nanomaterials for renewable energy applications. <i>Chemical Reviews</i> , <b>2014</b> , 114, 9662-707	68.1	368
941	In-situ synthesis of g-C <sub>3</sub> N <sub>4</sub> -P25 TiO <sub>2</sub> composite with enhanced visible light photoactivity. <b>2014</b> , 16, 1		29
940	Doping high-surface-area mesoporous TiO <sub>2</sub> microspheres with carbonate for visible light hydrogen production. <b>2014</b> , 7, 2592		232
939	Aligned Fe <sub>2</sub> TiO <sub>5</sub> -containing nanotube arrays with low onset potential for visible-light water oxidation. <b>2014</b> , 5, 5122		144
938	Nitrogen-doped titanium dioxide as visible-light-sensitive photocatalyst: designs, developments, and prospects. <i>Chemical Reviews</i> , <b>2014</b> , 114, 9824-52	68.1	899

937	Bio-inspired titanium dioxide materials with special wettability and their applications. <i>Chemical Reviews</i> , <b>2014</b> , 114, 10044-94	68.1	415
936	Photoexcited Electron Hopping between TiO <sub>2</sub> Particles: Effect of Single-Walled Carbon Nanotubes. <b>2014</b> , 118, 23614-23620		6
935	Hierarchically Grown CaMn <sub>3</sub> O <sub>6</sub> Nanorods by RF Magnetron Sputtering for Enhanced Visible-Light-Driven Photocatalysis. <b>2014</b> , 118, 24127-24135		14
934	Behavior and Energy States of Photogenerated Charge Carriers on Pt- or CoO <sub>x</sub> -Loaded LaTiO <sub>2</sub> N Photocatalysts: Time-Resolved Visible to Mid-Infrared Absorption Study. <b>2014</b> , 118, 23897-23906		102
933	Photocatalytic organic pollutants degradation in metal-organic frameworks. <b>2014</b> , 7, 2831-2867		1133
932	Recent advances in BiOX (X = Cl, Br and I) photocatalysts: synthesis, modification, facet effects and mechanisms. <b>2014</b> , 1, 90		522
931	Quasiparticle Level Alignment for Photocatalytic Interfaces. <b>2014</b> , 10, 2103-13		54
930	Introduction: titanium dioxide (TiO <sub>2</sub> ) nanomaterials. <i>Chemical Reviews</i> , <b>2014</b> , 114, 9281-2	68.1	289
929	Photocatalytic degradation of phenol in aqueous solution by rare earth-doped SnO <sub>2</sub> nanoparticles. <b>2014</b> , 49, 5151-5159		37
928	Adsorption of dopamine on rutile TiO <sub>2</sub> (110): a photoemission and near-edge X-ray absorption fine structure study. <b>2014</b> , 30, 8761-9		16
927	Electrokinetic and adsorption properties of different titanium dioxides at the solid/solution interface. <b>2014</b> , 12, 1194-1205		4
926	Superhydrophilic Cu-doped TiO <sub>2</sub> thin film for solar-driven photocatalysis. <b>2014</b> , 40, 5107-5110		49
925	Titanium dioxide crystals with tailored facets. <i>Chemical Reviews</i> , <b>2014</b> , 114, 9559-612	68.1	796
924	Theoretical studies on anatase and less common TiO <sub>2</sub> phases: bulk, surfaces, and nanomaterials. <i>Chemical Reviews</i> , <b>2014</b> , 114, 9708-53	68.1	310
923	Viable photocatalysts under solar-spectrum irradiation: nonplasmonic metal nanoparticles. <b>2014</b> , 53, 2935-40		195
922	Comprehensive Kinetic and Mechanistic Analysis of TiO <sub>2</sub> Photocatalytic Reactions According to the Direct/Indirect Model: (I) Theoretical Approach. <b>2014</b> , 118, 14266-14275		30
921	Preparation and enhanced photocatalytic activity of TiO <sub>2</sub> nanocrystals with internal pores. <b>2014</b> , 6, 1608-15		95
920	Preparation and photocatalytic activity of B, Ce Co-doped TiO <sub>2</sub> hollow fibers photocatalyst. <b>2014</b> , 88, 1236-1240		1

919	Electrocatalytic Enhancement of Salicylic Acid Oxidation at Electrochemically Reduced TiO <sub>2</sub> Nanotubes. <i>ACS Catalysis</i> , <b>2014</b> , 4, 2616-2622	13.1	44
918	Shape and morphology effects on the electronic structure of TiO <sub>2</sub> nanostructures: from nanocrystals to nanorods. <b>2014</b> , 6, 2471-8		20
917	Facile in situ synthesis of BiOCl nanoplates stacked to highly porous TiO <sub>2</sub> synergistic combination for environmental remediation. <b>2014</b> , 6, 13994-4000		43
916	Density of state determination of two types of intra-gap traps in dye-sensitized solar cells and its influence on device performance. <b>2014</b> , 16, 11626-32		24
915	Surface Chemistry of Formaldehyde on Rutile TiO <sub>2</sub> (110) Surface: Photocatalysis vs Thermal-Catalysis. <b>2014</b> , 118, 20420-20428		56
914	Constructing a Metallic/Semiconducting TaB <sub>2</sub> /Ta <sub>2</sub> O <sub>5</sub> Core/Shell Heterostructure for Photocatalytic Hydrogen Evolution. <b>2014</b> , 4, 1400057		35
913	Defect-related photoluminescence and photocatalytic properties of porous ZnO nanosheets. <b>2014</b> , 2, 15377		234
912	Visible-Light Photocatalysis in Ca <sub>0.6</sub> Ho <sub>0.4</sub> MnO <sub>3</sub> Films Deposited by RF-Magnetron Sputtering Using Nanosized Powder Compacted Target. <b>2014</b> , 118, 590-597		12
911	Quantum-confinement induced enhancement in photocatalytic properties of iron oxide nanoparticles prepared by ionic liquid. <b>2014</b> , 40, 15743-15751		16
910	Preparation of TiO <sub>2</sub> /SnO <sub>2</sub> thin films by sol-gel method and periodic B3LYP simulations. <b>2014</b> , 118, 5857-65		20
909	Titanium-Niobium oxide nanocomposite thin films: Synthesis, characterization and antibacterial activity. <b>2014</b> , 144, 538-546		10
908	Thermal evolution of structure and photocatalytic activity in polymer microsphere templated TiO <sub>2</sub> microbowls. <b>2014</b> , 308, 50-57		19
907	Influence of calcination parameters on the synthesis of N-doped TiO <sub>2</sub> by the polymeric precursors method. <b>2014</b> , 215, 211-218		17
906	Enhanced visible light photocatalytic activity of TiO <sub>2</sub> nanotube arrays modified with CdSe nanoparticles by electrodeposition method. <b>2014</b> , 242, 20-28		17
905	Enhanced photocatalytic activity of Ag doped TiO <sub>2</sub> nanoparticles synthesized by a microwave assisted method. <b>2014</b> , 40, 5489-5496		140
904	Self-assembled three-dimensional hierarchical Bi <sub>2</sub> WO <sub>6</sub> microspheres by sol-gel/hydrothermal route. <b>2014</b> , 40, 6203-6209		22
903	Surface structures and thermodynamics of low-index of rutile, brookite and anatase TiO <sub>2</sub> comparative DFT study. <b>2014</b> , 288, 275-287		54
902	Photo-oxidation of an endocrine disrupting chemical o-chloroaniline with the assistance of TiO <sub>2</sub> and iodate: Reaction parameters and kinetic models. <b>2014</b> , 248, 273-279		7



901	Synthesis and characterization of a microfibrinous TiO <sub>2</sub> /CdS/palygorskite nanostructured material with enhanced visible-light photocatalytic activity. <b>2014</b> , 87, 285-291		47
900	Facile synthesis of porous microspheres composed of TiO <sub>2</sub> nanorods with high photocatalytic activity for hydrogen production. <b>2014</b> , 148-149, 281-287		58
899	Surface characterization of sputtered N:TiO <sub>2</sub> thin films within a wide range of dopant concentration. <b>2014</b> , 40, 9989-9995		15
898	A unique semiconductor-metal-graphene stack design to harness charge flow for photocatalysis. <b>2014</b> , 26, 5689-95		116
897	Titanium dioxide nanomaterials for sensor applications. <i>Chemical Reviews</i> , <b>2014</b> , 114, 10131-76	68.1	573
896	Self-modification of titanium dioxide materials by Ti <sup>3+</sup> and/or oxygen vacancies: new insights into defect chemistry of metal oxides. <b>2014</b> , 4, 13979-13988		84
895	Fast-growing field of magnetically recyclable nanocatalysts. <i>Chemical Reviews</i> , <b>2014</b> , 114, 6949-85	68.1	608
894	Photochemical splitting of water for hydrogen production by photocatalysis: A review. <b>2014</b> , 128, 85-101		470
893	Photocatalytic effects of wool fibers modified with solely TiO <sub>2</sub> nanoparticles and N-doped TiO <sub>2</sub> nanoparticles by using hydrothermal method. <b>2014</b> , 254, 106-114		24
892	Fabrication of positively and negatively charged, double-shelled, nanostructured hollow spheres for photodegradation of cationic and anionic aromatic pollutants under sunlight irradiation. <b>2014</b> , 160-161, 279-285		25
891	Gold-modified N-doped TiO <sub>2</sub> and N-doped WO <sub>3</sub> /TiO <sub>2</sub> semiconductors as photocatalysts for UV-visible light destruction of aqueous 2,4,6-trinitrotoluene solution. <b>2014</b> , 392, 194-201		20
890	Nanoscale anatase TiO <sub>2</sub> with dominant {111} facets shows high photocatalytic activity. <b>2014</b> , 311, 521-528		40
889	Control of optical absorption edge of TiO <sub>2</sub> through co-doped acceptors: The chemical trend. <b>2014</b> , 378, 2275-2279		3
888	Novel coupled structures of FeWO <sub>4</sub> /TiO <sub>2</sub> and FeWO <sub>4</sub> /TiO <sub>2</sub> /CdS designed for highly efficient visible-light photocatalysis. <b>2014</b> , 6, 9654-63		53
887	One-pot synthesis of monodisperse Zn coordination polymer micro/nanostructures and their transformation to mesoporous ZnO photocatalysts. <b>2014</b> , 4, 25160		11
886	Influence of surface states on the evaluation of the flat band potential of TiO <sub>2</sub> . <b>2014</b> , 6, 2401-6		20
885	Fabrication, characterization, and photocatalytic performance of exfoliated g-C <sub>3</sub> N <sub>4</sub> /TiO <sub>2</sub> hybrids. <b>2014</b> , 311, 574-581		151
884	A new approach to prepare Ti <sup>3+</sup> self-doped TiO <sub>2</sub> via NaBH <sub>4</sub> reduction and hydrochloric acid treatment. <b>2014</b> , 160-161, 240-246		203



883	Preparation and Characterization of TiO <sub>2</sub> Nanotube Arrays in Ionic Liquid for Water Splitting. <b>2014</b> , 136, 404-411	32
882	Chromate enhanced visible light driven TiO <sub>2</sub> photocatalytic mechanism on Acid Orange 7 photodegradation. <b>2014</b> , 274, 420-7	19
881	Structural, optical and morphological analyses of pristine titanium di-oxide nanoparticles--synthesized via sol-gel route. <b>2014</b> , 117, 622-9	112
880	Photocatalytic hydrogen production from glycerol and water with NiOx/TiO <sub>2</sub> catalysts. <b>2014</b> , 144, 41-45	76
879	Dye-sensitized Pt@TiO <sub>2</sub> core-shell nanostructures for the efficient photocatalytic generation of hydrogen. <b>2014</b> , 5, 360-4	14
878	Ultrafast multiphoton pump-probe photoemission excitation pathways in rutile TiO <sub>2</sub> (110). <b>2015</b> , 91,	37
877	Engineering of Self-Organizing Electrochemistry: Porous Alumina and Titania Nanotubes. <b>2015</b> , 145-192	3
876	Lattice distortion mechanism study of TiO <sub>2</sub> nanoparticles during photocatalysis degradation and reactivation. <b>2015</b> , 5, 057105	10
875	Photocatalytic oxidation of the organic monolayers on TiO <sub>2</sub> surface investigated by in-situ sum frequency generation spectroscopy. <b>2015</b> , 3, 104402	4
874	TiO <sub>2</sub> nanofibers supported on Ti sheets prepared by hydrothermal corrosion: effect of the microstructure on their photochemical and photoelectrochemical properties. <b>2015</b> , 5, 95038-95046	6
873	Stable Co-Catalyst-Free Photocatalytic H <sub>2</sub> Evolution From Oxidized Titanium Nitride Nanopowders. <b>2015</b> , 54, 13385-9	31
872	Stable Co-Catalyst-Free Photocatalytic H <sub>2</sub> Evolution From Oxidized Titanium Nitride Nanopowders. <b>2015</b> , 127, 13583-13587	2
871	Dual-Wavelength Irradiation and Dox Delivery for -Cancer Cell Ablation with Photocatalytic Pr Doped TiO <sub>2</sub> /NGO -Hybrid Nanocomposite. <b>2015</b> , 4, 1833-40	12
870	An Amorphous Carbon Nitride Photocatalyst with Greatly Extended Visible-Light-Responsive Range for Photocatalytic Hydrogen Generation. <b>2015</b> , 27, 4572-7	599
869	Correlation between Energy and Spatial Distribution of Intragap Trap States in the TiO <sub>2</sub> Photoanode of Dye-Sensitized Solar Cells. <b>2015</b> , 16, 2253-9	25
868	Enhanced Photocatalytic Activity of Pure Anatase TiO <sub>2</sub> and Pt-TiO <sub>2</sub> Nanoparticles Synthesized by Green Microwave Assisted Route. <b>2015</b> , 18, 473-481	59
867	Facile Preparation of Efficient WO <sub>3</sub> Photocatalysts Based on Surface Modification. <b>2015</b> , 2015, 1-7	6
866	Excitation Wavelength Dependence of Photocatalyzed Oxidation of Methanol on TiO <sub>2</sub> (110) <b>2015</b> , 28, 459-464	3

865	Low-Temperature Fabrication of Mesoporous Titanium Dioxide Thin Films with Tunable Refractive Indices for One-Dimensional Photonic Crystals and Sensors on Rigid and Flexible Substrates. <b>2015</b> , 7, 13180-8	29
864	Quantum chemical investigation on the role of Li adsorbed on anatase (101) surface nano-materials on the storage of molecular hydrogen. <b>2015</b> , 21, 142	2
863	Preparation, characterization, and photocatalytic activity of La-doped TiO <sub>2</sub> supported on activated carbon at the decomposition of methylene orange. <b>2015</b> , 89, 1108-1114	2
862	Synthesis of TiO <sub>2</sub> thin films with highly efficient surfaces using a sol-gel technique. <b>2015</b> , 37, 207-214	10
861	Improving the photocatalytic activity of TiO <sub>2</sub> through reduction. <b>2015</b> , 5, 35661-35666	16
860	From Molecules to Materials. <b>2015</b> ,	7
859	Synthesis, characterization and photocatalytic behavior of Ag doped TiO <sub>2</sub> thin film. <b>2015</b> , 85, 255-265	39
858	Low temperature synthesis of rutile TiO <sub>2</sub> single crystal nanorods with exposed (002) facets and their decoration with gold nanoparticles for photocatalytic applications. <b>2015</b> , 5, 45122-45128	8
857	Development of ZnO and ZrO <sub>2</sub> nanoparticles: Their photocatalytic and bactericidal activity. <b>2015</b> , 3, 886-891	27
856	Gadolinium doped tin dioxide nanoparticles: an efficient visible light active photocatalyst. <b>2015</b> , 33, 1275-1283	23
855	Promoting the oxidative removal rate of oxalic acid on gold-doped CeO <sub>2</sub> /TiO <sub>2</sub> photocatalysts under UV and visible light irradiation. <b>2015</b> , 156, 715-723	29
854	Optical Properties of TiO <sub>2</sub> Thin Films. <b>2015</b> , 73, 100-107	27
853	Efficient water oxidation under visible light by tuning surface defects on ceria nanorods. <b>2015</b> , 3, 20465-20470	65
852	A Stationary Reaction Current Effect in Mesoporous Pt/ZrO <sub>2</sub> System Under H <sub>2</sub> /O <sub>2</sub> Environment. <b>2015</b> , 7, 27749-54	9
851	Sub-10 nm rutile titanium dioxide nanoparticles for efficient visible-light-driven photocatalytic hydrogen production. <b>2015</b> , 6, 5881	535
850	Microwave-assisted synthesis of Ag-doped MOFs-like organotitanium polymer with high activity in visible-light driven photocatalytic NO oxidization. <b>2015</b> , 172-173, 46-51	88
849	Simulation of IRRAS Spectra for Molecules on Oxide Surfaces: CO on TiO <sub>2</sub> (110). <b>2015</b> , 119, 5403-5411	13
848	TiO <sub>2</sub> (110) Charge Donation to an Extended $\pi$ -Conjugated Molecule. <i>Journal of Physical Chemistry Letters</i> , <b>2015</b> , 6, 308-13	6.4 18

847	A new visible light active multifunctional ternary composite based on TiO <sub>2</sub> /h <sub>2</sub> O <sub>3</sub> nanocrystals heterojunction decorated porous graphitic carbon nitride for photocatalytic treatment of hazardous pollutant and H <sub>2</sub> evolution. <b>2015</b> , 170-171, 195-205	140
846	Quasiparticle interfacial level alignment of highly hybridized frontier levels: H <sub>2</sub> O on TiO <sub>2</sub> (110). <b>2015</b> , 11, 239-51	25
845	Impact of Nonadiabatic Charge Transfer on the Rate of Redox Chemistry of Carbon Oxides on Rutile TiO <sub>2</sub> (110) Surface. <i>ACS Catalysis</i> , <b>2015</b> , 5, 1764-1771	13.1 14
844	Endowing single-electron-trapped oxygen vacancy self-modified titanium dioxide with visible-light photocatalytic activity by grafting Fe(III) nanocluster. <b>2015</b> , 172-173, 37-45	20
843	Nanostructured TiO <sub>2</sub> /KIT-6 catalysts for improved photocatalytic reduction of CO <sub>2</sub> to tunable energy products. <b>2015</b> , 170-171, 53-65	36
842	Silica nanoparticles assisted photodegradation of acridine orange in aqueous suspensions. <b>2015</b> , 168-169, 363-369	20
841	Hydroxylation of the Rutile TiO <sub>2</sub> (110) Surface Enhancing Its Reducing Power for Photocatalysis. <b>2015</b> , 119, 1451-1456	38
840	TiO <sub>2</sub> nanosheet array thin film for self-cleaning coating. <b>2015</b> , 5, 9861-9864	19
839	On the role of localized surface plasmon resonance in UV-Vis light irradiated Au/TiO <sub>2</sub> photocatalysis systems: pros and cons. <b>2015</b> , 7, 4114-23	89
838	Dramatic enhancement of visible light photocatalysis due to strong interaction between TiO <sub>2</sub> and end-group functionalized P3HT. <b>2015</b> , 174-175, 193-202	12
837	Effects of architectures and H <sub>2</sub> O <sub>2</sub> additions on the photocatalytic performance of hierarchical Cu <sub>2</sub> O nanostructures. <b>2015</b> , 10, 8	30
836	Enhanced visible light photocatalytic performance of a novel heterostructured Bi <sub>4</sub> O <sub>5</sub> Br <sub>2</sub> /Bi <sub>24</sub> O <sub>31</sub> Br <sub>10</sub> /Bi <sub>2</sub> SiO <sub>5</sub> photocatalyst. <b>2015</b> , 172-173, 100-107	74
835	Thin Film Structures in Energy Applications. <b>2015</b> ,	5
834	Effect of Surface Structure on the Photoreactivity of TiO <sub>2</sub> . <b>2015</b> , 119, 6121-6127	41
833	An ultrasensitive label-free immunosensor based on CdS sensitized Fe-TiO <sub>2</sub> with high visible-light photoelectrochemical activity. <b>2015</b> , 74, 843-8	35
832	Recent developments in TiO <sub>2</sub> as n- and p-type transparent semiconductors: synthesis, modification, properties, and energy-related applications. <b>2015</b> , 50, 7495-7536	75
831	Nitrogen-modified nano-titania: True phase composition, microstructure and visible-light induced photocatalytic NO abatement. <b>2015</b> , 231, 87-100	14
830	Rutile {111} Faceted TiO <sub>2</sub> Film with High Ability for Selective Adsorption of Aldehyde. <b>2015</b> , 119, 17680-17686	6

829	Ethanol photocatalysis on rutile TiO <sub>2</sub> (110): the role of defects and water. <b>2015</b> , 17, 22809-14	37
828	Fabrication of TiO <sub>2</sub> /porous carbon nanofibers with superior visible photocatalytic activity. <b>2015</b> , 39, 7863-7872	25
827	Competition between oxidation and anti-oxidation to guarantee visible light activity for a TiO <sub>2</sub> photocatalyst from the dissolution of TiO. <b>2015</b> , 40, 9155-9164	3
826	Facile synthesis of ZnO hollow microspheres and their high performance in photocatalytic degradation and dye sensitized solar cells. <i>Journal of Alloys and Compounds</i> , <b>2015</b> , 647, 57-62	5-7 41
825	Site Specific Interaction Between TiO <sub>2</sub> Nanoparticles and Phenanthrimidazole-A First Principles Quantum Mechanical Study. <b>2015</b> , 25, 1063-83	4
824	Tunneling Desorption of Single Hydrogen on the Surface of Titanium Dioxide. <b>2015</b> , 9, 6837-42	20
823	Fabrication and Characterization of Cobalt Sensitized Nanostructure Zinc Oxide Thin Film Coated on Glass by Sol-Gel Spin Coating Using Trans-bis(acetylacetonato)-bis(4-methylpyridine)cobalt(III). <b>2015</b> , 45, 1642-1646	1
822	Selective photoredox activity on specific facet-dominated TiO <sub>2</sub> mesocrystal superstructures incubated with directed nanocrystals. <b>2015</b> , 176-177, 678-686	26
821	Laser-Modified Black Titanium Oxide Nanospheres and Their Photocatalytic Activities under Visible Light. <b>2015</b> , 7, 16070-7	99
820	Electronic structures of bare and terephthalic acid adsorbed TiO <sub>2</sub> (110)-(1 × 1) reconstructed surfaces: origin and reactivity of the band gap states. <b>2015</b> , 17, 20144-53	12
819	Completely oriented anatase TiO <sub>2</sub> nanoarrays: topotactic growth and orientation-related efficient photocatalysis. <b>2015</b> , 7, 13888-97	18
818	SnO <sub>2</sub> /BrO based nanocomposites and their photocatalytic activity for the treatment of organic pollutants. <b>2015</b> , 1098, 393-399	28
817	Coupled Heterojunction SnTe@SnO <sub>2</sub> Cooperative Promotion of Effective Electron-Hole Separation and Superior Visible-light Absorption. <b>2015</b> , 7, 13905-14	19
816	Comparing Quasiparticle H <sub>2</sub> O Level Alignment on Anatase and Rutile TiO <sub>2</sub> . <i>ACS Catalysis</i> , <b>2015</b> , 5, 4242-4254	35
815	Localized Excitation of Ti(3+) Ions in the Photoabsorption and Photocatalytic Activity of Reduced Rutile TiO <sub>2</sub> . <b>2015</b> , 137, 9146-52	139
814	Surface-mediated selective photocatalytic aerobic oxidation reactions on TiO <sub>2</sub> nanofibres. <b>2015</b> , 5, 56820-56831	16
813	Environmental Photochemistry Part III. <b>2015</b> ,	2
812	Water-plasma-assisted synthesis of black titania spheres with efficient visible-light photocatalytic activity. <b>2015</b> , 17, 13794-9	71

811	The synthesis of CdS/TiO <sub>2</sub> hetero-nanofibers with enhanced visible photocatalytic activity. <b>2015</b> , 452, 89-97	56
810	Enhanced photocatalytic activity for the degradation of rhodamine B by TiO <sub>2</sub> modified with Gd <sub>2</sub> O <sub>3</sub> calcined at high temperature. <b>2015</b> , 344, 249-256	36
809	Preparation of Ti <sup>3+</sup> self-doped TiO <sub>2</sub> nanoparticles and their visible light photocatalytic activity. <b>2015</b> , 36, 389-399	46
808	A unique Z-scheme 2D/2D nanosheet heterojunction design to harness charge transfer for photocatalysis. <b>2015</b> , 3, 11006-11013	106
807	Remarkable enhancement in visible-light absorption and electron transfer of carbon nitride nanosheets with 1% tungstate dopant. <b>2015</b> , 176-177, 91-98	12
806	Recent advances in rare-earth elements modification of inorganic semiconductor-based photocatalysts for efficient solar energy conversion: A review. <b>2015</b> , 33, 453-462	54
805	Defects on TiO <sub>2</sub> Key Pathways to Important Surface Processes. <b>2015</b> , 81-121	1
804	Numerical Simulations of Defective Structures: The Nature of Oxygen Vacancy in Non-reducible (MgO, SiO <sub>2</sub> , ZrO <sub>2</sub> ) and Reducible (TiO <sub>2</sub> , NiO, WO <sub>3</sub> ) Oxides. <b>2015</b> , 1-28	3
803	Recent theoretical progress in the development of photoanode materials for solar water splitting photoelectrochemical cells. <b>2015</b> , 3, 10632-10659	119
802	Oxygen deficient ZnO 1-x nanosheets with high visible light photocatalytic activity. <b>2015</b> , 7, 7216-23	148
801	Structure, synthesis, and applications of TiO <sub>2</sub> nanobelts. <b>2015</b> , 27, 2557-82	247
800	High-Performance Planar Perovskite Optoelectronic Devices: A Morphological and Interfacial Control by Polar Solvent Treatment. <b>2015</b> , 27, 3492-500	187
799	Engineering the intermediate band states in amorphous Ti <sup>3+</sup> -doped TiO <sub>2</sub> for hybrid dye-sensitized solar cell applications. <b>2015</b> , 3, 11437-11443	59
798	N,F-Monodoping and N/F-codoping effects on the electronic structures and optical performances of Zn <sub>2</sub> GeO <sub>4</sub> . <b>2015</b> , 17, 5613-23	8
797	Light illuminated Fe <sub>2</sub> O <sub>3</sub> /Pt nanoparticles as water activation agent for photoelectrochemical water splitting. <b>2015</b> , 5, 9130	42
796	Management on the location and concentration of Ti <sup>3+</sup> in anatase TiO <sub>2</sub> for defects-induced visible-light photocatalysis. <b>2015</b> , 176-177, 354-362	174
795	Recyclable Sn-TiO <sub>2</sub> /polythiophene nanohybrid material for degradation of organic pollutants under visible-light irradiation. <b>2015</b> , 36, 1668-1677	13
794	New insights into electrolyte-component biased and transfer- and transport-limited charge recombination in dye-sensitized solar cells. <b>2015</b> , 5, 84959-84966	5

793	Solution combustion synthesis of metal oxide nanomaterials for energy storage and conversion. <b>2015</b> , 7, 17590-610	259
792	One step preparation of highly dispersed TiO <sub>2</sub> nanoparticles. <b>2015</b> , 31, 688-692	3
791	Preparation of Bi <sub>2</sub> WO <sub>4</sub> /SnO <sub>2</sub> heterostructure with enhanced visible-light-driven photocatalytic activity. <b>2015</b> , 357, 1528-1535	27
790	Synthesis of Ag <sub>2</sub> CO <sub>3</sub> /Bi <sub>2</sub> WO <sub>6</sub> heterojunctions with enhanced photocatalytic activity and cycling stability. <b>2015</b> , 5, 97195-97204	35
789	Communication: unraveling the (4)He droplet-mediated soft-landing from ab initio-assisted and time-resolved density functional simulations: Au@(4)He <sub>300</sub> /TiO <sub>2</sub> (110). <b>2015</b> , 142, 131101	34
788	Titanium functionalized Zirconium phosphate single layer nanosheets for photocatalyst applications. <b>2015</b> , 5, 93969-93978	21
787	Enhancement of visible-light photocatalytic activity in BiFeO <sub>3</sub> @carbon-microspheres heterostructures and its mechanism implication. <b>2015</b> , 26, 7496-7501	4
786	Facile synthesis of an iron doped rutile TiO <sub>2</sub> photocatalyst for enhanced visible-light-driven water oxidation. <b>2015</b> , 3, 21434-21438	44
785	Electric-dipole effect of defects on the energy band alignment of rutile and anatase TiO <sub>2</sub> . <b>2015</b> , 17, 29079-84	21
784	A Multitechnique Study of CO Adsorption on the TiO <sub>2</sub> Anatase (101) Surface. <b>2015</b> , 119, 21044-21052	48
783	Light-Induced Processes in Plasmonic Gold/TiO <sub>2</sub> Photocatalysts Studied by Electron Paramagnetic Resonance. <b>2015</b> , 58, 776-782	33
782	Sustainable Energy Application. <b>2015</b> , 181-231	
781	Impact of distributions on the photocatalytic performance of anatase nanoparticle ensembles. <b>2015</b> , 3, 60-64	8
780	Rational design of nanomaterials for water treatment. <b>2015</b> , 7, 17167-94	157
779	Borate-Mediated Hole Transfer from Irradiated Anatase TiO <sub>2</sub> to Phenol in Aqueous Solution. <b>2015</b> , 119, 21376-21385	8
778	Control synthesis and formation mechanism of sphere-like titanium dioxide. <b>2015</b> , 10, 23-27	1
777	Synthesis of Cr-doped SrTiO <sub>3</sub> photocatalyst and its application in visible-light-driven transformation of CO <sub>2</sub> into CH <sub>4</sub> . <b>2015</b> , 12, 43-48	66
776	Photocatalytic organic degradation over W-rich and Cu-rich CuWO <sub>4</sub> under UV and visible light. <b>2015</b> , 5, 8108-8113	36

775	Effect of oxygen and WO <sub>3</sub> additive on anatase-to-rutile phase transformation in TiO <sub>2</sub> nanoparticles. <b>2015</b> , 119, 435-439	7
774	Preparation and Photocatalytic Activity of Mesoporous TiO <sub>2</sub> Photocatalyst Co-doped with Fe and H <sub>3</sub> PW <sub>12</sub> O <sub>40</sub> . <b>2015</b> , 62, 163-169	4
773	Understanding the fate and biological effects of Ag- and TiO <sub>2</sub> nanoparticles in the environment: The quest for advanced analytics and interdisciplinary concepts. <b>2015</b> , 535, 3-19	137
772	Novel nanostructured-TiO <sub>2</sub> materials for the photocatalytic reduction of CO <sub>2</sub> greenhouse gas to hydrocarbons and syngas. <b>2015</b> , 149, 55-65	58
771	Near-infrared light photocatalysis with metallic/semiconducting H <sub>x</sub> WO <sub>3</sub> /WO <sub>3</sub> nanoheterostructure in situ formed in mesoporous template. <b>2015</b> , 168-169, 9-13	13
770	Enhanced visible light responsive photocatalytic activity of TiO <sub>2</sub> -based nanocrystallites: impact of doping sequence. <b>2015</b> , 5, 7363-7369	19
769	Probing electrons in TiO <sub>2</sub> polaronic trap states by IR-absorption: evidence for the existence of hydrogenic states. <b>2014</b> , 4, 3808	70
768	Defective TiO <sub>2</sub> -supported Cu nanoparticles as efficient and stable electrocatalysts for oxygen reduction in alkaline media. <b>2015</b> , 7, 1224-32	32
767	Fe <sub>3</sub> O <sub>4</sub> @TiO <sub>2</sub> preparation and catalytic activity in heterogeneous photocatalytic and ozonation processes. <b>2015</b> , 5, 1143-1152	23
766	Hierarchical TiO <sub>2</sub> nanowire/graphite fiber photoelectrocatalysis setup powered by a wind-driven nanogenerator: A highly efficient photoelectrocatalytic device entirely based on renewable energy. <b>2015</b> , 11, 19-27	92
765	TiO <sub>2</sub> nanoparticles with efficient photocatalytic activity towards gaseous benzene degradation. <b>2015</b> , 41, 2836-2839	15
764	Carbon quantum dots/hydrogenated TiO <sub>2</sub> nanobelt heterostructures and their broad spectrum photocatalytic properties under UV, visible, and near-infrared irradiation. <b>2015</b> , 11, 419-427	352
763	Adsorption of organic molecules at the TiO <sub>2</sub> (110) surface: The effect of van der Waals interactions. <b>2015</b> , 632, 142-153	49
762	Layered KTiNbO <sub>5</sub> photocatalyst modified with transitional metal ions (Mn <sup>2+</sup> , Ni <sup>2+</sup> ): Investigation of microstructure and photocatalytic reaction pathways for the oxidation of dimethyl sulfide and ethyl mercaptan. <b>2015</b> , 270, 154-162	17
761	Aberration-corrected Scanning Transmission Electron Microscopy and Spectroscopy of Nonprecious Metal Nanoparticles in Titania Aerogels. <b>2016</b> , 22, 324-325	
760	Pulsed Laser-Deposited TiO <sub>2</sub> -based Films: Synthesis, Electronic Structure and Photocatalytic Activity. <b>2016</b> ,	2
759	Effect of Temperature of Electron Beam Evaporated CdSe Thin Films. <b>2016</b> , 05,	1
758	Catalysis by Supported Gold Nanoparticles. <b>2016</b> ,	



757	A Modified Thermal Treatment Method for the Up-Scalable Synthesis of Size-Controlled Nanocrystalline Titania. <b>2016</b> , 6, 295	3
756	Microstructure and Characteristic of BiVO <sub>4</sub> Prepared under Different pH Values: Photocatalytic Efficiency and Antibacterial Activity. <b>2016</b> , 9,	20
755	Stoichiometry and structure driven optical properties of carbon incorporated titanium oxide thin films. <b>2016</b> , 6, 3594	3
754	BiOX (X = Cl, Br, and I) Photocatalysts. <b>2016</b> ,	5
753	Inorganic Antiflaming Wood Caused by aTiO <sub>2</sub> -Decorated ZnO Nanorod Arrays Coating Prepared by a Facile Hydrothermal Method. <b>2016</b> , 2016, 1-9	9
752	In Situ Synthesis of Ti <sup>3+</sup> Self-Doped TiO <sub>2</sub> /N-Doped Carbon Nanocomposites and its Visible Light Photocatalytic Performance. <b>2016</b> , 11, 1650088	3
751	Comparing the Contribution of Visible-Light Irradiation, Gold Nanoparticles, and Titania Supports in Photocatalytic Nitroaromatic Coupling and Aromatic Alcohol Oxidation. <b>2016</b> , 33, 628-634	7
750	Following the Reduction of Oxygen on TiO <sub>2</sub> Anatase (101) Step by Step. <b>2016</b> , 138, 9565-71	56
749	Progress of Carbon Quantum Dots in Photocatalysis Applications. <b>2016</b> , 33, 457-472	121
748	In Situ Fluorine Doping of TiO <sub>2</sub> Superstructures for Efficient Visible-Light Driven Hydrogen Generation. <b>2016</b> , 9, 617-23	46
747	Progress in Black Titania: A New Material for Advanced Photocatalysis. <b>2016</b> , 6, 1600452	193
746	Metal-Organic Framework (MOF) Compounds: Photocatalysts for Redox Reactions and Solar Fuel Production. <b>2016</b> , 55, 5414-45	675
745	Alumina coating with TiO <sub>2</sub> and its effect on catalytic photodegradation of phenol and p-cresol. <b>2016</b> , 91, 2211-2220	11
744	Comparative study on the effect of H <sub>2</sub> pre-adsorption on CO oxidation in O <sub>2</sub> -poor atmosphere over Au/TiO <sub>2</sub> and TiO <sub>2</sub> : Temperature programmed surface reaction by a multiplexed mass spectrometer testing. <b>2016</b> , 387, 1062-1071	5
743	Dramatic visible light photocatalytic degradation due to the synergetic effects of TiO <sub>2</sub> and PDA nanospheres. <b>2016</b> , 6, 64446-64449	23
742	Structural and Magnetic Properties of <sup>57</sup> Fe-Doped TiO <sub>2</sub> and <sup>57</sup> Fe/Sn-Codoped TiO <sub>2</sub> Prepared by a Soft-Chemical Process. <b>2016</b> , 2016, 2131-2135	6
741	Fe <sub>3</sub> O <sub>4</sub> /CuO/ZnO/Nano graphene platelets (Fe <sub>3</sub> O <sub>4</sub> /CuO/ZnO/NGP) composites prepared by sol-gel method with enhanced sonocatalytic activity for the removal of dye. <b>2016</b> ,	1
740	Effect of Heat Treatment on the Structural Properties of TiO <sub>2</sub> Films Produced by Sol-Gel Spin Coating Technique. <b>2016</b> , 766, 012026	7



739	Structural Change of the Rutile TiO <sub>2</sub> (110) Surface During the Photoinduced Wettability Conversion. <b>2016</b> , 120, 29107-29115	16
738	Donor defects and small polarons on the TiO <sub>2</sub> (110) surface. <b>2016</b> , 119, 181503	44
737	A nanosecond pulsed laser heating system for studying liquid and supercooled liquid films in ultrahigh vacuum. <b>2016</b> , 144, 164201	8
736	Gas phase vibrational spectroscopy of cold (TiO <sub>2</sub> ) <sub>n</sub> (-) (n = 3-8) clusters. <b>2016</b> , 144, 124308	13
735	Titania species on two-dimensional HNbMoO <sub>6</sub> nanosheets: structural feature, interaction model, and synergistic effect for photocatalytic degradation of methylene blue. <b>2016</b> , 10, 046015	3
734	Enhanced photo-catalytic activity of the composite of TiO <sub>2</sub> and conjugated derivative of polyvinyl alcohol immobilized on cordierite under visible light irradiation. <b>2016</b> , 25, 55-61	5
733	Efficient photo catalytic degradation of methyl orange over Ag <sub>2</sub> UO nanostructures grown on copper foil under visible light irradiation. <b>2016</b> , 27, 6542-6551	17
732	Performance of a modified hybrid functional in the simultaneous description of stoichiometric and reduced TiO <sub>2</sub> polymorphs. <b>2016</b> , 18, 12357-67	37
731	Photocatalytic H <sub>2</sub> Generation Using Dewetted Pt-Decorated TiO <sub>2</sub> Nanotubes: Optimized Dewetting and Oxide Crystallization by a Multiple Annealing Process. <b>2016</b> , 120, 15884-15892	39
730	Interaction of Formaldehyde with the Rutile TiO <sub>2</sub> (110) Surface: A Combined Experimental and Theoretical Study. <b>2016</b> , 120, 12626-12636	40
729	Ligand-directed rapid formation of ultralong ZnO nanowires by oriented attachment for UV photodetectors. <b>2016</b> , 4, 5755-5765	20
728	Graphitic Carbon Nitride (g-C <sub>3</sub> N <sub>4</sub> )-Based Photocatalysts for Artificial Photosynthesis and Environmental Remediation: Are We a Step Closer To Achieving Sustainability?. <i>Chemical Reviews</i> , <b>2016</b> , 116, 7159-329	68.1 4018
727	Quenching of electron transfer reactions through coadsorption: A study of oxygen photodesorption from TiO <sub>2</sub> (110). <b>2016</b> , 652, 183-188	10
726	Photoinduced Carbonyl Coupling of Aldehydes on Anatase TiO <sub>2</sub> (101). <b>2016</b> , 120, 9897-9903	7
725	Self-assembly graphitic carbon nitride quantum dots anchored on TiO <sub>2</sub> nanotube arrays: An efficient heterojunction for pollutants degradation under solar light. <b>2016</b> , 316, 159-68	78
724	Facile strategy for controllable synthesis of stable mesoporous black TiO <sub>2</sub> hollow spheres with efficient solar-driven photocatalytic hydrogen evolution. <b>2016</b> , 4, 7495-7502	173
723	Electronic properties and photoactivity of monolayer MoS <sub>2</sub> /fullerene van der Waals heterostructures. <b>2016</b> , 6, 43228-43236	26
722	Novel Titanium Oxide Materials Synthesized by Solvothermal and Supercritical Fluid Processes. <b>2016</b> , 3-21	

7 <sup>21</sup>	Decontamination of Chemical Warfare Agents on sensitive equipment materials using Zr 4+ and Ge 4+ co-doped TiO <sub>2</sub> and hydrofluoroether suspension. <b>2016</b> , 302, 111-119	11
7 <sup>20</sup>	Locating structures and evolution pathways of reconstructed rutile TiO <sub>2</sub> (011) using genetic algorithm aided density functional theory calculations. <b>2016</b> , 22, 114	2
7 <sup>19</sup>	Heterojunctions in g-C <sub>3</sub> N <sub>4</sub> /B-TiO <sub>2</sub> nanosheets with exposed {001} plane and enhanced visible-light photocatalytic activities. <b>2016</b> , 41, 7292-7300	48
7 <sup>18</sup>	Novel visible-light-responsive photo-catalysts based on palladium decorated nanotube films fabricated on titanium substrates. <b>2016</b> , 42, 11209-11216	10
7 <sup>17</sup>	A New Route for Surface Modification: Fluorine-Induced Superhydrophilicity. <b>2016</b> , 120, 11882-11888	13
7 <sup>16</sup>	TiO <sub>2</sub> /Graphene Composites with Excellent Performance in Photocatalysis. <b>2016</b> , 23-67	4
7 <sup>15</sup>	Hollow CoreShell Titania Photocatalysts for Selective Organic Synthesis. <b>2016</b> , 137-146	
7 <sup>14</sup>	A new form of chemisorbed photo- and electro-active atomic H species on the TiO <sub>2</sub> (110) surface. <b>2016</b> , 652, 195-199	9
7 <sup>13</sup>	Temperature study of magnetic resonance spectra of co-modified (Co,N)-TiO <sub>2</sub> nanocomposites. <b>2016</b> , 34, 242-250	3
7 <sup>12</sup>	Effect of surface charge of TiO <sub>2</sub> particles on hydroxyapatite formation in simulated body fluid. <b>2016</b> , 27, 2409-2415	3
7 <sup>11</sup>	Photocatalytic oxidation of methane over SrCO decorated SrTiO nanocatalysts via a synergistic effect. <b>2016</b> , 18, 31400-31409	28
7 <sup>10</sup>	Mechanism of enhanced photocatalytic activities on tungsten trioxide doped with sulfur: Dopant-type effects. <b>2016</b> , 30, 1650340	2
7 <sup>09</sup>	Efficient photocatalytic degradation of organic dyes and reaction mechanism with Ag <sub>2</sub> CO <sub>3</sub> /Bi <sub>2</sub> O <sub>2</sub> CO <sub>3</sub> photocatalyst under visible light irradiation. <b>2016</b> , 425, 124-135	65
7 <sup>08</sup>	First-principle study for influence of an external electric field on the electronic structure and optical properties of TiO <sub>2</sub> . <b>2016</b> , 6, 98908-98915	11
7 <sup>07</sup>	Clew-like hierarchical ZnO nanostructure assembled by nanosheets as an efficient photocatalyst for degradation of azure B. <b>2016</b> , 27, 10052-10058	9
7 <sup>06</sup>	Review of functional titanium oxides. I: TiO <sub>2</sub> and its modifications. <b>2016</b> , 44, 86-105	182
7 <sup>05</sup>	Unique Three-Dimensional InP Nanopore Arrays for Improved Photoelectrochemical Hydrogen Production. <b>2016</b> , 8, 22493-500	13
7 <sup>04</sup>	Adsorption of Noble-Gas Atoms on the TiO <sub>2</sub> (110) Surface: An Ab Initio-Assisted Study with van der Waals-Corrected DFT. <b>2016</b> , 120, 18126-18139	46

703	Functional Tantalum-based Oxides: From the Structure to the Applications. <b>2016</b> , 337-383	1
702	Emerging trends in photodegradation of petrochemical wastes: a review. <b>2016</b> , 23, 22340-22364	34
701	Titania Nanotube Arrays (TNAs) as Support for Oxygen Reduction Reaction (ORR) Platinum Thin Film Catalysts. <b>2016</b> , 7, 451-465	6
700	Liquid-exfoliation of layered MoS <sub>2</sub> for enhancing photocatalytic activity of TiO <sub>2</sub> /g-C <sub>3</sub> N <sub>4</sub> photocatalyst and DFT study. <b>2016</b> , 389, 496-506	102
699	N-Doped TiO <sub>2</sub> Nanotube Arrays: Synthesis by Anodization in an Ionic Liquid ([BMIM]BF <sub>4</sub> ) and Assessment of Photocatalytic Property. <b>2016</b> , 45, 561-566	9
698	Hydrothermal synthesis of the novel rutile-mixed anatase TiO <sub>2</sub> nanosheets with dominant {001} facets for high photocatalytic activity. <b>2016</b> , 6, 84035-84041	17
697	Photovoltaic properties of titanium dioxide nanowires with different crystal structures. <b>2016</b> , 32, 661-664	5
696	Improved visible light photocatalytic activity of WO <sub>3</sub> through CuWO <sub>4</sub> for phenol degradation. <b>2016</b> , 389, 491-495	23
695	Interfacial phenomena at a surface of individual and complex fumed nanooxides. <b>2016</b> , 235, 108-189	37
694	The annealing temperature dependence of anatase TiO <sub>2</sub> thin films prepared by the electron-beam evaporation method. <b>2016</b> , 31, 125012	37
693	Development of tailored TiO <sub>2</sub> mesocrystals for solar driven photocatalysis. <b>2016</b> , 25, 917-926	26
692	La-Doped Nanometer TiO <sub>2</sub> Powders Prepared by Sol-Gel Method. <b>2016</b> , 697, 97-100	
691	Novel application of metal-free graphitic carbon nitride (g-C <sub>3</sub> N <sub>4</sub> ) in photocatalytic reduction/Recovery of silver ions. <b>2016</b> , 4, 4165-4172	18
690	Molecular weight effects of PEG on the crystal structure and photocatalytic activities of PEG-capped TiO <sub>2</sub> nanoparticles. <b>2016</b> , 6, 83366-83372	11
689	Magnetically separable Fe <sub>3</sub> O <sub>4</sub> @TiO <sub>2</sub> nanospheres: preparation and photocatalytic activity. <b>2016</b> , 27, 9983-9988	9
688	X-Ray Powder Diffraction Characterization of Nanomaterials. <b>2016</b> , 545-608	8
687	Fabrication, characterization, and visible-light photocatalytic performance of ternary plasmonic composites. <b>2016</b> , 511, 329-338	1
686	Excitonic Interfacial Proton-Coupled Electron Transfer Mechanism in the Photocatalytic Oxidation of Methanol to Formaldehyde on TiO(110). <b>2016</b> , 138, 16165-16173	50

- 685 Hydrogen Oxidation-Mediated Current Discharge in Mesoporous Pt/TiO Nanocomposite. **2016**, 8, 32077-32082 **11**
- 684 Facile synthesis of MoS<sub>2</sub>/B-TiO<sub>2</sub> nanosheets with exposed {001} facets and enhanced visible-light-driven photocatalytic H<sub>2</sub> production activity. **2016**, 6, 107075-107080 **17**
- 683 In situ growth of small Au nanoparticles on ZnO nanorods via ultrasonic irradiation toward super-enhanced catalytic activity. **2016**, 6, 107433-107441 **15**
- 682 Exceptional performance of photoelectrochemical water oxidation of single-crystal rutile TiO<sub>2</sub> nanorods dependent on the hole trapping of modified chloride. **2016**, 6, 21430 **23**
- 681 Unravelling Site-Specific Photo-Reactions of Ethanol on Rutile TiO<sub>2</sub>(110). **2016**, 6, 21990 **39**
- 680 Unravelling the Efficient Photocatalytic Activity of Boron-induced Ti Species in the Surface Layer of TiO. **2016**, 6, 34765 **37**
- 679 A lanthanide-titanium (LnTi) oxo-cluster, a potential molecule based fluorescent labelling agent and photocatalyst. **2016**, 45, 17681-17686 **24**
- 678 Synthesis and characterization of UV-treated Fe-doped bismuth lanthanum titanate-doped TiO<sub>2</sub> layers in dye-sensitized solar cells. **2016**, 68, 1399-1402 **1**
- 677 Titanium mesh supported TiO<sub>2</sub> nanowire arrays/Nb-doped TiO<sub>2</sub> nanoparticles for fully flexible dye-sensitized solar cells with improved photovoltaic properties. **2016**, 4, 11118-11128 **20**
- 676 g-C<sub>3</sub>N<sub>4</sub>/TiO<sub>2</sub> Nanocomposites for Degradation of Ciprofloxacin under Visible Light Irradiation. **2016**, 1, 5679-5685 **35**
- 675 UV-TiO<sub>2</sub> photocatalytic disinfection and photoreactivation of pathogenic bacterium in municipal wastewater. **2016**, 23, 3115-3121 **2**
- 674 Photoelectrical characteristics of TiO<sub>2</sub>-N-Si heterostructures. **2016**, 58, 1113-1116 **12**
- 673 Metall-organische Gerüstverbindungen: Photokatalysatoren für Redoxreaktion und die Produktion von Solarbrennstoffen. **2016**, 128, 5504-5535 **69**
- 672 TiO<sub>2</sub> Nanotubes: Nitrogen-Ion Implantation at Low Dose Provides Noble-Metal-Free Photocatalytic H<sub>2</sub>-Evolution Activity. **2016**, 128, 3827-3831 **22**
- 671 TiO<sub>2</sub> Nanotubes: Nitrogen-Ion Implantation at Low Dose Provides Noble-Metal-Free Photocatalytic H<sub>2</sub> -Evolution Activity. **2016**, 55, 3763-7 **102**
- 670 Portable photocatalytic air cleaners: efficiencies and by-product generation. **2016**, 23, 7482-93 **23**
- 669 Pd-catalyzed instant hydrogenation of TiO<sub>2</sub> with enhanced photocatalytic performance. **2016**, 9, 2410-2417 **100**
- 668 Facet-dependent trapping and dynamics of excess electrons at anatase TiO<sub>2</sub> surfaces and aqueous interfaces. **2016**, 15, 1107-12 **241**

667	The effect of double impurity cluster of Ni and Co in TiO <sub>2</sub> bulk; a DFT study. <b>2016</b> , 37, 79-84		7
666	Solvothermal alcoholysis synthesis of hierarchical TiO <sub>2</sub> with enhanced activity in environmental and energy photocatalysis. <b>2016</b> , 28, 72-86		72
665	Copper nanoparticles supported on diamond nanoparticles as a cost-effective and efficient catalyst for natural sunlight assisted Fenton reaction. <b>2016</b> , 6, 7077-7085		18
664	Selenide and Sulfide Quantum Dots and Nanocrystals: Optical Properties. <b>2016</b> , 319-332		
663	Solar water-splitting using palladium modified tungsten trioxide-titania nanotube photocatalysts. <b>2016</b> , 27, 1805-1811		13
662	Synthesis of heterostructured Pd@TiO <sub>2</sub> /TiO <sub>2</sub> nanohybrids with enhanced photocatalytic performance. <i>Materials Research Bulletin</i> , <b>2016</b> , 80, 337-343	5.1	16
661	Role of surface water molecules in stabilizing trapped hole centres in titanium dioxide (anatase) as monitored by electron paramagnetic resonance. <b>2016</b> , 322-323, 27-34		32
660	Surface chemistry of Au/TiO <sub>2</sub> : Thermally and photolytically activated reactions. <b>2016</b> , 71, 77-271		88
659	Surface heterojunction between (001) and (101) facets of ultrafine anatase TiO <sub>2</sub> nanocrystals for highly efficient photoreduction CO <sub>2</sub> to CH <sub>4</sub> . <b>2016</b> , 198, 378-388		92
658	Novel photothermocatalytic synergetic effect leads to high catalytic activity and excellent durability of anatase TiO <sub>2</sub> nanosheets with dominant {001} facets for benzene abatement. <b>2016</b> , 198, 303-310		51
657	The effect of ionic Co presence on the structural, optical and photocatalytic properties of modified cobalt-titanate nanotubes. <b>2016</b> , 18, 18081-93		24
656	Niobium Doping Enhances Charge Transport in TiO <sub>2</sub> Nanorods. <b>2016</b> , 2, 660-664		9
655	N-Doped TiO <sub>2</sub> Nanobelts with Coexposed (001) and (101) Facets and Their Highly Efficient Visible-Light-Driven Photocatalytic Hydrogen Production. <b>2016</b> , 8, 18126-31		134
654	Preparation and characterization of TiO <sub>2</sub> /ZnO/CuO nanocomposite and application for phenol removal from wastewaters. <b>2016</b> , 57, 799-809		16
653	Synthesis of TiO <sub>2</sub> @WO <sub>3</sub> /Au Nanocomposite Hollow Spheres with Controllable Size and High Visible-Light-Driven Photocatalytic Activity. <b>2016</b> , 4, 1581-1590		66
652	Effect of Water Adsorption on Carrier Trapping Dynamics at the Surface of Anatase TiO <sub>2</sub> Nanoparticles. <b>2016</b> , 16, 1323-7		43
651	Preparation of polypyrrole/TiO <sub>2</sub> nanocomposites with enhanced photocatalytic performance. <b>2016</b> , 26, 73-78		56
650	Titanium incorporated with UiO-66(Zr)-type Metal-Organic Framework (MOF) for photocatalytic application. <b>2016</b> , 6, 3671-3679		109

649	Amino-terminated diamond surfaces: Photoelectron emission and photocatalytic properties. <b>2016</b> , 650, 295-301		22
648	Defective TiO <sub>2</sub> with oxygen vacancy and nanocluster modification for efficient visible light environment remediation. <b>2016</b> , 264, 236-242		33
647	Recent advances in the TiO <sub>2</sub> /CdS nanocomposite used for photocatalytic hydrogen production and quantum-dot-sensitized solar cells. <b>2016</b> , 54, 1048-1059		106
646	Correlation between donating or accepting electron behavior of the adsorbed CO or H <sub>2</sub> and its oxidation over TiO <sub>2</sub> under ultraviolet light irradiation. <b>2016</b> , 360, 698-706		19
645	Anatase nano-TiO <sub>2</sub> with exposed curved surface for high photocatalytic activity. <i>Journal of Alloys and Compounds</i> , <b>2016</b> , 661, 441-447	5-7	41
644	Synergistic promotion of solar-driven H <sub>2</sub> generation by three-dimensionally ordered macroporous structured TiO <sub>2</sub> -Au-CdS ternary photocatalyst. <b>2016</b> , 184, 182-190		117
643	Synthesis and characterization of RF sputtered WO <sub>3</sub> /TiO <sub>2</sub> bilayers. <b>2016</b> , 285, 197-202		14
642	Photoreductive transformation of fluorinated acetophenone derivatives on titanium dioxide: Defluorination vs. reduction of carbonyl group. <b>2016</b> , 521, 68-74		12
641	CO <sub>2</sub> photo-reduction: insights into CO <sub>2</sub> activation and reaction on surfaces of photocatalysts. <b>2016</b> , 9, 2177-2196		1038
640	TiO <sub>2</sub> encapsulated in Salicylaldehyde-NH <sub>2</sub> -MIL-101(Cr) for enhanced visible light-driven photodegradation of MB. <b>2016</b> , 191, 192-201		126
639	Graphene-linked graphitic carbon nitride/TiO <sub>2</sub> nanowire arrays heterojunction for efficient solar-driven water splitting. <b>2016</b> , 46, 807-817		16
638	Highly photocatalytic active thiomolybdate [Mo <sub>3</sub> S <sub>13</sub> ] <sub>2</sub> clusters/Bi <sub>2</sub> WO <sub>6</sub> nanocomposites. <b>2016</b> , 274, 22-27		10
637	Temperature influence on microstructure and optical properties of TiO <sub>2</sub> /Au thin films. <b>2016</b> , 122, 1		2
636	Carbon-dot-decorated TiO <sub>2</sub> nanotube arrays used for photo/voltage-induced organic pollutant degradation and the inactivation of bacteria. <b>2016</b> , 27, 115301		13
635	In situ infrared study of photoreaction of ethanol on Au and Ag/TiO <sub>2</sub> . <b>2016</b> , 264, 16-22		24
634	Superoxide Ion: Generation and Chemical Implications. <i>Chemical Reviews</i> , <b>2016</b> , 116, 3029-85	68.1	983
633	Photocatalytic activity of nanohybrid Co-TCPP@TiO <sub>2</sub> /WO <sub>3</sub> in aerobic oxidation of alcohols under visible light. <b>2016</b> , 4, 3933-3946		40
632	Structural, optical and morphological properties of post-growth calcined TiO <sub>2</sub> nanopowder for opto-electronic device application: Ex-situ studies. <i>Journal of Alloys and Compounds</i> , <b>2016</b> , 671, 486-492	5-7	52

631	A novel hexanuclear titanium(IV)-oxo-iminodiacetate cluster with a Ti <sub>6</sub> O <sub>9</sub> core: single-crystal structure and photocatalytic activities. <b>2016</b> , 45, 7581-8	18
630	Terbium doped ZnCr-layered double hydroxides with largely enhanced visible light photocatalytic performance. <b>2016</b> , 4, 3907-3913	53
629	Inductive effect of poly(vinyl pyrrolidone) on morphology and photocatalytic performance of Bi <sub>2</sub> WO <sub>6</sub> . <b>2016</b> , 368, 332-340	26
628	Silica supported TiO <sub>2</sub> nanostructures for highly efficient photocatalytic application under visible light irradiation. <i>Materials Research Bulletin</i> , <b>2016</b> , 76, 353-357	5.1 30
627	Influence of titanium doping on the structure and properties of hollow glass microspheres for inertial confinement fusion. <b>2016</b> , 436, 22-28	3
626	Photocatalytic production of hydrogen from biomass-derived feedstocks. <b>2016</b> , 315, 1-66	238
625	Feed-back action of nitrite in the oxidation of nitrophenols by bicarbonate-activated peroxide system. <b>2016</b> , 516, 90-99	6
624	Role of defects and metal coordination on adsorption of acid gases in MOFs and metal oxides: An in situ IR spectroscopic study. <b>2016</b> , 227, 65-75	24
623	Temperature- and Coverage-Dependent Kinetics of Photocatalytic Reaction of Methanol on TiO <sub>2</sub> (110)-(1 × 1) Surface. <b>2016</b> , 120, 5503-5514	39
622	Synthesis of TiO <sub>2</sub> nanoparticles containing Fe, Si, and V using multiple diffusion flames and catalytic oxidation capability of carbon-coated nanoparticles. <b>2016</b> , 18, 1	10
621	Enhanced photoactivities of TiO <sub>2</sub> particles induced by bio-inspired micro-nanoscale substrate. <b>2016</b> , 470, 10-13	2
620	Fabrication, characterization and photocatalytic properties of Au/TiO <sub>2</sub> -WO <sub>3</sub> nanotubular composite synthesized by photo-assisted deposition and electrochemical anodizing methods. <b>2016</b> , 417, 107-115	76
619	Combined biological and photocatalytic treatment of real coke oven wastewater. <b>2016</b> , 295, 20-28	45
618	Formaldehyde adsorption and decomposition on rutile (110): A first-principles study. <b>2016</b> , 652, 156-162	18
617	Influence of doping on chain-like TiO <sub>2</sub> clusters: A DFT study. <b>2016</b> , 16, 197-206	5
616	Enhanced photovoltaic performance of fully flexible dye-sensitized solar cells based on the Nb <sub>2</sub> O <sub>5</sub> coated hierarchical TiO <sub>2</sub> nanowire-nanosheet arrays. <b>2016</b> , 364, 676-685	17
615	Synthesis of hollow carbon-W <sub>18</sub> O <sub>49</sub> composite and its photocatalytic properties. <b>2016</b> , 27, 2662-2669	1
614	Removal of rhodamine 6G dye contaminant by visible light driven immobilized Ca <sup>1/2</sup> Ln MnO <sub>3</sub> (Ln = Sm, Ho; 0.1 × 0.4) photocatalysts. <b>2016</b> , 360, 798-806	20



613	Heterogeneous Photocatalysis. <b>2016</b> ,	42
612	Shape controllers enhance the efficiency of graphene-TiO <sub>2</sub> hybrids in pollutant abatement. <b>2016</b> , 8, 3407-15	12
611	Fundamental Processes in Surface Photocatalysis on TiO <sub>2</sub> . <b>2016</b> , 361-416	1
610	Ultrasmall graphitic carbon nitride quantum dots decorated self-organized TiO <sub>2</sub> nanotube arrays with highly efficient photoelectrochemical activity. <b>2016</b> , 186, 127-135	131
609	Facile synthesis of CdS/C core-shell nanospheres with ultrathin carbon layer for enhanced photocatalytic properties and stability. <b>2016</b> , 362, 126-131	46
608	Truncated tetragonal bipyramidal anatase nanocrystals formed without use of capping agents from the supercritical drying of a TiO <sub>2</sub> sol. <b>2016</b> , 18, 164-176	12
607	A facile and novel strategy to synthesize reduced TiO <sub>2</sub> nanotubes photoelectrode for photoelectrocatalytic degradation of diclofenac. <b>2016</b> , 144, 888-94	49
606	An easier method of preparation of mesoporous anatase TiO <sub>2</sub> nanoparticles via ultrasonic irradiation. <b>2016</b> , 11, 540-549	16
605	Enhanced photocatalytic activities of vacuum activated TiO <sub>2</sub> catalysts with Ti <sup>3+</sup> and N co-doped. <b>2016</b> , 266, 188-196	56
604	A heterostructured TiO <sub>2</sub> /Ti <sub>3</sub> N <sub>4</sub> support for gold catalysts: a superior preferential oxidation of CO in the presence of H <sub>2</sub> under visible light irradiation and without visible light irradiation. <b>2016</b> , 6, 829-839	46
603	Elementary photocatalytic chemistry on TiO <sub>2</sub> surfaces. <b>2016</b> , 45, 3701-30	242
602	The pivotal effect of the interaction between reactant and anatase TiO <sub>2</sub> nanosheets with exposed {0 0 1} facets on photocatalysis for the photocatalytic purification of VOCs. <b>2016</b> , 181, 625-634	83
601	Photocatalytic hydrogen production from aqueous glycerol solution using NiO/TiO <sub>2</sub> catalysts: Effects of preparation and reaction conditions. <b>2016</b> , 181, 818-824	117
600	Interaction of carboxylic acids with rutile TiO <sub>2</sub> (110): IR-investigations of terephthalic and benzoic acid adsorbed on a single crystal substrate. <b>2016</b> , 643, 117-123	31
599	Facile fabrication of an aptasensor for thrombin based on graphitic carbon nitride/TiO <sub>2</sub> with high visible-light photoelectrochemical activity. <b>2016</b> , 75, 116-22	73
598	Photocatalytic properties of titania thin films prepared by sputtering versus evaporation and aging of induced oxygen vacancy defects. <b>2016</b> , 180, 362-371	45
597	Photocatalytic process in TiO <sub>2</sub> /graphene hybrid materials. Evidence of charge separation by electron transfer from reduced graphene oxide to TiO <sub>2</sub> . <b>2017</b> , 281, 29-37	88
596	Atom surface diffusion of catalytic metals on the anatase TiO <sub>2</sub> (101) surface. <b>2017</b> , 19, 4541-4552	24



595	Effects of Defects on Photocatalytic Activity of Hydrogen-Treated Titanium Oxide Nanobelts. <i>ACS Catalysis</i> , <b>2017</b> , 7, 1742-1748	13.1	129
594	Mechanism of Ethanol Photooxidation on Single-Crystal Anatase TiO <sub>2</sub> (101). <b>2017</b> , 121, 2940-2950		27
593	Fabrication of Ag-Ag <sub>2</sub> O/reduced TiO <sub>2</sub> nanophotocatalyst and its enhanced visible light driven photocatalytic performance for degradation of diclofenac solution. <b>2017</b> , 206, 136-145		104
592	A highly efficient visible-light-responding Cu <sub>2</sub> O/TiO <sub>2</sub> /g-C <sub>3</sub> N <sub>4</sub> photocatalyst for instantaneous discolorations of organic dyes. <b>2017</b> , 193, 18-21		25
591	Tin dioxide as a photocatalyst for water treatment: A review. <b>2017</b> , 107, 190-205		143
590	Influence of electronic structure on visible light photocatalytic activity of nitrogen-doped TiO <sub>2</sub> . <b>2017</b> , 7, 1887-1898		27
589	One-pot solvothermal preparation of mesoporous Cu(II)Porphyrin-TiO <sub>2</sub> composites with enhanced photocatalytic activity and stability. <b>2017</b> , 47, 783-787		1
588	Full visible-light absorption of TiO <sub>2</sub> nanotubes induced by anionic S <sub>2</sub> S <sub>2</sub> doping and their greatly enhanced photocatalytic hydrogen production abilities. <b>2017</b> , 206, 168-174		47
587	Catalytic role of bridging oxygens in TiO <sub>2</sub> liquid phase photocatalytic reactions: analysis of H <sub>2</sub> 16O photooxidation on labeled Ti <sub>18</sub> O <sub>2</sub> . <b>2017</b> , 7, 902-910		7
586	Structural Rearrangement of Au-Pd Nanoparticles under Reaction Conditions: An ab Initio Molecular Dynamics Study. <b>2017</b> , 11, 1649-1658		41
585	IR spectroscopic investigations of chemical and photochemical reactions on metal oxides: bridging the materials gap. <b>2017</b> , 46, 1875-1932		120
584	Identifying the Role of Photogenerated Holes in Photocatalytic Methanol Dissociation on Rutile TiO <sub>2</sub> (110). <i>ACS Catalysis</i> , <b>2017</b> , 7, 2374-2380	13.1	52
583	Enhancing photocatalytic CO <sub>2</sub> reduction by coating an ultrathin Al <sub>2</sub> O <sub>3</sub> layer on oxygen deficient TiO <sub>2</sub> nanorods through atomic layer deposition. <b>2017</b> , 404, 49-56		45
582	Water Oxidation Mechanisms of Metal Oxide Catalysts by Vibrational Spectroscopy of Transient Intermediates. <b>2017</b> , 68, 209-231		25
581	Photon-induced interfacial charge transfer mechanism of porous silicon/TiO <sub>2</sub> nanoparticles for photoelectrochemical performance. <b>2017</b> , 338, 72-84		4
580	Photodeposited Pd Nanoparticles with Disordered Structure for Phenylacetylene Semihydrogenation. <b>2017</b> , 7, 42172		30
579	Enhancing visible light photocatalytic activity of nitrogen-deficient g-CN via thermal polymerization of acetic acid-treated melamine. <b>2017</b> , 495, 27-36		86
578	Structural features of N-containing titanium dioxide thin films deposited by magnetron sputtering. <b>2017</b> , 627, 9-16		16

577	Proton-Promoted Electron Transfer in Photocatalysis: Key Step for Photocatalytic Hydrogen Evolution on Metal/Titania Composites. <i>ACS Catalysis</i> , <b>2017</b> , 7, 2744-2752	13.1	47
576	Smart surface in pool boiling: Thermally-induced wetting transition. <b>2017</b> , 109, 231-241		18
575	Comparative study of ultraviolet light and visible light on the photo-assisted conductivity and gas sensing property of TiO <sub>2</sub> . <b>2017</b> , 248, 724-732		15
574	Photocatalyst performance in wastewater treatment applications: Towards the role of TiO <sub>2</sub> properties. <b>2017</b> , 434, 167-174		33
573	Controllable nanothorns on TiO mesocrystals for efficient charge separation in hydrogen evolution. <b>2017</b> , 53, 5306-5309		17
572	Structural Dependence of Competitive Adsorption of Water and Methanol on TiO <sub>2</sub> Surfaces. <b>2017</b> , 35, 889-895		10
571	Photocatalytic degradation of dye using CeO/SCB composite catalysts. <b>2017</b> , 183, 218-224		18
570	Photoelectrocatalytic H evolution in water with molecular catalysts immobilised on p-Si a stabilising mesoporous TiO interlayer. <b>2017</b> , 8, 5172-5180		72
569	Preparation and characterization of nanocomposite of graphitic carbon nitride and TiO <sub>2</sub> as a porous support for nano catalyst for desulfurization process. <b>2017</b> , 21, 943-953		2
568	Instantaneous photoinitiated synthesis and rapid pulsed photothermal treatment of three-dimensional nanostructured TiO <sub>2</sub> thin films through pulsed light irradiation. <b>2017</b> , 32, 1701-1709		13
567	Computational investigation of the co-doping effect of sulphur and nitrogen on the electronics of CsTaWO <sub>6</sub> . <b>2017</b> , 3, 71-76		
566	SnS <sub>2</sub> Nanoplates with Specific Facets Exposed for Enhanced Visible-Light-Driven Photocatalysis. <b>2017</b> , 1, 60-69		21
565	The mechanism of H <sub>2</sub> and H <sub>2</sub> O desorption from bridging hydroxyls of a TiO <sub>2</sub> (110) surface. <b>2017</b> , 7, 251-264		10
564	Anisotropic Metal Deposition on TiO Particles by Electric-Field-Induced Charge Separation. <b>2017</b> , 56, 11431-11435		25
563	Present Perspectives of Advanced Characterization Techniques in TiO-Based Photocatalysts. <b>2017</b> , 9, 23265-23286		78
562	Inorganic Colloidal Perovskite Quantum Dots for Robust Solar CO Reduction. <b>2017</b> , 23, 9481-9485		161
561	Bifunctional property of Pt nanoparticles deposited on TiO <sub>2</sub> for the photocatalytic sp <sup>3</sup> Csp <sup>3</sup> C cross-coupling reactions between THF and alkanes. <b>2017</b> , 7, 2616-2623		19
560	Zirconium doped TiO <sub>2</sub> nano-powder via halide free non-aqueous solvent controlled sol-gel route. <b>2017</b> , 5, 2955-2963		19

559	VOCs photocatalytic abatement using nanostructured titania-silica catalysts. <b>2017</b> , 5, 3100-3107		19
558	Photocatalytic membrane processes, and respective modelling, for removal of pharmaceutical residues in wastewaters. A case study with 2-[2,6-(dichlorophenyl)amino]phenyl acetic acid as model molecule. <b>2017</b> , 6, 69-77		1
557	Investigation on the effect of an anion layer on photocatalytic activity: carbonate vs. oxalate. <b>2017</b> , 41, 7073-7080		8
556	Visible-Light-Mediated [4+2] Annulation of N-Cyclobutylanilines with Alkynes Catalyzed by Self-Doped Ti @TiO. <b>2017</b> , 23, 15396-15403		6
555	Role of Surface Stress on the Reactivity of Anatase TiO(001). <i>Journal of Physical Chemistry Letters</i> , <b>2017</b> , 8, 1764-1771	6.4	29
554	Efficient production of acrylic acid by dehydration of lactic acid over BaSO <sub>4</sub> with crystal defects. <b>2017</b> , 7, 10278-10286		13
553	Evolution of microstructural defects of TiO <sub>2</sub> nanocrystals by Zr <sup>4+</sup> or/and Ge <sup>4+</sup> doping lead to high disinfection efficiency for CWAs. <b>2017</b> , 678, 146-152		6
552	Comparative Study of Structural and Photocatalytic Properties of M-Doped (M = Ce <sup>3+</sup> , Zn <sup>2+</sup> , Cu <sup>2+</sup> ) Dendritic-Like CdS. <b>2017</b> , 46, 1598-1606		4
551	Microwave-assisted synthesis of Ag <sub>2</sub> O/reduced TiO <sub>2</sub> nano-tube arrays photoelectrode with enhanced visible photocatalytic activity for degradation of organic pollutants. <b>2017</b> , 182, 230-237		7
550	IR spectroscopy applied to metal oxide surfaces: adsorbate vibrations and beyond. <b>2017</b> , 2, 373-408		32
549	Electron transfer between anatase TiO and an O molecule directly observed by atomic force microscopy. <b>2017</b> , 114, E2556-E2562		65
548	Time-Resolved Spectroscopic Investigation of Charge Trapping in Carbon Nitrides Photocatalysts for Hydrogen Generation. <b>2017</b> , 139, 5216-5224		307
547	Surface chemistry of pure tetragonal ZrO and gas-phase dependence of the tetragonal-to-monoclinic ZrO transformation. <b>2017</b> , 46, 4554-4570		14
546	Engineering the surface charge states of nanostructures for enhanced catalytic performance. <b>2017</b> , 1, 1951-1964		51
545	Surface Localization of Defects in Black TiO: Enhancing Photoactivity or Reactivity. <i>Journal of Physical Chemistry Letters</i> , <b>2017</b> , 8, 199-207	6.4	79
544	A review on the effects of TiO <sub>2</sub> surface point defects on CO <sub>2</sub> photoreduction with H <sub>2</sub> O. <b>2017</b> , 3, 17-32		78
543	Photo-reduction assisted synthesis of W-doped TiO <sub>2</sub> coupled with Au nanoparticles for highly efficient photocatalytic hydrogen evolution. <b>2017</b> , 19, 675-683		14
542	Mechanistic Insight into the Photocatalytic Working of Fluorinated Anatase {001} Nanosheets. <b>2017</b> , 121, 26275-26286		17

541	Mesoporous TiO <sub>2</sub> /g-C <sub>3</sub> N <sub>4</sub> Microspheres with Enhanced Visible-Light Photocatalytic Activity. <b>2017</b> , 121, 22114-22122		89
540	Achievement of safer palladium nanocrystals by enlargement of {100} crystallographic facets. <b>2017</b> , 11, 907-922		9
539	A new recipe for preparing oxidized TiO <sub>2</sub> (110) surfaces: An STM study. <b>2017</b> , 666, 113-122		4
538	Synthesis of anatase nano wire and its application as a functional top layer for alumina membrane. <b>2017</b> , 43, 17104-17110		5
537	Considering photocatalytic activity of N/F/S-doped TiO <sub>2</sub> thin films in degradation of textile waste under visible and sunlight irradiation. <b>2017</b> , 158, 636-643		28
536	Facile and large-scale preparation of N doped TiO <sub>2</sub> photocatalyst with high visible light photocatalytic activity. <b>2017</b> , 209, 585-588		18
535	Adsorption and Photodesorption of CO from Charged Point Defects on TiO(110). <i>Journal of Physical Chemistry Letters</i> , <b>2017</b> , 8, 4565-4572	6.4	14
534	3D Foam Strutted Graphene Carbon Nitride with Highly Stable Optoelectronic Properties. <b>2017</b> , 27, 1703711		64
533	Molecular Ion Formation by Photoinduced Electron Transfer at the Tetracyanoquinodimethane/Au(111) Interface. <i>Journal of Physical Chemistry Letters</i> , <b>2017</b> , 8, 4685-4690	6.4	5
532	Identifying the Site-Dependent Photoactivity of Anatase TiO <sub>2</sub> (001)-(100) Surface. <b>2017</b> , 121, 19930-19937		14
531	Methanol on Anatase TiO (101): Mechanistic Insights into Photocatalysis. <i>ACS Catalysis</i> , <b>2017</b> , 7, 7081-7091	3.1	62
530	Laser-Induced Surface Modification at Anatase TiO <sub>2</sub> Nanotube Array Photoanodes for Photoelectrochemical Water Oxidation. <b>2017</b> , 121, 17121-17128		27
529	TiO <sub>2</sub> and F-TiO <sub>2</sub> photocatalytic deactivation in gas phase. <b>2017</b> , 684, 164-170		6
528	Bi metal-modified Bi <sub>4</sub> O <sub>5</sub> I <sub>2</sub> hierarchical microspheres with oxygen vacancies for improved photocatalytic performance and mechanism insights. <b>2017</b> , 7, 3580-3590		50
527	Anisotropic Metal Deposition on TiO <sub>2</sub> Particles by Electric-Field-Induced Charge Separation. <b>2017</b> , 129, 11589-11593		3
526	Nanostructured TiO <sub>2</sub> /CuO dual-coated copper meshes with superhydrophilic, underwater superoleophobic and self-cleaning properties for highly efficient oil/water separation. <b>2017</b> , 328, 497-510		86
525	Scenarios of polaron-involved molecular adsorption on reduced TiO(110) surfaces. <b>2017</b> , 7, 6148		11
524	Facile preparation of defective black TiO <sub>2</sub> through the solution plasma process: Effect of parametric changes for plasma discharge on its structural and optical properties. <i>Journal of Alloys and Compounds</i> , <b>2017</b> , 726, 567-577	5.7	30

523	Increasing Oxide Reducibility: The Role of Metal/Oxide Interfaces in the Formation of Oxygen Vacancies. <i>ACS Catalysis</i> , <b>2017</b> , 7, 6493-6513	13.1	375
522	Microwave synthesis of In-doped TiO <sub>2</sub> nanoparticles for photocatalytic application. <b>2017</b> , 28, 17140-17147		5
521	Excess charge driven dissociative hydrogen adsorption on TiO. <b>2017</b> , 19, 23154-23161		15
520	Heterogeneous Fenton degradation of oxalic acid by using silica supported iron catalysts prepared from raw rice husk. <b>2017</b> , 19, 156-163		20
519	Surface Chemistry of Formaldehyde on Rutile TiO <sub>2</sub> (011)-(2 × 1) Surface: Photocatalysis Versus Thermal-Catalysis. <b>2017</b> , 121, 25921-25929		15
518	Titania-Modified Silver Electrocatalyst for Selective CO <sub>2</sub> Reduction to CH <sub>3</sub> OH and CH <sub>4</sub> from DFT Study. <b>2017</b> , 121, 16275-16282		29
517	The effects of transition-metal doping and chromophore anchoring on the photocurrent response of titanium-oxo-clusters. <b>2017</b> , 46, 9639-9645		24
516	Syntheses of Novel Lanthanide Metal-Organic Frameworks for Highly Efficient Visible-Light-Driven Dye Degradation. <b>2017</b> , 17, 4189-4195		71
515	Massive Ti <sup>3+</sup> self-doped by the injected electrons from external Pt and the efficient photocatalytic hydrogen production under visible-Light. <b>2017</b> , 218, 751-757		37
514	Effects of Molecular Structure and Solvent Polarity on Adsorption of Carboxylic Anchoring Dyes onto TiO Particles in Aprotic Solvents. <b>2017</b> , 33, 7036-7042		15
513	On the apparent visible-light and enhanced UV-light photocatalytic activity of nitrogen-doped TiO <sub>2</sub> thin films. <b>2017</b> , 333, 49-55		26
512	Novel three-dimensionally ordered macroporous Fe <sup>3+</sup> -doped TiO <sub>2</sub> photocatalysts for H <sub>2</sub> production and degradation applications. <b>2017</b> , 394, 248-257		67
511	Green and low cost tetracycline degradation processes by nanometric and immobilized TiO <sub>2</sub> systems. <b>2017</b> , 281, 38-44		51
510	Synthetic porous materials applied in hydrogenation reactions. <b>2017</b> , 237, 246-259		35
509	Enhanced visible-light photocatalytic activity of carbonate-doped anatase TiO <sub>2</sub> based on the electron-withdrawing bidentate carboxylate linkage. <b>2017</b> , 202, 642-652		88
508	Facilitation of the visible light-induced Fenton-like excitation of H <sub>2</sub> O <sub>2</sub> via heterojunction of g-C <sub>3</sub> N <sub>4</sub> /NH <sub>2</sub> -Iron terephthalate metal-organic framework for MB degradation. <b>2017</b> , 202, 653-663		231
507	Photocatalytic and Luminescent Properties of SrMoO <sub>4</sub> Phosphors Prepared via Hydrothermal Method with Different Stirring Speeds. <b>2017</b> , 33, 23-29		25
506	Enhanced adsorbability and photocatalytic activity of TiO-graphene composite for polycyclic aromatic hydrocarbons removal in aqueous phase. <b>2017</b> , 150, 68-77		48

505	Photo-Induced Morphology Changes at the RuO <sub>2</sub> (110)/TiO <sub>2</sub> (110) Surface: A Scanning Tunneling Microscopy Study. <b>2017</b> , 60, 533-541	4
504	Synthesis, characterization and properties of titanium dioxide obtained by hydrolytic method. <b>2017</b> , ,	5
503	Influence of doping with Co, Cu, Ce and Fe on structure and photocatalytic activity of TiO <sub>2</sub> nanoparticles. <b>2017</b> , 35, 725-732	9
502	Modeling atmospheric mineral aerosol chemistry to predict heterogeneous photooxidation of SO <sub>2</sub> . <b>2017</b> , 17, 10001-10017	18
501	Surface force analysis of glycine adsorption on different crystal surfaces of titanium dioxide (TiO <sub>2</sub> ). <b>2017</b> , 4, 38	3
500	Acetone Formation from Photolysis of 2-Propanol on Anatase-TiO <sub>2</sub> (101). <b>2017</b> , 30, 1-6	5
499	Markedly Enhanced Surface Hydroxyl Groups of TiO <sub>2</sub> Nanoparticles with Superior Water-Dispersion for Photocatalysis. <b>2017</b> , 10,	94
498	Water Diffusion through a Titanium Dioxide/Poly(Carbonate Urethane) Nanocomposite for Protecting Cultural Heritage: Interactions and Viscoelastic Behavior. <b>2017</b> , 7,	5
497	Preparation of Titania on Stainless Steel by the Spray-ILGAR Technique as Active Photocatalyst under UV Light Irradiation for the Decomposition of Acetaldehyde. <b>2017</b> , 7, 698	4
496	Reactivity of Trapped and Accumulated Electrons in Titanium Dioxide Photocatalysis. <b>2017</b> , 7, 303	43
495	Metabolomic effects of CeO <sub>2</sub> , SiO <sub>2</sub> and CuO metal oxide nanomaterials on HepG2 cells. <b>2017</b> , 14, 50	21
494	Modelling Atmospheric Mineral Aerosol Chemistry to Predict Heterogeneous Photooxidation of SO <sub>2</sub> . <b>2017</b> ,	
493	Pronounced Visible Light Photocatalytic Activity Obtained from Coupling of TiO <sub>2</sub> with Metal Organic Macromolecule. <b>2017</b> , 727, 508-513	
492	Review on selective hydrogenation of nitroarene by catalytic, photocatalytic and electrocatalytic reactions. <b>2018</b> , 227, 386-408	226
491	Effects of atomic oxygen on titanium dioxide thin film. <b>2018</b> , 146, 1-6	4
490	Facet-dependent photocatalytic decomposition of NO on the anatase TiO <sub>2</sub> : a DFT study. <b>2018</b> , 10, 6024-6038	25
489	Progress in TiO <sub>2</sub> nanotube coatings for biomedical applications: a review. <b>2018</b> , 6, 1862-1886	94
488	Photocatalytic selectivity switch to C-C scission: Methyl ejection of tert-butanol on TiO <sub>2</sub> (110). <b>2018</b> , 20, 7105-7111	6

487	Enhanced Hydrogen Production from Methanol Photolysis on a Formate-Modified Rutile-TiO <sub>2</sub> (110) Surface. <b>2018</b> , 122, 13774-13781	2
486	Surface states as electron transfer pathway enhanced charge separation in TiO <sub>2</sub> nanotube water splitting photoanodes. <b>2018</b> , 234, 100-108	54
485	Identifying the key obstacle in photocatalytic oxygen evolution on rutile TiO <sub>2</sub> . <b>2018</b> , 1, 291-299	131
484	Synthesis of Biphasic Defective TiO <sub>2</sub> /Reduced Graphene Oxide Nanocomposites with Highly Enhanced Photocatalytic Activity. <b>2018</b> , 34, 158-163	0
483	Dependence of morphology, substrate and thickness of iron phthalocyanine thin films on the photocatalytic degradation of rhodamine B dye. <b>2018</b> , 72, 2327-2337	2
482	Excess electrons in reduced rutile and anatase TiO <sub>2</sub> . <b>2018</b> , 73, 58-82	75
481	Bulk oxygen vacancies enriched TiO <sub>2</sub> and its enhanced visible photocatalytic performance. <b>2018</b> , 441, 150-155	19
480	Enhanced photocatalytic hydrogen production activity of noble metal free MWCNT-TiO <sub>2</sub> nanocomposites. <b>2018</b> , 43, 4036-4043	36
479	Two pure MOF-photocatalysts readily prepared for the degradation of methylene blue dye under visible light. <b>2018</b> , 47, 4251-4258	115
478	Delocalized Impurity Phonon Induced Electron-Hole Recombination in Doped Semiconductors. <b>2018</b> , 18, 1592-1599	63
477	On the relationship between rutile/anatase ratio and the nature of defect states in sub-100 nm TiO <sub>2</sub> nanostructures: experimental insights. <b>2018</b> , 20, 5975-5982	20
476	Preparation of nano-TiO <sub>2</sub> /diatomite-based porous ceramics and their photocatalytic kinetics for formaldehyde degradation. <b>2018</b> , 25, 73-79	20
475	Photofunctional hybrids of TiO <sub>2</sub> and titanium metal-organic frameworks for dye degradation and lanthanide ion-tuned multi-color luminescence. <b>2018</b> , 42, 4394-4401	12
474	Engineering an N-doped TiO <sub>2</sub> @N-doped C butterfly-like nanostructure with long-lived photo-generated carriers for efficient photocatalytic selective amine oxidation. <b>2018</b> , 6, 2091-2099	53
473	Influence of Nb Doping Concentration on Bolometric Properties of RF Magnetron Sputtered Nb:TiO <sub>2</sub> Films. <b>2018</b> , 47, 2171-2176	1
472	TiO <sub>2</sub> nanotubes/Ti plates modified by silver/benzene with enhanced photocatalytic antibacterial properties. <b>2018</b> , 42, 2058-2066	5
471	Hydrogenated Blue Titania for Efficient Solar to Chemical Conversions: Preparation, Characterization, and Reaction Mechanism of CO <sub>2</sub> Reduction. <i>ACS Catalysis</i> , <b>2018</b> , 8, 1009-1017	13.1 164
470	Water-Assisted Hole Trapping at the Highly Curved Surface of Nano-TiO Photocatalyst. <b>2018</b> , 140, 1415-1422	59



469	MoS quantum dots@TiO nanotube composites with enhanced photoexcited charge separation and high-efficiency visible-light driven photocatalysis. <b>2018</b> , 29, 105403	30
468	Observation of Structure of Surfaces and Interfaces by Synchrotron X-ray Diffraction: Atomic-Scale Imaging and Time-Resolved Measurements. <b>2018</b> , 87, 061010	5
467	Aryl-Aryl Covalent Coupling on Rutile TiO <sub>2</sub> Surfaces. <b>2018</b> , 153-177	
466	CdS-Based photocatalysts. <b>2018</b> , 11, 1362-1391	765
465	On-Surface Synthesis II. <b>2018</b> ,	11
464	Improving methane selectivity of photo-induced CO <sub>2</sub> reduction on carbon dots through modification of nitrogen-containing groups and graphitization. <b>2018</b> , 232, 86-92	31
463	Fe-based bimetallic catalysts supported on TiO <sub>2</sub> for selective CO <sub>2</sub> hydrogenation to hydrocarbons. <b>2018</b> , 25, 330-337	36
462	Sodium dodecyl sulphate-assisted synthesis, optical properties and catalytic activities of silver/manganese dioxide nanocomposites. <b>2018</b> , 258, 310-318	4
461	Heterostructure TiO <sub>2</sub> polymorphs design and structure adjustment for photocatalysis. <b>2018</b> , 63, 314-321	6
460	A Comparative Study of the Activity of TiO <sub>2</sub> Degussa P25 and Millennium PCs in the Photocatalytic Degradation of Bromothymol Blue. <b>2018</b> , 16,	6
459	Bridging Hydroxyls on Anatase TiO(101) by Water Dissociation in Oxygen Vacancies. <b>2018</b> , 122, 834-839	30
458	The location of excess electrons on H <sub>2</sub> O/TiO <sub>2</sub> (110) surface and its role in the surface reactions. <b>2018</b> , 116, 171-178	5
457	Synthesis of iron and copper cluster-grafted zinc oxide nanorod with enhanced visible-light-induced photocatalytic activity. <b>2018</b> , 509, 68-72	23
456	Surface-Plasmon-Driven Hot Electron Photochemistry. <i>Chemical Reviews</i> , <b>2018</b> , 118, 2927-2954	68.1 661
455	Unveiling the Atomic Structures of the Minority Surfaces of TiO <sub>2</sub> Nanocrystals. <b>2018</b> , 30, 288-295	12
454	Morphology-controlled synthesis of TiO <sub>2</sub> /MoS <sub>2</sub> nanocomposites with enhanced visible-light photocatalytic activity. <b>2018</b> , 5, 145-152	29
453	Synthesis of novel silver chromate incorporated copper-metal-organic framework composites with exceptionally high photocatalytic activity and stability. <b>2018</b> , 29, 3358-3369	5
452	Enhanced visible-light photocatalytic activity of Bi <sub>2</sub> MoO <sub>6</sub> nanoplates with heterogeneous Bi <sub>2</sub> MoO <sub>6</sub> -x@Bi <sub>2</sub> MoO <sub>6</sub> core-shell structure. <b>2018</b> , 224, 692-704	77



451	Preparation of new photocatalytic materials using ion implantation method. <b>2018</b> , 671, 156-163	0
450	Insights into the adsorption of organic molecules on rutile TiO <sub>2</sub> (1 1 0) surface: A theoretical study. <b>2018</b> , 56, 751-756	3
449	Decomposition of organic pollutant in waste water using magnetic catalyst nanocomposite. <b>2018</b> , 1091, 012011	
448	Exogenous Physical Irradiation on Titania Semiconductors: Materials Chemistry and Tumor-Specific Nanomedicine. <b>2018</b> , 5, 1801175	30
447	Photoactive metal-organic framework as a bifunctional material for 4-hydroxy-4'-nitrobiphenyl detection and photodegradation of methylene blue. <b>2018</b> , 47, 16551-16557	23
446	Hierarchically ordered macro-mesoporous anatase TiO prepared by pearl oyster shell and triblock copolymer dual templates for high photocatalytic activity.. <b>2018</b> , 8, 38461-38469	4
445	Visible-light-induced photo-Fenton process for the facile degradation of metronidazole by Fe/Si codoped TiO <sub>2</sub> . <b>2018</b> , 8, 40022-40034	17
444	Thermodynamic Modelling and Characterisation of TiO <sub>2</sub> nanoparticles Produced by Wire Explosion Process. <b>2018</b> , 5, 17304-17311	3
443	Preparation of Mesoporous Titania Using a Sol-Gel Method in a Deep Eutectic Solvent. <b>2018</b> , 51, 620-624	1
442	Modeling Heterogeneous Oxidation of NO <sub>x</sub> , SO <sub>2</sub> and Hydrocarbons in the Presence of Mineral Dust Particles under Various Atmospheric Environments. <i>ACS Symposium Series</i> , <b>2018</b> , 301-326	0.4 2
441	Enhanced photocatalytic performance of Bi <sub>4</sub> Ti <sub>3</sub> O <sub>12</sub> nanosheets synthesized by a self-catalyzed fast reaction process. <b>2018</b> , 44, 23014-23023	9
440	Particularities of photocatalysis and formation of reactive oxygen species on insulators and semiconductors: cases of SiO <sub>2</sub> , TiO <sub>2</sub> and their composite SiO <sub>2</sub> /TiO <sub>2</sub> . <b>2018</b> , 8, 5657-5668	13
439	Mechanistic aspect based on the role of reactive oxidizing species (ROS) in macroscopic level on the glycerol photooxidation over defected and defected-free TiO <sub>2</sub> . <b>2018</b> , 367, 270-281	16
438	Roles of Chenodeoxycholic Acid Coadsorbent in Anthracene-Based Dye-Sensitized Solar Cells: A Density Functional Theory Study. <b>2018</b> , 122, 23280-23287	10
437	Surface Strategies for Particulate Photocatalysts toward Artificial Photosynthesis. <b>2018</b> , 2, 2260-2288	89
436	Correlation between surface carrier dynamics and water oxidation activity of commercially available rutile-type TiO <sub>2</sub> powders. <b>2018</b> , 712, 123-127	2
435	Branched multiphase TiO <sub>2</sub> with enhanced photoelectrochemical water splitting activity. <b>2018</b> , 43, 21365-21373	1
434	Simulation of heterogeneous photooxidation of SO <sub>2</sub> and NO <sub>x</sub> in the presence of Gobi Desert dust particles under ambient sunlight. <b>2018</b> , 18, 14609-14622	14

433	Enhanced Photocatalytic Efficiency of a Least Active Ag-TiO by Amine Adsorption. <i>ACS Omega</i> , <b>2018</b> , 3, 12802-12812	3.9	12
432	Graphene-Modified TiO <sub>2</sub> with Enhanced Visible Light Photocatalytic Activities. <b>2018</b> , 107-131		
431	Fabrication of Bi <sub>2</sub> WO <sub>6</sub> quantum dots/ultrathin nanosheets 0D/2D homojunctions with enhanced photocatalytic activity under visible light irradiation. <b>2018</b> , 39, 1910-1918		23
430	TiNF and Related Analogues of TiO : A Combined Experimental and Theoretical Study. <b>2018</b> , 19, 3410-3417		6
429	Microstructure, fractal geometry and dye-sensitized solar cells performance of CdS/TiO <sub>2</sub> nanostructures. <b>2018</b> , 830-831, 80-87		17
428	Alumina anchored CQDs/TiO <sub>2</sub> nanorods by atomic layer deposition for efficient photoelectrochemical water splitting under solar light. <b>2018</b> , 6, 18293-18303		24
427	TiO <sub>2</sub> nano-flakes with high activity obtained from phosphorus doped TiO <sub>2</sub> nanoparticles by hydrothermal method. <b>2018</b> , 44, 22129-22134		15
426	Facet-Dependent Interfacial Charge Transfer in Fe(III)-Grafted TiO <sub>2</sub> Nanostructures Activated by Visible Light. <i>ACS Catalysis</i> , <b>2018</b> , 8, 9399-9407	13.1	34
425	Enhanced activity of TiO <sub>2</sub> by concentrating light for photoreduction of CO <sub>2</sub> with H <sub>2</sub> O to CH <sub>4</sub> . <b>2018</b> , 113, 6-9		15
424	Covalent immobilization of TiO <sub>2</sub> within macroporous polymer monolith as a facilely recyclable photocatalyst for water decontamination. <b>2018</b> , 296, 1419-1429		11
423	Dissociation behavior of water molecules on defect-free and defective rutile TiO <sub>2</sub> (1 0 1) surfaces. <b>2018</b> , 457, 295-302		5
422	How Far Are We From Large-Scale PMR Applications?. <b>2018</b> , 233-295		2
421	The role of lithium cations on the photochemistry of ruthenium complexes in dye-sensitized solar cells: A TDDFT study with the BCL model. <b>2018</b> , 364, 510-515		4
420	Structural and Electronic Properties of Na <sub>2</sub> Ti <sub>3</sub> O <sub>7</sub> and H <sub>2</sub> Ti <sub>3</sub> O <sub>7</sub> . <b>2018</b> , 255, 1700612		6
419	Revealing the Size Effect of Platinum Cocatalyst for Photocatalytic Hydrogen Evolution on TiO <sub>2</sub> Support: A DFT Study. <i>ACS Catalysis</i> , <b>2018</b> , 8, 7270-7278	13.1	90
418	Highly Active TiO <sub>2</sub> Microspheres Formation in the Presence of Ethylammonium Nitrate Ionic Liquid. <b>2018</b> , 8, 279		8
417	Ti <sup>3+</sup> -doped TiO <sub>2</sub> hollow sphere with mixed phases of anatase and rutile prepared by dual-frequency atmospheric pressure plasma jet. <b>2018</b> , 20, 1		6
416	Simulation of Heterogeneous Photooxidation of SO <sub>2</sub> and NO <sub>x</sub> in the presence of Gobi Desert Dust Particles under Ambient Sunlight. <b>2018</b> ,		

415	Fabrication of hierarchical meso/macroporous TiO <sub>2</sub> scaffolds by evaporation-induced self-assembly technique for bone tissue engineering applications. <b>2018</b> , 144, 35-41	6
414	Recyclable Aggregates of Mesoporous Titania Synthesized by Thermal Treatment of Amorphous or Peptized Precursors. <b>2018</b> , 11,	3
413	A Facile Method for the Preparation of Colored BiTiO <sub>2</sub> Nanosheets with Enhanced Visible-Light Photocatalytic Hydrogen Evolution Activity. <b>2018</b> , 8,	18
412	A new 3D Gd-based metal-organic framework with paddle-wheel unit: Structure and photocatalytic property. <b>2018</b> , 95, 104-106	5
411	Theoretical Modeling of Electronic Excitations of Gas-Phase and Solvated TiO Nanoclusters and Nanoparticles of Interest in Photocatalysis. <b>2018</b> , 14, 4391-4404	16
410	TiO <sub>2</sub> nanorods thin-films embedded with gold nanoparticles for enhanced photocatalytic activity. <b>2018</b> ,	
409	Titanium dioxide nanostructures for photoelectrochemical applications. <b>2018</b> , 98, 299-385	148
408	Influence of plasma functionalization treatment and gold nanoparticles on surface chemistry and wettability of reactive-sputtered TiO <sub>2</sub> thin films. <b>2018</b> , 458, 678-685	16
407	Effect of oxygen vacancies on Li-storage of anatase (hbox {TiO}_{2}) (001) Facets: a first principles study. <b>2018</b> , 41, 1	1
406	Flowing nitrogen atmosphere induced rich oxygen vacancies overspread the surface of TiO <sub>2</sub> /kaolinite composite for enhanced photocatalytic activity within broad radiation spectrum. <b>2018</b> , 236, 76-87	71
405	Hydroxyapatite/Anatase Photocatalytic CoreShell Composite Prepared by Sol-Gel Processing. <b>2018</b> , 63, 254-260	5
404	Morphology Conserving High Efficiency Nitrogen Doping of Titanate Nanotubes by NH <sub>3</sub> Plasma. <b>2018</b> , 61, 1263-1273	4
403	Carbon Nitride-Modified Defective TiO <sub>2</sub> @Carbon Spheres for Photocatalytic H <sub>2</sub> Evolution and Pollutants Removal: Synergistic Effect and Mechanism Insight. <b>2018</b> , 122, 20444-20458	29
402	Recent advances in syntheses, properties and applications of TiO nanostructures.. <b>2018</b> , 8, 30125-30147	124
401	Understanding the visible-light photocatalytic activity of GaN:ZnO solid solution: the role of Rh Cr O cocatalyst and charge carrier lifetimes over tens of seconds. <b>2018</b> , 9, 7546-7555	30
400	Tailoring the rate-determining step in photocatalysis via localized excess electrons for efficient and safe air cleaning. <b>2018</b> , 239, 187-195	113
399	Intrinsically Activated SrTiO: Photocatalytic H Evolution from Neutral Aqueous Methanol Solution in the Absence of Any Noble Metal Cocatalyst. <b>2018</b> , 10, 29532-29542	32
398	Interactions of Molecular Titanium Oxides TiO (x = 1-3) with Carbon Dioxide in Cluster Anions. <b>2018</b> , 122, 6909-6917	11

397	A novel "signal-on" photoelectrochemical sensor for ultrasensitive detection of alkaline phosphatase activity based on a TiO <sub>2</sub> /g-CN heterojunction. <b>2018</b> , 143, 3399-3407	23
396	A New Synthetic Strategy of Ag-TiO <sub>2</sub> Nanocomposites Based on Ligand-to-Metal Charge Transfer under Visible Light Irradiation: Characterizations and Photocatalytic Activity. <b>2018</b> , 215, 1800026	2
395	Fundamentals of metal oxide-based photocatalysis. <b>2018</b> , 3-50	3
394	Magnetoelectric $\gamma$ -FeO: DFT study of a potential candidate for electrode material in photoelectrochemical cells. <b>2018</b> , 148, 214707	9
393	Ultra-trace (parts per million-ppm) W <sup>6+</sup> dopant ions induced anatase to rutile transition (ART) of phase pure anatase TiO <sub>2</sub> nanoparticles for highly efficient visible light-active photocatalytic degradation of organic pollutants. <b>2018</b> , 456, 676-693	11
392	Polypyrrole- and polyaniline-supported TiO <sub>2</sub> for removal of pollutants from water. <b>2019</b> , 14, 67-89	6
391	Removal of aqueous chromium and environmental CO by using photocatalytic TiO doped with tungsten. <b>2019</b> , 370, 196-202	10
390	Ecotoxicity of nano-metal oxides: A case study on daphnia magna. <b>2019</b> , 28, 878-889	9
389	Self-doping of Ti <sup>3+</sup> in TiO <sub>2</sub> through incomplete hydrolysis of titanium (IV) isopropoxide: An efficient visible light sonophotocatalyst for organic pollutants degradation. <b>2019</b> , 585, 117208	22
388	Fundamentals of TiO Photocatalysis: Concepts, Mechanisms, and Challenges. <b>2019</b> , 31, e1901997	403
387	Photocatalytic efficacy of supported tetrazine on MgZnO nanoparticles for the heterogeneous photodegradation of methylene blue and ciprofloxacin.. <b>2019</b> , 9, 23818-23831	22
386	Cathodoluminescence of TiO <sub>2</sub> Films Formed by Molecular Layer Deposition. <b>2019</b> , 45, 256-258	2
385	Nanoscale Photocatalytic Layers with Titania on Stainless Steel Foil. <b>2019</b> , 121-129	
384	Study of a Nanostructured Anatase Coating on the Rutile Surface. <b>2019</b> , 60, 194-199	1
383	Nanocatalytic Medicine. <b>2019</b> , 31, e1901778	227
382	Synthesis of Diamond-Shaped Mesoporous Titania Nanobricks as pH-Responsive Drug Delivery Vehicles for Cancer Therapy. <b>2019</b> , 4, 8225-8228	5
381	Surface chemistry and catalysis of oxide model catalysts from single crystals to nanocrystals. <b>2019</b> , 74, 100471	65
380	Photoresponses of Supported Au Single Atoms on TiO(110) through the Metal-Induced Gap States. <i>Journal of Physical Chemistry Letters</i> , <b>2019</b> , 10, 4683-4691	6.4 11

379	Facile synthesis of Ti <sup>3+</sup> self-doped and sulfur-doped TiO <sub>2</sub> nanotube arrays with enhanced visible-light photoelectrochemical performance. <i>Journal of Alloys and Compounds</i> , <b>2019</b> , 804, 10-17	5-7	21
378	Highly photoactive TiO <sub>2</sub> microspheres for photocatalytic production of hydrogen. <b>2019</b> , 44, 24653-24666		12
377	Chemical diffusion analysis of the oxidation kinetics of oxygen-deficient, nitrogen doped TiO <sub>2</sub> thin films. <b>2019</b> , 341, 115044		2
376	An EPR characterisation of stable and transient reactive oxygen species formed under radiative and non-radiative conditions. <b>2019</b> , 45, 5763-5779		5
375	Insights into the Most Suitable TiO <sub>2</sub> Surfaces for Photocatalytic O <sub>2</sub> and H <sub>2</sub> Evolution Reactions from DFT Calculations. <b>2019</b> , 123, 28210-28218		25
374	Excited states in the conduction band and long-lifetime hot electrons in TiO <sub>2</sub> nanoparticles observed with photoemission electron microscopy. <b>2019</b> , 9, 085321		4
373	Effect of Na-Doping on Electron Decay Kinetics in SrTiO <sub>3</sub> Photocatalyst. <b>2019</b> , 11, 6349-6354		13
372	Natural Variation and Domestication Selection of Affects Plant Architecture and Yield-Related Traits in Maize. <b>2019</b> , 10,		6
371	Graphene oxide dispersed in N-TiO <sub>2</sub> nanoplatelets and their implication in wastewater remediation under visible light illumination: Photoelectrocatalytic and photocatalytic properties. <b>2019</b> , 7, 102884		10
370	Probing Photocatalytic Nitrogen Reduction to Ammonia with Water on the Rutile TiO <sub>2</sub> (110) Surface by First-Principles Calculations. <i>ACS Catalysis</i> , <b>2019</b> , 9, 9178-9187	13.1	28
369	Investigation of growth mechanism for highly oriented TiO <sub>2</sub> nanorods: the role of reaction time and annealing temperature. <b>2019</b> , 1, 1		8
368	Atmospheric Processes of Aromatic Hydrocarbons in the Presence of Mineral Dust Particles in an Urban Environment. <b>2019</b> , 3, 2404-2414		6
367	Adsorption and Reaction of Methanol on Anatase TiO <sub>2</sub> (101) Single Crystals and Faceted Nanoparticles. <b>2019</b> , 123, 24133-24145		10
366	Single Molecule Photocatalysis on TiO Surfaces. <i>Chemical Reviews</i> , <b>2019</b> , 119, 11020-11041	68.1	115
365	Frequencies and Thermal Stability of Isolated Surface Hydroxyls on Pyrogenic TiO <sub>2</sub> Nanoparticles. <b>2019</b> , 123, 24533-24548		21
364	Anatase TiO <sub>2</sub> (001)-(1 × 4) Surface Is Intrinsically More Photocatalytically Active than the Rutile TiO <sub>2</sub> (110)-(1 × 1) Surface. <b>2019</b> , 123, 24558-24565		9
363	Real-time Observation of Interface Atomic Structures by an Energy-Dispersive Surface X-ray Diffraction. <b>2019</b> , 17, 155-162		3
362	One-step synthesis of magnetic-TiO <sub>2</sub> -nanocomposites with high iron oxide-composing ratio for photocatalysis of rhodamine 6G. <b>2019</b> , 14, e0221221		3

361	Plasmonic-Enhanced Near-Infrared Photocatalytic Activity of F-Doped (NH <sub>4</sub> ) <sub>0.33</sub> WO <sub>3</sub> Nanorods. <b>2019</b> , 7, 4210-4219	17
360	Defects Promote Ultrafast Charge Separation in Graphitic Carbon Nitride for Enhanced Visible-Light-Driven CO Reduction Activity. <b>2019</b> , 25, 5028-5035	62
359	Fabrication and applications of dual-responsive microencapsulated phase change material with enhanced solar energy-storage and solar photocatalytic effectiveness. <b>2019</b> , 193, 184-197	38
358	Electronic Structure and Band Alignments of Various Phases of Titania Using the Self-Consistent Hybrid Density Functional and DFT+ Methods. <b>2019</b> , 7, 47	7
357	Evaluation of Solar-Driven Photocatalytic Activity of Thermal Treated TiO <sub>2</sub> under Various Atmospheres. <b>2019</b> , 9,	14
356	Visible light driven degradation of brilliant green dye using titanium based ternary metal oxide photocatalyst. <b>2019</b> , 12, 1850-1858	23
355	Synergism of oxygen vacancies, Ti <sup>3+</sup> and N dopants on the visible-light photocatalytic activity of N-doped TiO <sub>2</sub> . <b>2019</b> , 382, 111928	16
354	Advanced diffuse reflectance spectroscopy for studies of photochromic/photoactive solids. <b>2019</b> , 31, 424001	3
353	An evaluation of fluorinated titanium oxide nanocrystals with UV exposure treatment for oxygen vacancy control. <b>2019</b> , 489, 824-830	2
352	Significant improvement in photocatalytic activity by forming homojunction between anatase TiO <sub>2</sub> nanosheets and anatase TiO <sub>2</sub> nanoparticles. <b>2019</b> , 490, 283-292	18
351	Sn <sup>4+</sup> doping combined with hydrogen treatment for CdS/TiO <sub>2</sub> photoelectrodes: An efficient strategy to improve quantum dots loading and charge transport for high photoelectrochemical performance. <b>2019</b> , 430, 80-89	23
350	Development of a self-powered photoelectrochemical system (SPPS) for the determination of propyl gallate. <b>2019</b> , 148, 424-432	6
349	Active Species in Photocatalytic Reactions of Methanol on TiO <sub>2</sub> (110) Identified by Surface Sum Frequency Generation Vibrational Spectroscopy. <b>2019</b> , 123, 13789-13794	7
348	Efficient Charge Carrier Separation in L-Alanine Acids Derived N-TiO Nanospheres: The Role of Oxygen Vacancies in Tetrahedral Ti Sites. <b>2019</b> , 9,	8
347	UV-induced desorption of oxygen at the TiO <sub>2</sub> surface for highly sensitive room temperature O <sub>2</sub> sensing. <i>Journal of Alloys and Compounds</i> , <b>2019</b> , 793, 583-589	5-7 9
346	Solar to chemical energy conversion using titania nanorod photoanodes augmented by size distribution of plasmonic Au-nanoparticle. <b>2019</b> , 231, 322-334	5
345	Photogenerated carrier dynamics at the anatase/rutile TiO <sub>2</sub> interface. <b>2019</b> , 99,	11
344	Semiconductor Nanocatalysts for CO <sub>2</sub> Photoconversion Giving Organic Compounds: Design and Physicochemical Characteristics: A Review. <b>2019</b> , 55, 2-28	3

343	Difference of visible-light photocatalytic activity behaviors between nitrogen- and phosphorus-doped titanium(IV) oxide films. <b>2019</b> , 185, 469-476		2
342	Synthesis and optimization of photocatalytic performance of WO <sub>3</sub> -loaded TiO <sub>2</sub> nanotube array layers. <b>2019</b> , 34, 075027		2
341	A simple high-intensity UV-photon source for photochemical studies in UHV: Application to the photoconversion of norbornadiene to quadricyclane. <b>2019</b> , 90, 024105		7
340	In Situ Studies on Temperature-Dependent Photocatalytic Reactions of Methanol on TiO <sub>2</sub> (110). <b>2019</b> , 123, 9993-9999		12
339	Transparent Ta <sub>2</sub> O <sub>5</sub> Protective Layer for Stable Silicon Photocathode under Full Solar Spectrum. <b>2019</b> , 58, 5510-5515		16
338	Removal of groundwater nitrates by heterogeneous supramolecular complexes-like photocatalytic system based on in-situ generated and highly active Ti <sup>3+</sup> /Ti <sup>2+</sup> states in the reduced TiO <sub>2</sub> . <b>2019</b> , 470, 89-96		10
337	Reactive Oxygen Species (ROS)-Based Nanomedicine. <i>Chemical Reviews</i> , <b>2019</b> , 119, 4881-4985	68.1	776
336	Visible light photocatalytic performance of laser-modified TiO <sub>2</sub> /SnO <sub>2</sub> powders decorated with SiC nanocrystals. <b>2019</b> , 45, 12449-12454		12
335	Band Gap Modification of TiO <sub>2</sub> Nanoparticles by Ascorbic Acid-Stabilized Pd Nanoparticles for Photocatalytic SuzukiMiyaura and Ullmann Coupling Reactions. <b>2019</b> , 149, 1595-1610		20
334	Niobium-Doped TiO: Effect of an Interstitial Oxygen Atom on the Charge State of Niobium. <b>2019</b> , 58, 3090-3098		7
333	Generation of oxygen vacancies on Sr <sub>2</sub> FeMoO <sub>6</sub> to improve its photocatalytic performance through a novel preparation method involving pH adjustment and use of surfactant. <b>2019</b> , 480, 262-275		9
332	Interface and Defect Engineering for Metal Halide Perovskite Optoelectronic Devices. <b>2019</b> , 31, e1803515		201
331	Investigation of temperature-dependent optical properties of TiO <sub>2</sub> using diffuse reflectance spectroscopy. <b>2019</b> , 1, 1		23
330	Solar Concentration for Wastewaters Remediation: A Review of Materials and Technologies. <b>2019</b> , 9, 118		27
329	Multifunctional Fe <sub>3</sub> O <sub>4</sub> @mTiO <sub>2</sub> @noble metal composite NPs as ultrasensitive SERS substrates for trace detection. <b>2019</b> , 12, 2017-2027		6
328	Fabrication of Ti <sup>3+</sup> Self-doped TiO <sub>2</sub> via a Facile Carbothermal Reduction with Enhanced Photodegradation Activities. <b>2019</b> , 4, 14103-14110		3
327	Features of the Preparation and Study of Electrophysical Characteristics (BeO+TiO <sub>2</sub> )-Ceramics by Impedance Spectroscopy. <b>2019</b> , 60, 309-317		3
326	Nitrogen doping on the core-shell structured Au@TiO <sub>2</sub> nanoparticles and its enhanced photocatalytic hydrogen evolution under visible light irradiation. <i>Journal of Alloys and Compounds</i> , <b>2019</b> , 771, 505-512	5.7	21



325	Self-template synthesis of double-shell TiO <sub>2</sub> @ZIF-8 hollow nanospheres via sonocrystallization with enhanced photocatalytic activities in hydrogen generation. <b>2019</b> , 241, 149-158	118
324	Photocatalytic oxidation of gaseous benzene, toluene and xylene under UV and visible irradiation over Mn-doped TiO <sub>2</sub> nanoparticles. <b>2019</b> , 5, 56-65	27
323	Ti-Based Catalysts and Photocatalysts: Characterization and Modeling. <b>2019</b> , 19, 1319-1336	4
322	Nanoparticle transport and sequestration: Intracellular titanium dioxide nanoparticles in a neotropical fish. <b>2019</b> , 658, 798-808	19
321	Synergetic promotional effect of oxygen vacancy-rich ultrathin TiO <sub>2</sub> and photochemical induced highly dispersed Pt for photoreduction of CO <sub>2</sub> with H <sub>2</sub> O. <b>2019</b> , 244, 919-930	81
320	Hollowsphere Nanoheterojunction of g-CN@TiO with High Visible Light Photocatalytic Property. <b>2019</b> , 35, 779-786	51
319	Cascade electronic band structured zinc oxide/bismuth vanadate/three-dimensional ordered macroporous titanium dioxide ternary nanocomposites for enhanced visible light photocatalysis. <b>2019</b> , 539, 585-597	8
318	Biomimetic Hierarchical TiO <sub>2</sub> @CuO Nanowire Arrays-Coated Copper Meshes with Superwetting and Self-Cleaning Properties for Efficient Oil/Water Separation. <b>2019</b> , 7, 2569-2577	44
317	Facile synthesis of TiO <sub>2</sub> microspheres via solvothermal alcoholysis method for high performance dye-sensitized solar cells. <b>2019</b> , 177, 448-454	8
316	Boron-Doped TiO <sub>2</sub> for Efficient Electrocatalytic N <sub>2</sub> Fixation to NH <sub>3</sub> at Ambient Conditions. <b>2019</b> , 7, 117-122	94
315	Nanotechnology: Applications in Energy, Drug and Food. <b>2019</b> ,	3
314	Hydrogenated Titanium Oxide Decorated Upconversion Nanoparticles: Facile Laser Modified Synthesis and 808 nm Near-Infrared Light Triggered Phototherapy. <b>2019</b> , 31, 774-784	68
313	Nano TiO <sub>2</sub> for Biomedical Applications. <b>2019</b> , 267-281	1
312	Acetic Anhydride as an Oxygen Donor in the Non-Hydrolytic Sol-Gel Synthesis of Mesoporous TiO with High Electrochemical Lithium Storage Performances. <b>2019</b> , 25, 4767-4774	5
311	Study on the controlled synthesis and photocatalytic performance of rare earth Nd deposited on mesoporous TiO photocatalysts. <b>2019</b> , 652, 85-92	22
310	Influence of Surface-Related Phenomena on Mechanism, Selectivity, and Conversion of TiO -Induced Photocatalytic Reactions. <b>2019</b> , 12, 589-602	21
309	Biochemical effects of some CeO, SiO, and TiO nanomaterials in HepG2 cells. <b>2019</b> , 35, 129-145	2
308	An acidBase resistant paddle-wheel Cu(II) coordination polymer for visible-light-driven photodegradation of organic dyes. <b>2019</b> , 157, 367-373	12



307	Synthesis and applications of nano-TiO: a review. <b>2019</b> , 26, 3262-3291		139
306	N <sub>2</sub> <sup>+</sup> ion bombardment effect on the band gap of anatase TiO <sub>2</sub> ultrathin films. <b>2019</b> , 88, 282-288		10
305	CO <sub>2</sub> Adsorption on Ti <sub>3</sub> O <sub>6</sub> A Novel Carbonate Binding Motif. <b>2019</b> , 123, 8439-8446		12
304	Synergistic Effect of the Electronic Structure and Defect Formation Enhances Photocatalytic Efficiency of Gallium Tin Oxide Nanocrystals. <b>2019</b> , 123, 433-442		7
303	Effect of NO <sub>2</sub> and NO <sub>3</sub> <sup>-</sup> /HNO <sub>3</sub> adsorption on NO photocatalytic conversion. <b>2019</b> , 244, 660-670		20
302	Effect of metal doped and co-doped TiO <sub>2</sub> photocatalysts oriented to degrade indoor/outdoor pollutants for air quality improvement. A kinetic and product study using acetaldehyde as probe molecule. <b>2019</b> , 371, 255-263		30
301	Tailoring morphology, enhancing magnetization and photocatalytic activity via Cr doping in Bi <sub>25</sub> FeO <sub>40</sub> . <i>Journal of Alloys and Compounds</i> , <b>2019</b> , 773, 828-837	5-7	32
300	Photophysics of color centers in visible-light-active rutile titania. Evidence of the photoformation and trapping of charge carriers from advanced diffuse reflectance spectroscopy and mass spectrometry. <b>2020</b> , 340, 58-69		2
299	Facile one-pot preparation of Ti <sup>3+</sup> , N co-doping TiO <sub>2</sub> nanotube arrays and enhanced photodegradation activities by tuning tube lengths and diameters. <b>2020</b> , 355, 563-572		6
298	Recent Development of Ni/Fe-Based Micro/Nanostructures toward Photo/Electrochemical Water Oxidation. <b>2020</b> , 10, 1900954		200
297	A photocatalytic comparison study between tin complex and carboxylic acid derivatives of porphyrin/TiO <sub>2</sub> composites. <b>2020</b> , 46, 313-328		5
296	Ultraschallaktivierte Sensibilisatoren. <b>2020</b> , 132, 14316-14338		7
295	Synthesis, structure and magnetism of a novel Cu <sub>14</sub> Ti <sub>15</sub> heterometallic cluster. <b>2020</b> , 31, 809-812		13
294	Ultrasound-Activated Sensitizers and Applications. <b>2020</b> , 59, 14212-14233		108
293	Photo-catalytic destruction of acetaldehyde using cobalt, copper co-doped titania dioxide nanoparticles beneath Visible light. <b>2020</b> , 10, 931-939		5
292	Hybrid TiO <sub>2</sub> @ phthalocyanine catalysts in photooxidation of 4-nitrophenol: Effect of the matrix and sensitizer type. <b>2020</b> , 387, 112124		5
291	Photocatalytic surfaces obtained through one-step thermal spraying of titanium. <b>2020</b> , 504, 144173		4
290	Fe <sup>3+</sup> @ ZnO/polyester based solar photocatalytic membrane reactor for abatement of RB5 dye. <b>2020</b> , 246, 119010		27

289	Recent advances in heterometallic polyoxotitanium clusters. <b>2020</b> , 404, 213099	27
288	Enhancement of UV-responsive photocatalysts aided by visible-light responsive photocatalysts: Role of WO <sub>3</sub> for H <sub>2</sub> evolution on CuCl. <b>2020</b> , 263, 118333	9
287	Two-dimensional photocatalyst design: A critical review of recent experimental and computational advances. <b>2020</b> , 34, 78-91	116
286	Limitations and Prospects for Wastewater Treatment by UV and Visible-Light-Active Heterogeneous Photocatalysis: A Critical Review. <b>2019</b> , 378, 7	48
285	Enhancing the photocatalytic activity of Ga <sub>2</sub> O <sub>3</sub> @TiO <sub>2</sub> nanocomposites using sonication amplitudes for the degradation of Rhodamine B dye. <b>2020</b> , 34, e5336	14
284	A review on spectral converting nanomaterials as a photoanode layer in dye-sensitized solar cells with implementation in energy storage devices. <b>2020</b> , 2, e120	7
283	Stable anatase phase with a bandgap in visible light region by a charge compensated Ga <sup>IV</sup> (1:1) co-doping in TiO <sub>2</sub> . <b>2020</b> , 46, 8958-8970	5
282	Anatase-rutile phase transformation and photocatalysis in peroxide gel route prepared TiO <sub>2</sub> nanocrystals: Role of defect states. <b>2020</b> , 108, 106392	14
281	Recent Progress in the Abatement of Hazardous Pollutants Using Photocatalytic TiO-Based Building Materials. <b>2020</b> , 10,	23
280	The role of oxygen vacancies in water splitting photoanodes. <b>2020</b> , 4, 5916-5926	27
279	Rutile-Coated B-Phase TiO <sub>2</sub> Heterojunction Nanobelts for Photocatalytic H <sub>2</sub> Evolution. <b>2020</b> , 3, 10349-10359	8
278	Selective synthesis of visible light active Bi <sub>2</sub> WO <sub>6</sub> nanoparticles for efficient photocatalytic degradation of methylene blue, reduction of 4-nitrophenol, and antimicrobial activity.. <b>2020</b> , 10, 36636-36643	2
277	Highly efficient solar water evaporation of TiO <sub>2</sub> @TiN hyperbranched nanowires-carbonized wood hierarchical photothermal conversion material. <b>2020</b> , 18, 100546	9
276	All-inorganic metal oxide transparent solar cells. <b>2020</b> , 217, 110708	7
275	Heterogeneous photocatalysis. <b>2020</b> , 285-301	1
274	The color center singlet state of oxygen vacancies in TiO. <b>2020</b> , 153, 204704	7
273	Picosecond Lifetime Hot Electrons in TiO <sub>2</sub> Nanoparticles for High Catalytic Activity. <b>2020</b> , 10, 916	3
272	Preparation of TiO <sub>2</sub> Nanoparticle Aggregates and Capsules by the Two-Emulsion Method <b>2020</b> , 4, 57	

271	Adsorption and Motion of Single Molecular Motors on TiO <sub>2</sub> (110). <b>2020</b> , 124, 24776-24785	4
270	Photoinduced Surface Activation of Semiconductor Photocatalysts under Reaction Conditions: A Commonly Overlooked Phenomenon in Photocatalysis. <i>ACS Catalysis</i> , <b>2020</b> , 10, 5941-5948	13.1 23
269	Substitution of Titanium for Magnesium Ions at the Surface of Mg-Doped Rutile. <b>2020</b> , 124, 11490-11498	3
268	Theoretical insights into the surface physics and chemistry of redox-active oxides. <b>2020</b> , 5, 460-475	41
267	Design of TiO <sub>2</sub> nanocrystals with enhanced sunlight photocatalytic activity by exploring calcining conditions. <b>2020</b> , 46, 21268-21274	4
266	Resolving the adsorption of molecular O on the rutile TiO(110) surface by noncontact atomic force microscopy. <b>2020</b> , 117, 14827-14837	16
265	The mechanism of photodriven oxidation of CO over anatase and rutile TiO <sub>2</sub> investigated from the hydrogen adsorption behavior. <b>2020</b> , 277, 119169	11
264	Rapid proton exchange between surface bridging hydroxyls and adsorbed molecules on TiO <sub>2</sub> . <b>2020</b> , 277, 119234	10
263	Photocatalytic properties of graphene-supported titania clusters from density-functional theory. <b>2020</b> , 41, 1921-1930	6
262	Probing Pd <sub>n</sub> (n=1-5) Clusters on Rutile TiO <sub>2</sub> Surfaces by Using First-Principle Calculations. <b>2020</b> , 5, 6939-6945	2
261	Partial Cu ion exchange induced triangle hexagonal MnCuCdS nanocrystals for enhanced photocatalytic hydrogen evolution. <b>2020</b> , 56, 8127-8130	7
260	Affordable and environmentally friendly method for the synthesis of a green silver nanophotocatalyst based on <i>Mespilus germanica</i> . <b>2020</b> , 2, 1	1
259	A TiO nanowire photocatalyst for dual-ion production in laser desorption/ionization (LDI) mass spectrometry. <b>2020</b> , 56, 4420-4423	6
258	Preparation of Gd-Doped TiO <sub>2</sub> Nanotube Arrays by Anodization Method and Its Photocatalytic Activity for Methyl Orange Degradation. <b>2020</b> , 10, 298	12
257	Small polarons and the Janus nature of TiO <sub>2</sub> (110). <b>2020</b> , 101,	7
256	Recent developments in reduced graphene oxide nanocomposites for photoelectrochemical water-splitting applications. <b>2020</b> , 45, 11976-11994	32
255	Manipulating Atomic Structures at the Au/TiO Interface for O Activation. <b>2020</b> , 142, 6456-6460	35
254	Theoretical study of kinetics of proton coupled electron transfer in photocatalysis. <b>2020</b> , 152, 124705	5

253	Blue/red light-triggered reversible color switching based on CeO nanodots for constructing rewritable smart fabrics. <b>2020</b> , 12, 10335-10346		6
252	Effect of crystal field on the formation and diffusion of oxygen vacancy at anatase (101) surface and sub-surface. <b>2020</b> , 30, 128-133		4
251	Fabrication of micro-patterned ZrO <sub>2</sub> /TiO <sub>2</sub> composite surfaces with tunable super-wettability via a photosensitive sol-gel technique. <b>2020</b> , 529, 147136		7
250	Hollow tubular graphitic carbon nitride catalyst with adjustable nitrogen vacancy: Enhanced optical absorption and carrier separation for improving photocatalytic activity. <b>2020</b> , 402, 126185		39
249	What triggers dye adsorption by metal organic frameworks? The current perspectives. <b>2020</b> , 1, 1575-1601		61
248	Heterogeneous Photocatalysis. <b>2020</b> ,		2
247	Synthesis of Ti <sup>3+</sup> self-doped mesoporous TiO <sub>2</sub> cube with enhanced visible-light photoactivity by a simple reduction method. <i>Journal of Alloys and Compounds</i> , <b>2020</b> , 845, 156138	5-7	16
246	TiO <sub>2</sub> Nanoparticles. <b>2020</b> , 1-66		1
245	Surface oxygen vacancies promoted photodegradation of benzene on TiO <sub>2</sub> film. <b>2020</b> , 511, 145597		21
244	Carbon Sphere Template Derived Hollow Nanostructure for Photocatalysis and Gas Sensing. <b>2020</b> , 10,		5
243	Citric Acid Regulated Fabrication of Macroporous TiO <sub>2</sub> . <b>2020</b> , 3, 50-60		1
242	Black TiO <sub>2</sub> : What are exact functions of disorder layer. <b>2020</b> , 2, 44-53		28
241	Enhancing selectivity and reducing cost for dehydrogenation of dodecahydro-N-ethylcarbazole by supporting platinum on titanium dioxide. <b>2020</b> , 45, 6838-6847		18
240	Photocatalytic activities of antimony, iodide, and rare earth metals on SnO <sub>2</sub> for the photodegradation of phenol under UV, solar, and visible light irradiations. <b>2020</b> , 129-288		1
239	Over 20% Efficiency in Methylammonium Lead Iodide Perovskite Solar Cells with Enhanced Stability via "in Situ Solidification" of the TiO Compact Layer. <b>2020</b> , 12, 7135-7143		8
238	Large-scale preparation of titania film for water splitting reaction. <b>2020</b> , 179, 114348		1
237	Preparation and characterization of g-C <sub>3</sub> N <sub>4</sub> /Ag <sup>+</sup> /TiO <sub>2</sub> ternary hollowsphere nanoheterojunction catalyst with high visible light photocatalytic performance. <i>Journal of Alloys and Compounds</i> , <b>2020</b> , 823, 153851	5-7	44
236	Modification of photocatalyst with enhanced photocatalytic activity for water treatment. <b>2020</b> , 289-366		3

235	Construction of visible-light-responsive metal-organic framework with pillared structure for dye degradation and Cr(VI) reduction. <b>2020</b> , 34, e5487		6
234	Photocatalysis as a Tool for in Vitro Drug Metabolism Simulation: Multivariate Comparison of Twelve Metal Oxides on a Set of Twenty Model Drugs. <b>2020</b> , 10, 26		2
233	A review of recent progress in gas phase CO <sub>2</sub> reduction and suggestions on future advancement. <b>2020</b> , 16, 100264		15
232	DFT insights into electrocatalytic CO reduction to methanol on FeO(0001) surfaces. <b>2020</b> , 22, 10819-10827		11
231	N-Promoted Ru/TiO single-atom catalysts for photocatalytic water splitting for hydrogen production: a density functional theory study. <b>2020</b> , 22, 11392-11399		15
230	Au-Mediated Charge Transfer Process of Ternary CuO/Au/TiO-NAs Nanoheterostructures for Improved Photoelectrochemical Performance. <i>ACS Omega</i> , <b>2020</b> , 5, 7503-7518	3-9	5
229	Surface chemistry of TiO connecting thermal catalysis and photocatalysis. <b>2020</b> , 22, 9875-9909		20
228	Reduced Ti-MOFs encapsulated black phosphorus with high stability and enhanced photocatalytic activity. <b>2021</b> , 53, 185-191		13
227	Growth and Atomic-Scale Characterization of Ultrathin Silica and Germania Films: The Crucial Role of the Metal Support. <b>2021</b> , 27, 1870-1885		7
226	One-pot thermal polymerization route to prepare N-deficient modified g-C <sub>3</sub> N <sub>4</sub> for the degradation of tetracycline by the synergistic effect of photocatalysis and persulfate-based advanced oxidation process. <b>2021</b> , 406, 126844		96
225	Ultrathin nanoflake-assembled hierarchical BiOBr microflower with highly exposed {001} facets for efficient photocatalytic degradation of gaseous ortho-dichlorobenzene. <b>2021</b> , 281, 119478		45
224	Stannates, titanates and tantalates modified with carbon and graphene quantum dots for enhancement of visible-light photocatalytic activity. <b>2021</b> , 541, 148425		7
223	Time-resolved infrared spectroscopic investigation of Ga <sub>2</sub> O <sub>3</sub> photocatalysts loaded with Cr <sub>2</sub> O <sub>3</sub> -Rh cocatalysts for photocatalytic water splitting. <b>2021</b> , 42, 808-816		7
222	Cubic-cubic perovskite quantum dots/PbS mixed dimensional materials for highly efficient CO <sub>2</sub> reduction. <b>2021</b> , 481, 228838		9
221	A coordinated regulation strategy to improve electronic conductivity and Li-ion transport for TiO <sub>2</sub> lithium battery anode materials. <i>Journal of Alloys and Compounds</i> , <b>2021</b> , 860, 158282	5-7	4
220	Angle, Spin, and Depth Resolved Photoelectron Spectroscopy on Quantum Materials. <i>Chemical Reviews</i> , <b>2021</b> , 121, 2816-2856	68.1	3
219	Synchronous etching and W-doping for 3D CdS/ZnO/TiO <sub>2</sub> hierarchical heterostructure photoelectrodes to significantly enhance the photoelectrochemical performance. <b>2021</b> , 537, 147998		4
218	Size dependence of CdS nanoparticles on the precursor concentration and visible light driven photocatalytic degradation of methylene blue. <b>2021</b> , 45, 12227-12235		6

217	Fabrication of Fe <sub>2</sub> TiO <sub>5</sub> /TiO <sub>2</sub> binary nanocomposite from natural ilmenite and their photocatalytic activity under solar energy. <b>2021</b> , 4, 100156	9
216	Defects and doping effects in TiO <sub>2</sub> and ZnO thin films of transparent and conductive oxides. <b>2021</b> , 509-554	
215	Facile synthetic routes for photocatalytic Pb(BTC)HO coordination polymers.. <b>2021</b> , 11, 21979-21985	
214	Structural and Electronic Properties of Various Useful Metal Oxides. <b>2021</b> , 49-84	
213	Rational design of bimetallic photocatalysts based on plasmonically-derived hot carriers. <b>2021</b> , 3, 767-780	3
212	Photoinduced Hydrophilicity of Surfaces of Thin Films. <b>2021</b> , 83, 20-48	3
211	Function-oriented design of robust metal cocatalyst for photocatalytic hydrogen evolution on metal/titania composites. <b>2021</b> , 12, 158	22
210	TiO-Based photocatalyst modified with a covalent triazine-based framework organocatalyst for carbamazepine photodegradation.. <b>2021</b> , 11, 6943-6951	2
209	Self-assembly and activation of a titania-nanotube based photocatalyst for H evolution. <b>2021</b> , 57, 7120-7123	1
208	Novel prism shaped CN-doped Fe@CoO nanocomposites and their dye degradation and bactericidal potential with molecular docking study.. <b>2021</b> , 11, 23330-23344	10
207	Study on the self-cleaning and thermal reducing abilities of TiO <sub>2</sub> coated clay roof tile. <b>2021</b> ,	2
206	Comparison of the heat-treatment effect on carrier dynamics in TiO thin films deposited by different methods. <b>2021</b> , 23, 17672-17682	1
205	Structural and electronic properties of TiO <sub>2</sub> from first principles calculations. <b>2021</b> , 67-85	0
204	Refining active sites and hydrogen spillover for boosting visible-light-driven ammonia synthesis at room temperature.	1
203	Fundamental developments in the zeolite process. <b>2021</b> , 32, 499-556	1
202	Efficient photocatalytic degradation of phenol by Ag-doped TiO <sub>2</sub> nanocomposite photocatalysts under visible light irradiation in a three-phase fluidized bed reactor. <b>2021</b> , 75, 3181-3196	4
201	Photoconversion of 2-Propanol on Rutile Titania: A Combined Liquid-Phase and Surface Science Study. <b>2021</b> , 125, 3355-3367	6
200	Density Functional Theory Investigation of Structure-Activity Relationship for Efficient Electrochemical CO <sub>2</sub> Reduction on Defective SnSe <sub>2</sub> Nanosheets. <b>2021</b> , 4, 2760-2767	2

199	Photocatalytic Hydrogen Evolution. <b>2021</b> , 77-105	
198	Breath Acetone Sensing Based on Single-Walled Carbon Nanotube-Titanium Dioxide Hybrids Enabled by a Custom-Built Dehumidifier. <b>2021</b> , 6, 871-880	5
197	Preparation and application of defective graphite phase carbon nitride photocatalysts. <b>2021</b> ,	
196	2D square nanosheets of Anatase TiO <sub>2</sub> : A surfactant free nanofiller for transformer oil nanofluids. <b>2021</b> , 325, 115000	3
195	Photocatalytic oxidation removal of fluoride ion in wastewater by g-C <sub>3</sub> N <sub>4</sub> /TiO <sub>2</sub> under simulated visible light. <b>2021</b> , 4, 339-349	28
194	Fluorine-Induced Surface Metallization for Ammonia Synthesis under Photoexcitation up to 1550 nm. <b>2021</b> , 133, 11273-11279	
193	Fluorine-Induced Surface Metallization for Ammonia Synthesis under Photoexcitation up to 1550 nm. <b>2021</b> , 60, 11173-11179	6
192	Self-powered transparent photodetectors for broadband applications. <b>2021</b> , 23, 100934	4
191	Recent Development in Defects Engineered Photocatalysts: An Overview of the Experimental and Theoretical Strategies.	17
190	Enhancement and stabilization of isolated hydroxyl groups via the construction of coordinatively unsaturated sites on surface and subsurface of hydrogenated TiO <sub>2</sub> nanotube arrays for photocatalytic complete mineralization of toluene. <b>2021</b> , 9, 105080	4
189	Production of green electricity from strained BaTiO <sub>3</sub> and TiO <sub>2</sub> ceramics based hydroelectric cells. <b>2021</b> , 262, 124277	5
188	Advanced Photocatalysts: Pinning Single Atom Co-Catalysts on Titania Nanotubes. <b>2021</b> , 31, 2102843	16
187	The effect of mechanochemical, microwave and hydrothermal modification of precipitated TiO <sub>2</sub> on its physical-chemical and photocatalytic properties. <i>Journal of Alloys and Compounds</i> , <b>2021</b> , 862, 158011 <sup>5-7</sup>	2
186	Halide Perovskite Materials for Photo(Electro)Chemical Applications: Dimensionality, Heterojunction, and Performance. 2004002	21
185	Interaction of Water with Atomic Layer Deposited Titanium Dioxide on p-Si Photocathode: Modeling of Photoelectrochemical Interfaces in Ultrahigh Vacuum with Cryo-Photoelectron Spectroscopy. <b>2021</b> , 8, 2002257	3
184	Carboxylate Adsorption on Rutile TiO(100): Role of Coulomb Repulsion, Relaxation, and Steric Hindrance. <b>2021</b> , 125, 13770-13779	3
183	Crystal phase-dependent generation of mobile OH radicals on TiO <sub>2</sub> : Revisiting the photocatalytic oxidation mechanism of anatase and rutile. <b>2021</b> , 286, 119905	28
182	ZIF-8 Derived ZnO Decorated with Polydopamine and Au Nanoparticles for Efficient Photocatalytic Degradation of Rhodamine B. <b>2021</b> , 6, 5356-5365	0



181	Unexpected impact of oxygen vacancies on photoelectrochemical performance of Au@TiO <sub>2</sub> photoanodes. <b>2021</b> , 127, 105714	1
180	Photoinduced Strong Metal-Support Interaction for Enhanced Catalysis. <b>2021</b> , 143, 8521-8526	21
179	Recent Advances in Aerobic Photo-Oxidation of Methanol to Valuable Chemicals. <b>2021</b> , 13, 3381-3395	11
178	Co-doping of P(V) and Ti(III) in leaf-architected TiO <sub>2</sub> for enhanced visible light harvesting and solar photocatalysis. <b>2021</b> , 104, 5719-5732	1
177	Electron dynamics of tip-tunable oxygen species on TiO <sub>2</sub> surface. <b>2021</b> , 2,	2
176	Nanostructured Bi <sub>2</sub> O <sub>3</sub> /PbS heterojunction as np-junction photoanode for enhanced photoelectrochemical performance. <i>Journal of Alloys and Compounds</i> , <b>2021</b> , 870, 159545	5-7 4
175	TiO <sub>2</sub> Nanotubes Architectures for Solar Energy Conversion. <b>2021</b> , 11, 931	3
174	Oxygen Vacancy and Adsorbed Superoxides Dependent Photocatalytic Activity of TiO <sub>2</sub> Quantum Dot Thin Films for Degradation of Methylene Blue with Variation of Precursor Concentration. <b>2021</b> , 10, 081011	1
173	Optical Properties: UV/Vis Diffuse Reflectance Spectroscopy and Photoluminescence. <b>2021</b> , 435-482	
172	Fabricating Cu <sub>2</sub> O-CuO submicron-cubes for efficient catalytic CO oxidation: The significant effect of heterojunction interface. <b>2021</b> ,	1
171	The Effect of Photoinduced Surface Oxygen Vacancies on the Charge Carrier Dynamics in TiO Films. <b>2021</b> , 21, 8348-8354	10
170	Recent advances on Bi <sub>2</sub> WO <sub>6</sub> -based photocatalysts for environmental and energy applications. <b>2021</b> , 42, 1413-1438	62
169	Electronic and Interface Regulation of Wurtzite Surfaces Promotes Photocatalytic Ammonia Synthesis under Visible Light Irradiation.	1
168	Enhanced visible-light-induced photocatalytic NO <sub>x</sub> degradation over (Ti,C)-BiOBr/Ti <sub>3</sub> C <sub>2</sub> T <sub>x</sub> MXene nanocomposites: Role of Ti and C doping. <b>2021</b> , 270, 118815	11
167	Generalizing Continuum Solvation in Crystal to Nonaqueous Solvents: Implementation, Parametrization, and Application to Molecules and Surfaces. <b>2021</b> , 17, 6432-6448	0
166	A multi-functional Cd(II)-based coordination polymer for the highly sensitive detection of nitrofurazone and photocatalytic efficiency of Rhodamine B. <b>2021</b> , 527, 120566	2
165	Insights on interfacial charge transfer across MoS <sub>2</sub> /TiO <sub>2</sub> -NTAs nanoheterostructures for enhanced photodegradation and biosensing&gas-sensing performance. <b>2021</b> , 1244, 131240	1
164	Surface engineering of copper sulfide-titania-graphitic carbon nitride ternary nanohybrid as an efficient visible-light photocatalyst for pollutant photodegradation. <b>2021</b> , 604, 198-207	5



163	Design of 3D-supramolecular metal organic framework of zinc as photocatalyst for the degradation of methylene blue through advanced oxidation process. <b>2021</b> , 1245, 131039	2
162	Solar-driven Ag@NH <sub>2</sub> -MIL-125/PAES-CF <sub>3</sub> -COOH tight reactive hybrid ultrafiltration membranes for high self-cleaning efficiency. <b>2022</b> , 641, 119866	4
161	Ce ion surface-modified TiO <sub>2</sub> aerogel powders: a comprehensive study of their excellent photocatalytic efficiency in organic pollutant removal. <b>2021</b> , 45, 4174-4184	1
160	Self-supported CPs Materials for Photodegrading Toxic Organics in Water. <b>2021</b> , 215-232	1
159	TiO <sub>2</sub> with controllable oxygen vacancies for efficient isopropanol degradation: photoactivity and reaction mechanism. <b>2021</b> , 11, 4060-4071	4
158	Visible light active g-C <sub>3</sub> N <sub>4</sub> sheets/CdS heterojunction photocatalyst for decolourisation of acid blue (AB-25). <b>2021</b> , 23, 1	2
157	Properties of titanium dioxide. <b>2021</b> , 13-66	3
156	Effect of diatomite addition on crystalline phase formation of TiO <sub>2</sub> and photocatalytic degradation of MDMA. <b>2021</b> , 45, 13463-13474	3
155	Photocatalytic degradation of methylene blue under UV and visible light by brookite rutile bi-crystalline phase of TiO <sub>2</sub> . <b>2021</b> , 45, 3485-3497	11
154	Implication of Porous TiO <sub>2</sub> Nanoparticles in PEDOT:PSS Photovoltaic Devices. <b>2014</b> , 389-447	2
153	Artificial Photosynthesis: From Molecular to Hybrid Nanoconstructs. <b>2015</b> , 71-98	3
152	Automatic Evaluation of Surface Nanostructuring Using Image Processing. <b>2018</b> , 110-119	1
151	Fabrication and Photocatalytic Performance of Sb <sub>2</sub> S <sub>3</sub> Film/ITO Combination. <b>2017</b> , 147, 2592-2599	5
150	Silver/Platinum Supported on TiO <sub>2</sub> P25 Nanocatalysts for Non-photocatalytic and Photocatalytic Denitration of Water. <b>2017</b> , 60, 1156-1170	5
149	Adsorption Mechanisms of Typical Carbonyl-Containing Volatile Organic Compounds on Anatase TiO <sub>2</sub> (001) Surface: A DFT Investigation. <b>2017</b> , 121, 13717-13722	35
148	Facet-Specific Mineralization Behavior of Nano-CaP on Anatase Polyhedral Microcrystals. <b>2017</b> , 3, 875-881	4
147	Study on dynamic scaling of morphological evolution of TiO <sub>2</sub> film deposited with different O <sub>2</sub> /Ar flow ratio. <b>2019</b> , 14, 967-971	1
146	Distinct behavior of localized and delocalized carriers in anatase TiO <sub>2</sub> (001) during reaction with O <sub>2</sub> . <b>2020</b> , 4,	16

145	Biochemical Effects of Silver Nanomaterials in Human Hepatocellular Carcinoma (HepG2) Cells. <b>2020</b> , 20, 5833-5858	6
144	Controlled synthesis of mesoporous codoped titania nanoparticles and their photocatalytic activity. <b>2016</b> , 4, 157-165	3
143	Theoretical calculation of a TiO <sub>2</sub> -based photocatalyst in the field of water splitting: A review. <b>2020</b> , 9, 1080-1103	23
142	Characterization and Photoactivity of Titanium (IV) Oxide Obtained from Different Precursors. <b>2015</b> , 6, 85-96	1
141	Impedance Spectroscopy (BeO+TiO <sub>2</sub> )-Ceramics with Additive of TiO <sub>2</sub> Nanoparticles. <b>2019</b> , 366-380	1
140	Synthesis and Characterization of SnO <sub>2</sub> -TiO <sub>2</sub> Nanocomposites Photocatalysts. <b>2019</b> , 15, 398-406	5
139	Optical and photocatalytic properties of photoactive paper with polycrystalline TiO <sub>2</sub> nanopigment for optimal product design. <b>2012</b> , 11, 33-38	7
138	Characterization and Photocatalytic Activity of ZnO/AgNbO <sub>3</sub> . <b>2010</b> , 25, 935-941	5
137	Preparation of 2D Hexagonal p6mm Ordered Mesoporous WO <sub>3</sub> -TiO <sub>2</sub> Composite Materials and Their Visible-Light Photocatalytic Activity. <b>2013</b> , 33, 308-316	1
136	Effects of a chayotte ( <i>Sechium edule</i> ) extract (macerated) on the biochemistry of blood of Wistar rats and on the action against the stannous chloride effect. <b>2007</b> , 10, 823-7	4
135	Graphitic g-C <sub>3</sub> N <sub>4</sub> -WO <sub>3</sub> Composite: Synthesis and Photocatalytic Properties. <b>2014</b> , 35, 1794-1798	7
134	Controlling Size, Shape and Polymorph of TiO <sub>2</sub> Nanoparticles by Temperature-Controlled Hydrothermal Treatment. <b>2015</b> , 59, 238-245	1
133	Unconventional grain growth suppression in oxygen-rich metal oxide nanoribbons. <b>2021</b> , 7, eabh2012	3
132	Kinetics and Thermodynamics of CO Oxidation by (TiO). <b>2021</b> , 26,	
131	Analysis of the origin of lateral interactions in the adsorption of small organic molecules on oxide surfaces. <b>2014</b> , 177-183	
130	Soft X-Ray Spectroscopy and Electronic Structure of 3d Transition Metal Compounds in Artificial Photosynthesis Materials. <b>2015</b> , 269-296	1
129	Time-Domain Ab Initio Modeling of Charge and Exciton Dynamics in Nanomaterials. <b>2015</b> , 353-392	
128	Titania Nano-architectures for Energy. <b>2015</b> , 129-165	

- 127 Binary Oxides of Transition Metals. **2015**, 429-543
- 126 Structural Change of TiO<sub>2</sub>(110) Surface Involved in the Photoinduced Wettability Transition. **2017**, 38, 620-625
- 125 Preparation and Characterization of Visible Light-Sensitive N-doped TiO<sub>2</sub> Using a Sol-gel Method. **2017**, 24, 477-482
- 124 Degradation of Phenol With A Microwave-Uv Irradiation Treatment System Using NANO-TiO<sub>2</sub>. **2017**, 4, 10-23
- 123 Titanium dioxide defect structures as catalytic sites. **2017**, 9(24), 44-56 1
- 122 Clean surfaces of titanium dioxide TiO<sub>2</sub> and other rutile structures. **2018**, 111-115
- 121 Microstructure and optical and electrical properties of TiO<sub>2</sub> nanotube thin films prepared by spin-coating method. **2019**, 14, 1208-1212 2
- 120 Features of the production and study of electrophysical characteristics (BeO + TiO<sub>2</sub>)-ceramics by impedance spectroscopy. **2019**, 55-63 1
- 119 The physico-chemical properties of  $\beta$ -containing stainless steel composites and its photoactivity. **2019**, 10, 410-418
- 118 Interfacial phenomena at a surface of individual and complex fumed nanooxides. **2019**, 11(26), 3-269 5
- 117 Binary Oxides of Transition Metals: ZnO, TiO<sub>2</sub>, ZrO<sub>2</sub>, HfO<sub>2</sub>. **2020**, 255-451
- 116 Impact of Nanoparticle Consolidation on Charge Separation Efficiency in Anatase TiO<sub>2</sub> Films. **2021**, 9, 772116 0
- 115 Photocatalytically Enhanced Inactivation of Internalized Pathogenic Bacteria in Fresh Produce Using UV Irradiation with Nano-Titanium Dioxide. **2021**, 84, 820-826
- 114 Ti-Implanted Nanoscale Layers for the Chloramphenicol Photocatalytic Decomposition. **2021**, 103-115 0
- 113 Effects of nanomaterials on biodegradation of biomaterials. **2022**, 105-135
- 112 Visualization and Quantification of the Laser-Induced ART of TiO<sub>2</sub> by Photoexcitation of Adsorbed Dyes. **2020**, 36, 1651-1661 1
- 111 Growth of transparent conducting rutile TiO<sub>2</sub>:Nb and diode characteristics of n-TiO<sub>2</sub>:Nb/p-Si. **2020**,
- 110 Optimized Pt Single Atom Harvesting on TiO<sub>2</sub> Nanotubes-Towards a Most Efficient Photocatalyst. **2021**, e2104892 13

109	Acetone Formation from Photolysis of 2-Propanol on Anatase-TiO <sub>2</sub> (101). <b>2017</b> , 30, 1-6	
108	Regulation of surface properties of photocatalysis material TiO <sub>2</sub> by strain engineering. <b>2020</b> , 41, 091703	0
107	Size Dependent Photocatalytic Activity of ZnO Nanosheets for Degradation of Methyl Red. <b>2020</b> , 7,	1
106	Metal Substitution in Rutile TiO <sub>2</sub> : Segregation Energy and Conductivity. <b>2022</b> , 51, 609	2
105	C <sub>18</sub> versus C <sub>17</sub> Bond Cleavage in Ethylene Glycol Photochemistry on Rutile TiO <sub>2</sub> (110): Selectivity Depends on Excess Electrons. <b>2021</b> , 125, 25580-25588	1
104	Self-assembled monolayers enhance the efficiency of Pt single atom co-catalysts in photocatalytic H <sub>2</sub> generation. <b>2021</b> , 133, 107166	2
103	Effect of oxidation on excited state dynamics of neutral TiO (n 2021, 155, 211102	0
102	Customizing New Titanium Dioxide Nanoparticles with Controlled Particle Size and Shape Distribution: A Feasibility Study Toward Reference Materials for Quality Assurance of Nonspherical Nanoparticle Characterization. 2101347	0
101	Superwetting and photocatalytic Ag <sub>2</sub> O/TiO <sub>2</sub> @Cu <sub>2</sub> O <sub>4</sub> nanocomposite-coated mesh membranes for oil/water separation and soluble dye removal. <b>2022</b> , 23, 100717	4
100	Recent progress in defective TiO <sub>2</sub> photocatalysts for energy and environmental applications. <b>2022</b> , 156, 111980	18
99	Fermi-level-tuned MOF-derived N-ZnO@NC for photocatalysis: A key role of pyridine-N-Zn bond. <b>2022</b> , 112, 68-76	3
98	Studying the Photocatalytic Activity of Iron Oxides Synthesized by Plasma Dynamic Method. <b>2020</b> ,	
97	Depth Profiling Characterization of Titanium Chemical State on Electrode Surfaces for Technological Applications.	1
96	Study on the homogeneous design of ultra-thin protonated g-C <sub>3</sub> N <sub>4</sub> composite TiO <sub>2</sub> hollow spheres and its photocatalytic performance for RHB. <b>2022</b> , 33, 4482	0
95	A Comprehensive Review of Graphitic Carbon Nitride (g-CN)-Metal Oxide-Based Nanocomposites: Potential for Photocatalysis and Sensing.. <b>2022</b> , 12,	15
94	Oxygen Deficiencies in Titanium Oxide Clusters as Models for Bulk Defects.. <b>2022</b> ,	0
93	Heating-Induced Transformation of Anatase TiO Nanorods into Rock-Salt TiO Nanoparticles: Implications for Photocatalytic and Gas-Sensing Applications.. <b>2022</b> , 5, 1600-1606	1
92	A Few Pt Single Atoms Are Responsible for the Overall Co-Catalytic Activity in Pt/TiO <sub>2</sub> Photocatalytic H <sub>2</sub> Generation. 2101026	5

91	An Overview of Hydrogen Production: Current Status, Potential, and Challenges. <b>2022</b> , 316, 123317	10
90	Titanium dioxide (TiO <sub>2</sub> )-based photocatalyst materials activity enhancement for contaminants of emerging concern (CECs) degradation: In the light of modification strategies. <b>2022</b> , 10, 100262	8
89	Photochemistry of 2-Propanol on Rutile TiO <sub>2</sub> (110). <b>2022</b> , 126, 3949-3956	
88	Photocatalytic oxidative degradation of methyl orange by a novel g-C <sub>3</sub> N <sub>4</sub> @ZnO based on graphene oxide composites with ternary heterojunction construction. 1	
87	Ultrahigh Photocatalytic CO Reduction Efficiency and Selectivity Manipulation by Single-Tungsten-Atom Oxide at the Atomic Step of TiO <sub>2</sub> . <b>2022</b> , e2109074	7
86	Holes as Catalysts for CO Photo-Oxidation on Rutile TiO <sub>2</sub> (110).	0
85	Photoinduced Superhydrophilicity of Gd-Doped TiO Ellipsoidal Nanoparticles Boosts Contrast Enhancement for Magnetic Resonance Imaging.. <b>2022</b> ,	4
84	A facile Dark-Deposition approach for Pt single-atom trapping on faceted anatase TiO <sub>2</sub> nanoflakes and use in photocatalytic H <sub>2</sub> generation. <b>2022</b> , 412, 140129	4
83	APATITIC NANOPOWDERS AND COATINGS: A COMPREHENSIVE REVIEW.	0
82	INVESTIGATION OF Pd@g-C <sub>3</sub> N <sub>4</sub> /TiO <sub>2</sub> NANOPARTICLES AS PHOTOCATALYST IN THE DEGRADATION OF METHYLENE BLUE UNDER VISIBLE LIGHT IRRADIATION. <b>2021</b> , 7, 100-111	
81	Effect of Nitrogen Doping on Structural and Optical Properties of TiO <sub>2</sub> Nanoparticles. <b>2021</b> , 400, 2100071	0
80	Contribution of photocatalytic and Fenton-based processes in nanotwin structured anodic TiO nanotube layers modified by Ce and V.. <b>2022</b> ,	0
79	CHAPTER 9. Hybrid Solar Cells. 298-340	
78	2D/2D Heterojunction of TiO Nanoparticles and Ultrathin G-CN Nanosheets for Efficient Photocatalytic Hydrogen Evolution.. <b>2022</b> , 12,	0
77	Role of Water in Methanol Photochemistry on TiO <sub>2</sub> Nanocrystals: An In Situ DRIFTS Study.	1
76	Synthesis and structural, optical and photovoltaic characteristics of pure and Ag doped TiO <sub>2</sub> nanoparticles for dye sensitized solar cell application. <b>2022</b> ,	0
75	Surface State-Assisted Delayed Photocurrent Response of Au Nanocluster/TiO <sub>2</sub> Photoelectrodes.	0
74	Effect of Doping on Rutile TiO <sub>2</sub> Surface Stability and Crystal Shapes. <b>2022</b> , 11,	0

73	Revealing different depth boron substitution on interfacial charge transfer in TiO <sub>2</sub> for enhanced visible-light H <sub>2</sub> production. <b>2022</b> , 121570		0
72	Improving Water Quality Using Metal-Organic Frameworks. <i>ACS Symposium Series</i> , 171-191	0.4	1
71	Understanding the fundamentals of TiO <sub>2</sub> surfaces. Part I. The influence of defect states on the correlation between crystallographic structure, electronic structure and physical properties of single-crystal surfaces. <i>Surface Engineering</i> , <b>2022</b> , 38, 91-149	2.6	3
70	High Photoreactivity on a Reconstructed Anatase TiO <sub>2</sub> (001) Surface Predicted by Ab Initio Nonadiabatic Molecular Dynamics. <i>Journal of Physical Chemistry Letters</i> , 5766-5775	6.4	
69	Hybrid Lithographic Arbitrary Patterning of TiO <sub>2</sub> Nanorod Arrays. <i>ACS Omega</i> ,	3.9	1
68	Elucidating the role of adsorption during artificial photosynthesis: H <sub>2</sub> O and CO <sub>2</sub> adsorption isotherms over TiO <sub>2</sub> reveal thermal effects under UV illumination. <i>Photosynthesis Research</i> ,	3.7	
67	Photodegradation and Mineralization of Phenol Using TiO <sub>2</sub> Coated $\gamma$ -Al <sub>2</sub> O <sub>3</sub> : Effect of Thermic Treatment. <i>Processes</i> , <b>2022</b> , 10, 1186	2.9	0
66	Quantum chemical and molecular dynamics simulation approach to investigate adsorption behaviour of organic azo dyes on TiO <sub>2</sub> and ZnO surfaces. <i>Journal of Adhesion Science and Technology</i> , 1-17	2	2
65	Structural and XPS studies of polyhedral europium doped gadolinium orthovanadate (Eu <sup>3+</sup> :GdVO <sub>4</sub> ) nanocatalyst for augmented photodegradation against Congo-red. <i>Physica E: Low-Dimensional Systems and Nanostructures</i> , <b>2022</b> , 143, 115357	3	
64	Photo-assisted (waste)water treatment technologies [A scientometric-based critical review. <i>Desalination</i> , <b>2022</b> , 538, 115905	10.3	1
63	Subtle Structure Matters: The Vicinity of Surface Ti <sup>5c</sup> Cations Alters the Photooxidation Behaviors of Anatase and Rutile TiO <sub>2</sub> under Aqueous Environments. <i>ACS Catalysis</i> , <b>2022</b> , 12, 8242-8251	13.1	0
62	Interfacial optimization of Oxygen-Vacancy-Induced 1D/2D CeO <sub>2</sub> Nanotubes/g-C <sub>3</sub> N <sub>4</sub> Step-Scheme Heterojunction with Enhanced Visible-Light Photocatalysis and Mechanism Insight. <i>Journal of Alloys and Compounds</i> , <b>2022</b> , 166330	5.7	1
61	The effect of Ti/TiO <sub>2</sub> treatment on morphology, phase composition and semiconductor properties. <i>Voprosy Khimii I Khimicheskoi Tekhnologii</i> , <b>2022</b> , 18-23	0.7	
60	The experimental design and mechanism study of the rifampin photodegradation by PbS-Co <sub>3</sub> O <sub>4</sub> coupled catalyst. <i>Materials Research Bulletin</i> , <b>2022</b> , 155, 111972	5.1	1
59	Biochemical effects of copper nanomaterials in human hepatocellular carcinoma (HepG2) cells.		
58	DFT study of TiO <sub>2</sub> brookite (210) surface doped with silver and molybdenum.		
57	Dithizone, carminic acid and pyrocatechol violet dyes sensitized metal (Ho, Ba& Cd) doped TiO <sub>2</sub> /CdS nanocomposite as a photoanode in hybrid heterojunction solar cell. <b>2022</b> ,		
56	Adsorption and Oxidation of NO <sub>2</sub> on Anatase TiO <sub>2</sub> : Concerted Nitrate Interaction and Photon-Stimulated Reaction. <b>2022</b> , 12, 10472-10481		

55	UV protective fabric for face covering utility article using TiO <sub>2</sub> nanoparticles. <b>2022</b> ,	
54	Aggregation and support effects in the oxidation of fluxional atomic metal clusters. The paradigmatic Cu <sub>5</sub> case.	2
53	A CdS/rGO QDs/TiO <sub>2</sub> nanolawn photoanode co-decorated by reduced graphene oxide quantum dots and CdS nanoparticles with photoinduced cathodic protection characteristic for 316L SS and Cu.	0
52	Room temperature bilayer water structures on a rutile TiO <sub>2</sub> (110) surface: hydrophobic or hydrophilic?. <b>2022</b> , 13, 10546-10554	1
51	Photodegradation of Dyes in Visible Light by TiO <sub>2</sub> /PPy/GO Nanocomposites. <b>2022</b> , 29-52	0
50	Designing Highly Efficient Cu <sub>2</sub> O-CuO Heterojunction CO Oxidation Catalysts: The Roles of the Support Type and Cu <sub>2</sub> O-CuO Interface Effect. <b>2022</b> , 12, 3020	0
49	Preparation and modification methods of defective titanium dioxide-based nanoparticles for photocatalytic wastewater treatment – comprehensive review. <b>2022</b> , 29, 70706-70745	0
48	First-principles Investigations on the Magnetic, Electronic, and Optical Properties of Honeycomb-Kagome-Structured Fe <sub>2</sub> O <sub>3</sub> Monolayer.	0
47	Modified HSE06 functional applied to anatase TiO <sub>2</sub> : influence of exchange fraction on the quasiparticle electronic structure and optical response.	0
46	Hydrothermal synthesis of 3D cauliflower anatase TiO <sub>2</sub> and bio sourced activated carbon: adsorption and photocatalytic activity in real water matrices. 1-16	1
45	Application and synthesis of nano-TiO <sub>2</sub> photocatalytic materials.	0
44	Novel nanocomposite thin films for efficient degradation of Rhodamine B and Rhodamine 6G under visible light irradiation: Reaction Mechanism and Pathway studies. <b>2023</b> , 28, 220430-0	0
43	Photocatalytic destruction of prometryn on Ti-containing aluminum foil nanocomposites.	0
42	Molybdenum and chitosan-doped MnO <sub>2</sub> nanostructures used as dye degrader and antibacterial agent.	0
41	Investigations on structural, electronic and optical properties of ZnO in two-dimensional configurations by first-principles calculations. <b>2023</b> , 51, 014002	0
40	Application of Rh/TiO <sub>2</sub> Nanotube Array in Photocatalytic Hydrogen Production from Formic Acid Solution. <b>2022</b> , 6, 327	0
39	Fabrication of S-scheme hollow TiO <sub>2</sub> @Bi <sub>2</sub> MoO <sub>6</sub> composite for efficiently photocatalytic CO <sub>2</sub> reduction. <b>2023</b> , 27, 101260	0
38	Photoelectrochemical study of Ti <sup>3+</sup> self-doped Titania nanotubes arrays: A comparative study between chemical and electrochemical reduction. <b>2023</b> , 811, 140219	0

37	Structural influence of strontium titanate nanocubes for photocatalytic dye degradation and electrochemical applications. <b>2023</b> , 148, 110299	0
36	Enhanced photocatalytic degradation of Rhodamine B and Methylene blue by novel TiO <sub>2</sub> /SnSe-SnO <sub>2</sub> hybrid nanocomposites under sunlight irradiation: Correlation of photoluminescence property with photocatalytic activity. <b>2023</b> , 159, 112109	0
35	Untangling product selectivity on clean low indexed rutile TiO <sub>2</sub> surfaces using first-principles calculations.	1
34	In Situ Synchrotron-Based Studies of IrO <sub>2</sub> (110)∥TiO <sub>2</sub> (110) under Harsh Acidic Water Splitting Conditions: Anodic Stability and Radiation Damages. <b>2022</b> , 126, 20243-20250	0
33	Electrophysical properties of ceramics sintered at elevated temperatures BeO + 30 wt.% TiO <sub>2</sub> . <b>2022</b> , 1, 21-27	0
32	Progress and challenges in full spectrum photocatalysts: Mechanism and photocatalytic applications. <b>2022</b> ,	0
31	Pt-surface oxygen vacancies coupling accelerated photo-charge extraction and activated hydrogen evolution.	0
30	Electrophysical Properties of BeO + 30 wt.% TiO <sub>2</sub> Ceramics Sintered at Elevated Temperatures.	0
29	Novel cubical Ag(NP) decorated titanium dioxide supported bentonite thin film in the efficient removal of bisphenol A using visible light.	0
28	Operando Identification of Dynamic Photoexcited Oxygen Vacancies as True Catalytic Active Sites. 191-203	1
27	Mixed Molecular and Dissociative Water Adsorption on Hydroxylated TiO <sub>2</sub> (110): An Infrared Spectroscopy and Ab Initio Molecular Dynamics Study.	0
26	Cost-effective equipment for surface pre-treatment for cleaning and excitation of substrates in semiconductor technology. <b>2023</b> , 5,	0
25	Fluorine Aided Stabilization of Pt Single Atoms on TiO <sub>2</sub> Nanosheets and Strongly Enhanced Photocatalytic H <sub>2</sub> Evolution. 33-41	0
24	Anodic TiO <sub>2</sub> Nanotube Layers for Wastewater and Air Treatments: Assessment of Performance Using Sulfamethoxazole Degradation and N <sub>2</sub> O Reduction. <b>2022</b> , 27, 8959	1
23	Methanol Adsorption and Reaction on TiO <sub>2</sub> (110) at Near Ambient Pressure.	0
22	Titanium Dioxide Promotes New Particle Formation: A Smog Chamber Study. <b>2023</b> , 57, 920-928	0
21	Superoxide Anion ChemistryIts Role at the Core of the Innate Immunity. <b>2023</b> , 24, 1841	3
20	Preparation and Numerical Optimization of TiO <sub>2</sub> :CdS Thin Films in Double Perovskite Solar Cell. <b>2023</b> , 16, 900	0



- 19 Hybrid additive manufacturing based on vat photopolymerization and laser-activated selective metallization for three-dimensional conformal electronics. **2023**, 63, 103388 ○
- 18 Ni-based Electro/Photo-Catalysts in HER  $\square$  Review. **2023**, 36, 102619 ○
- 17 High-performance triboelectric nanogenerator via photon-generated carriers for green low-carbon system. **2023**, 108, 108206 ○
- 16 Sol-Gel Obtaining of TiO<sub>2</sub>/TeO<sub>2</sub> Nanopowders with Biocidal and Environmental Applications. **2023**, 13, 257 2
- 15 A Novel Hydrothermal CdS with Enhanced Photocatalytic Activity and Photostability for Visible Light Hydrogenation of Azo Bond: Synthesis and Characterization. **2023**, 13, 413 ○
- 14 Anisotropic Heavy-Metal-Free Semiconductor Nanocrystals: Synthesis, Properties, and Applications. **2023**, 123, 3625-3692 ○
- 13 Improved charge transfer by Ca<sup>2+</sup> modified TiO<sub>2</sub>/graphene conductive material for enhancing conductivity. **2023**, 38, 102779 ○
- 12 TiO<sub>2</sub>-based nanocomposites for cancer diagnosis and therapy: A comprehensive review. **2023**, 82, 104370 ○
- 11 Ordered/Disordered Structures of Water at Solid/Liquid Interfaces. **2023**, 13, 263 ○
- 10 Unraveling the Water Oxidation Mechanism on a Stoichiometric and Reduced Rutile TiO<sub>2</sub> (100) Surface Using First-Principles Calculations. **2023**, 127, 3444-3451 ○
- 9 Surface oxygen vacancy engineering on TiO<sub>2</sub> (101) via ALD technology for simultaneously enhancing charge separation and transfer. **2023**, 59, 3237-3240 ○
- 8 Selective Catalytic Hydrogenation of Nitroarenes to Anilines. **2023**, 1479-1524 ○
- 7 Structural design, biomimetic synthesis, and environmental sustainability of graphene-supported g-C<sub>3</sub>N<sub>4</sub>/TiO<sub>2</sub> hetero-aerogels. ○
- 6 Understanding the fundamentals of TiO<sub>2</sub> surfaces Part II. Reactivity and surface chemistry of TiO<sub>2</sub> single crystals. **2022**, 38, 846-906 ○
- 5 Use of materials based on cobalt alloys for the eco- and energy technologies. **2023**, 30, ○
- 4 Preparation of Hydrated TiO<sub>2</sub> Particles by Hydrothermal Hydrolysis of Mg/Al-Bearing TiOSO<sub>4</sub> Solution. **2023**, 13, 1179 ○
- 3 Effect of Decoration of C@TiO<sub>2</sub> Core-Shell Composites with Nano-Ag Particles on Photocatalytic Activity in 4-Nitrophenol Degradation. **2023**, 13, 764 ○
- 2 Adsorption-Controlled Wettability and Self-Cleaning of TiO<sub>2</sub>. ○

- 1 Mechanochemistry-Induced Strong MetalSupport Interactions Construction toward Enhanced Hydrogenation. 6114-6125

o